https://doi.org/10.15388/vu.thesis.66
https://orcid.org/0000-0002-0896-9209

VILNIUS UNIVERSITY

Renatas
KRASAUSKAS

The role of *Acinetobacter baumannii* BfmRS system in environmental fitness and inter-bacterial competition

DOCTORAL DISSERTATION

Life Sciences,
Biochemistry (N 004)

VILNIUS 2020

This dissertation was written between 2015 and 2019 in the Institute of Biosciences, Life Sciences Center, Vilnius University.

Academic supervisor:
Prof. Dr. Edita Sužiedėlienė
(Vilnius University Life Sciences, Biochemistry – N 004).

https://doi.org/10.15388/vu.thesis.66
https://orcid.org/0000-0002-0896-9209

VILNIAUS UNIVERSITETAS

Renatas
KRASAUSKAS

A. baumannii BfmRS sistemos įtaka patogeno išlikimui aplinkoje ir tarpbakterinėje konkurencijoje

DAKTARO DISERTACIJA

Gamtos mokslai,
Biochemija (N 004)

VILNIUS 2020

Disertacija rengta 2015– 2019 metais Vilniaus universiteto Gyvybės mokslų centro Biomokslų institute.

Mokslinė vadovė:
prof. dr. Edita Sužiedėlienė
(Vilniaus universitetas, gamtos mokslai, biochemija – N 004).

Table of Contents

LIST OF ABBREVIATIONS

aa	amino acids
CDI	contact-dependent growth inhibition
CDI+/-	contact-dependent growth inhibition positive/negative
CdiA-CT	C-terminus domain of CdiA
CFU	colony forming unit
IC	international clone
ICU	intensive care unit
IPTG	isopropyl β-D-1-thiogalactopyranoside
kb	kilobase
kDa	kilodalton
LB	lysogeny broth
MIC	minimal inhibitory concentration
nt	nucleotide
OD	optical density
PBS	phosphate-buffered saline buffer
PCR	polymerase chain reaction
qPCR	quantitative polymerase chain reaction
SDS-PAGE	sodium dodecyl sulphate-polyacrylamide gel electrophoresis
T1SS	type I secretion system
T2SS	type II secretion system
T5SS	type V secretion system
T6SS	type VI secretion system
T6SS+/-	type 6 secretion system positive/negative
TSB	tryptic soy broth
WT	wild-type

INTRODUCTION

Acinetobacter baumannii is one of the most clinically important pathogens worldwide. This Gram-negative bacteria have spread in health-care institutions and affect individuals with critical conditions and those who have experienced a prolong stay in hospital. Infections caused by *A. baumannii* are difficult to treat and represent a serious risk for people with a compromised immune system.

It has been estimated that *A. baumannii* is responsible for up to a tenth of all Gram-negative hospital infections (Antunes *et al.*, 2014), with a mortality rate of the most common ones reaching as high as 70 % (McConnell *et al.*, 2013). The spectrum of infections includes pneumonia, bacteremia (blood infection), urinary tract infections, wound infections, endocarditis, post-neurosurgical meningitis, and necrotizing fasciitis (Peleg *et al.*, 2008).

The success of *A. baumannii* in clinical settings comes from its ability to persist in the environment, which is unfavourable for a majority of bacteria. The adaptation modes include such traits as multidrug-resistance, tolerance to desiccation, ability to form biofilms, motility, and tolerance to oxidative stress (Harding *et al.*, 2018; Morris *et al.*, 2019). Recently, various traits that can directly aid in the colonisation of a host have been described and include virulence factors, secretion systems, and nutrient acquisition systems (Morris *et al.*, 2019).

In bacteria, gene regulation is commonly performed via two-component systems composed of a membrane anchored histidine kinases and cytosolic response regulators, which are regulated via phosphoryl group transfer to a conserved aspartate from the cognate histidine kinase (Groisman, 2016). Recent research provided compelling evidence that *A. baumannii* two-component system BfmRS is one of the most important systems contributing to *A. baumannii* virulent traits such as biofilms, motility, capsule formation, drug resistance, desiccation resistance, adhesion to epithelial cells, resistance to immune system (Clemmer *et al.*, 2011; Farrow *et al.*, 2018; Geisinger *et al.*, 2018; Geisinger and Isberg, 2015; Russo *et al.*, 2010; Tomaras *et al.*, 2008).

Additional mechanism that allows *A. baumannii* to respond and persist in the environment is the presence of secretion systems (Harding *et al.*, 2018; Weber *et al.*, 2017). Recently, it has been shown that the pathogen uses Type VI secretion and contact-dependent growth inhibition systems, which theoretically can provide an *in vivo* fitness advantage in microbial

communities (Harding *et al.*, 2018). This phenotype is especially important in clinical settings, where food sources are scarce, therefore competitions are unavoidable. In addition, these systems in some organisms modulate the secretion of virulence factors, adhesion to surfaces, or mediate micro-nutrient uptake, suggesting their role in pathogenesis.

However, very few studies have been performed elucidating the regulatory circuits of these secretion systems. Understanding of how they are regulated in bacteria and how beneficial they are for the interaction with the environment is of significant importance for the design of potential treating strategies.

In this work, we characterise the contribution of the two-component system BfmRS to *A. baumannii* phenotypes important for the establishment of bacterial communities in the environment and inter-bacterial competition. We also characterise a contact-dependent growth inhibition system encoded by *A. baumannii* V15 clinical isolate.

Therefore, **the goal of this thesis** is to describe the role of BfmRS two-component system in *A. baumannii* ability to persist in the environment and in microbial communities.

To reach the goal the following **objectives** were formulated:

- To investigate the role of BfmRS system in *A. baumannii* ability to form pellicle and to mediate motility;
- To investigate the role of BfmRS system in *A. baumannii* inter-bacterial competition via Type VI secretion system;
- To determine the regulatory action of BfmRS system in *A. baumannii* contact-dependent growth inhibition;
- To evaluate the role of *A. baumannii* polysaccharide capsule in the defence against contact-dependent growth inhibition;
- To determine the mechanism of action of *A. baumannii* CdiA protein in contact-dependent growth inhibition system.

Scientific novelty statement

This work presents novel findings regarding the regulatory network of *Acinetobacter baumannii* two-component system BfmRS, a Gram-negative opportunistic pathogen responsible for a growing number of severe nosocomial infections.

A. baumannii forms a biofilm-like structure at the air/liquid interface known as a pellicle, which increases bacterial survival and persistence in a hostile environment. So far, no regulatory mechanisms have been described that influence *A. baumannii* pellicle formation. In this work, for the first time we show that *A. baumannii* BfmR regulator promotes pellicle formation. We provide evidence that at the same time BfmR protein reciprocally regulates *A. baumannii* surface-associated motility. Although it has already been known that the loss of the BfmS sensor coding gene results in the loss of motility, the role of BfmR regulator in this phenotype remained unexplained. We demonstrated for the first time that the inhibition of motility results from the up-regulation of BfmR coding gene.

BfmR positively regulates the secretion of Hcp protein into the growth media. Hcp in complex along with other proteins form a needle-like apparatus, called Type VI secretion system (T6SS), which is able to puncture and deliver effectors (toxins) into adjacent cells. We demonstrated for the first time that the BfmRS system up-regulates Type VI secretion system. However, the BfmR-dependent increase in the secretion of Hcp protein does not influence the T6SS-mediated interbacterial competition, suggesting that Hcp secretion performs an alternative role in *A. baumannii* physiology.

We have also linked the BfmRS system with the repression of the contact-dependent growth inhibition system in *A. baumannii*. These inhibition systems in Gram-negative bacteria mediate intra-species competition by binding to neighbouring cells of the same species and delivering various toxins to them. This results in the inhibition of the target cell growth. To date, knowledge regarding the regulatory mechanisms of contact-dependent growth inhibition systems is scarce.

It is generally accepted, that a cell-cell contact is essential for contact-dependent growth inhibition activity. However, our results showed that *A. baumannii* CdiA toxin, the component of contact-dependent growth inhibition system, released from bacterial cell into the growth media, retains its toxicity, and effectively induces the growth arrest of susceptible strains. This unique feature indicates that *A. baumannii* does not require a cell to cell interaction to mediate contact-dependent growth inhibition, suggesting that

the pathogen could expand the sphere of influence, leading to the establishment of a more homogeneous population.

This work also introduces novel findings regarding *A. baumannii* defence mechanisms against contact-dependent growth inhibition. It has been known that the outer polysaccharide layer, the capsule, protects *Escherichia coli* from this type of inhibition. In this work, we showed for the first time that *A. baumannii* capsule performs the same protective role, indicating that this defence mechanism is a common phenomenon among bacteria.

Lastly, we found that the presence of the BfmRS system impacts the susceptibility against contact-dependent growth inhibition in some *A. baumannii* clinical strains. This work is the first study that established a direct link between the BfmRS system and the protection against contact-dependent growth inhibition. It has been shown that the loss of BfmRS in some *A. baumannii* strains resulted in the down-regulation of the capsule, which might render them susceptible to the inhibition. However, we did not find that the *bfmRS* deletion caused any apparent reduction in the quantity of capsule in all our tested strains. We concluded that the BfmRS system mediates resistance to contact-dependent growth inhibition via other mechanisms.

In sum, this work demonstrates that the BfmRS system plays a central role in *A. baumannii* ability to survive under unfavourable environmental conditions as well as its ability to perform inter-bacterial competition.

Major findings presented for the defence of this thesis:

- BfmRS system acts as a positive regulator of *A. baumannii* pellicle formation and a negative regulator of surface-associated motility;
- BfmRS system positively regulates the secretion of Hcp protein, a component of the Type VI secretion system into the growth media without impacting the killing phenotype;
- *A. baumannii* contains a functional contact-dependent growth inhibition system negatively regulated by the two-component system BfmRS;
- *A. baumannii* capsule efficiently protects clinical *A. baumannii* isolates from contact-dependent growth inhibition;
- *A. baumannii* V15 strain secretes a functional CdiA toxin into the growth media causing the growth arrest of susceptible cells.

1. LITERATURE REVIEW

1.1. General features of the genus *Acinetobacter*

The genus *Acinetobacter* includes bacteria that can be isolated from various sources of natural ecosystems and opportunistic pathogens that cause human infections. Currently, the genus include 59 distinct species (https://lpsn.dsmz.de/genus/acinetobacter, last accessed March 09, 2020), that should be classified in the Family *Moraxellaceae*, within the Order *Pseudomonadales*, the Class *Gammaproteobacteria*, The Phylum *Proteobacteria*, and the Domain *Bacteria* (George Garrity *et al.*, 2005).

Based on the protein similarity between orthologs in the core genomes, the proposed age of *Acinetobacter* is ~500 million years old, meaning that the genus is as ancient as *Enterobacteriacea*, explaining a great phenotypic and genotypic variation within it (Touchon *et al.*, 2014). Isolated strains can be assigned to *Acinetobacter* if they have a G + C content of 38 – 47 %, are Gram-negative coccobacilli, oxidase negative, catalase positive, aerobic (nonfermenting), non-motile, and do not reduce nitrate (for most strains) (George Garrity *et al.*, 2005). Among all *Acinetobacter* species, which are predominantly isolated from environmental samples, *Acinetobacter baumannii* is found almost uniquely in the hospital environment (Antunes *et al.*, 2014).

Special attention should be paid to the *Acinetobacter calcoaceticus* – *Acinetobacter baumannii* complex (*Acb*), which includes species that can not be properly distinguished based only on phenotypic characterisation. The *Acb* complex includes *A. baumannii*, *Acinetobacter pittii*, *Acinetobacter nosocomialis*, *A. calcoaceticus*, and *Acinetobacter seifertii* species (Mateo-Estrada *et al.*, 2019; Peleg *et al.*, 2008). A recent phylogenetic analysis of the *Acinetobacter* genus not only has identified a few additional species that classify under the *Acb* complex, namely *Acinetobacter oleivorans* and *Acinetobacter lactucae*, but also has found that some strains in the complex are misclassified (Mateo-Estrada *et al.*, 2019). Out of all species from the genus, *A. baumannii, A. nosocomialis* and *A. pittii*, appear to be the most clinically important. These species emerged recently in health institutions worldwide as opportunistic pathogens causing various hospital-acquired infections (Peleg *et al.*, 2008).

Due to the clinical importance of some of the species from *Acinetobacter* genus, methods that identify *Acinetobacter* down to the species level, are of

high priority. Currently these include various phenotypic and genotypic analysis techniques that involve but are not limited to: matrix-assisted laser desorption/ionization time-of-flight mass spectrometry, DNA-DNA hybridisation, 16S rRNA gene restriction analysis, high-resolution fingerprint analysis by amplified fragment length polymorphism, ribotyping, tRNA spacer fingerprinting, restriction or sequence analysis of the 16S-23S rRNA intergenic spacer sequences, sequencing of various other phylogenetic markers, and whole genome sequencing along with average nucleotide identity (Mateo-Estrada *et al.*, 2019; Peleg *et al.*, 2008).

1.1.1 Clonal lineages of *A. baumannii*

It has been observed that bacterial cells within a population might form so-called clonal groups that differ between each other by various properties such as virulence, epidemicity and other. These groups can be identified by performing multi-locus sequence typing of several house-keeping genes (Diancourt et al., 2010). The comparison of resulting profiles allows to track global distribution, spread, and common features among groups of *A. baumannii*. Data from various typing schemes indicate that population structure of *A. baumannii* can be separated into at least nine distinct clonal lineages that are widespread (Zarrilli *et al.*, 2013). Two of these, termed International Clones (IC) I and II, are the most widespread and responsible for the majority of infections worldwide (Giannouli *et al.*, 2013; Zarrilli *et al.*, 2013). It has been suggested that these clusters originated in the mid-1970s with resistance determinants for early antibiotics. The introduction of currently used modern antibiotics from the 1980s caused a rapid, resistance-driven diversification of strains within lineages (Hamidian *et al.*, 2019; Wright *et al.*, 2014). Recent observations of the variations in capsular polysaccharide and lipooligosaccharide outer core loci (Holt *et al.*, 2016; Schultz *et al.*, 2016; Wyres *et al.*, 2020) show an additional level of the diversity of *A. baumannii*. These changes can significantly impact surface polysaccharide structure, host interactions, resistance to predators, and various virulence phenotypes (Holt *et al.*, 2016; Russo *et al.*, 2010; Tipton *et al.*, 2018).

The comparative analyses of genome sequences between strains belonging to IC I and IC II clusters revealed a striking variations within them that can not be observed by conventional typing methods (Holt *et al.*, 2016; Schultz *et al.*, 2016; Wright *et al.*, 2014). Also, these variant strains are seemingly widespread indicating the necessity to characterise each individual isolate (Wright *et al.*, 2014). An interesting observation was made

recently that several different strains can colonise a single patient at the same time. This suggests a possibility for lateral gene transfer between populations, which additionally contributes to the increase of diversity within *A. baumannii* (Snitkin *et al.*, 2013; Wright *et al.*, 2014).

Despite high variations within clusters, some generalities can be drawn. For instance, a tendency has been observed for IC II strains to form larger biofilms, when compared to IC I strains. Moreover, the former group of strains displayed a higher adherence to airway epithelial cells (de Breij *et al.*, 2010; Giannouli *et al.*, 2013), suggesting their more pronounced virulence, and partially explaining the prevalence of IC II clones (Higgins *et al.*, 2010; Karah *et al.*, 2012). Our recent analysis indicated that carbapenem-resistant *A. baumannii* strains from IC II cluster, were the most prevalent carbapenemase producers in Lithuanian hospitals (Povilonis *et al.*, 2013). It was reported that IC I strains display increased resistance to desiccation, while IC II strains are only moderately resistant (Giannouli *et al.*, 2013). Also, when compared to IC II strains, IC I clones display the ability to twitch. It is one out of two motility phenotypes displayed by *A. baumannii* strains (please see section 1.3.1) (Eijkelkamp *et al.*, 2011b). In summary, *A. baumannii* displays a high level of genomic and phenotypic variability, allowing it to rapidly evolve and adapt to life under unfavourable conditions.

1.2. *Acinetobacter baumannii* epidemiology and clinical manifestations

It was calculated that *Acinetobacter* infections account for up to 20 % of all infections in intensive care units worldwide (Vincent *et al.*, 2009). The pathogen targets critically ill people with pre-existing health conditions or patients that have received major surgical interventions, thereby causing nosocomial infections (Antunes *et al.*, 2014). Additionally, the rise of community-acquired *A. baumannii* infections has also been noted (Dijkshoorn *et al.*, 2007).

A recent epidemiological study surveying *in vitro* activities of tigecycline and other antimicrobials against clinically important pathogens, indicated that during the period of 2004-2014, multidrug-resistant *A. baumannii* isolate numbers increased globally from 23 % to 63 %, while all other Gram-negative pathogen numbers remained relatively stable (Fig. 1.1. A). Most important was the fact that ~90 % of surveyed *A. baumannii* isolates were resistant to at least three antibiotics (Giammanco *et al.*, 2017). The epidemiological data on the prevalence of multidrug-resistant *A. baumannii* in Eastern Europe between 2011 and 2016 show an increase from 44.1 % in 2011 to 71.0 % in 2015, before decreasing to ~50.0 % (Fig. 1.1 B). A

worrying observation was made that resistance to fluoroquinolones, aminoglycosides and carbapenems in isolates from Eastern Europe was approximately two-times higher than reported average for European Union/European Economic Area (EU/EEA) countries (Dowzicky and Chmelařová, 2019).

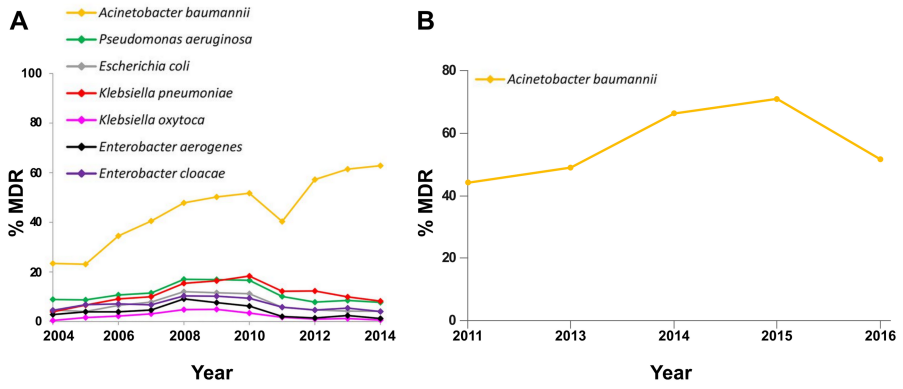

Fig. 1.1. Percentages of multi-drug resistant (MDR) isolates collected: (**A**) globally, between 2004-2014 (adapted from Giammanco *et al.*, (2017)); (**B**) in Eastern Europe, between 2011–2016 (adapted from Dowzicky and Chmelařová, (2019)).

Particular attention should be paid to *A. baumannii* caused outbreaks in neonatal care units. A recently published study aggregating 12 studies from 2004 to 2017 showed that the risk factors associated with neonatal care units including low birthweight, use of various assisted devices, and extensive use of antibiotics, resulted in bloodstream and respiratory tract infections caused by multidrug-resistant and extensively multi-drug resistant *A. baumannii* (Zarrilli *et al.*, 2018).

A. baumannii predominantly causes two types of infections: nosocomial pneumonia and bacteremia (blood infection) (Wong *et al.*, 2017). The former results when the pathogen reaches alveoli of a ventilated patient. This is usually mediated via an invasive endotracheal tube, to which the pathogen might adhere and subsequently be inhaled (Gil-Perotin *et al.*, 2012). Additionally, community-acquired pneumonia has also been documented (Peleg *et al.*, 2008). In general, these cases are associated with pre-existing health conditions such as diabetes or cancer, and are common for patients that smoke heavily, or consume excessive amounts of alcohol (Peleg *et al.*, 2008; Wong *et al.*, 2017). Bacteremia is caused when the pathogen reaches the bloodstream. This happens via various means, such as via contaminated catheter, or secondarily due to the extensive pneumonia (Wong *et al.*, 2017).

The disease is associated with the risk factors such as loss of functionality, steroid and antibiotic use, and prolonged hospital stay (Ballouz *et al.*, 2017). It also demonstrates highly increased mortality rates (between 30 % and 76 %) (Ballouz *et al.*, 2017; Peleg *et al.*, 2008). Other infections caused by *A. baumannii* include urinary tract infections, wound infections, endocarditis, post-neurosurgical meningitis, and necrotizing fasciitis (Peleg *et al.*, 2008).

1.3. Environmental persistence and virulence of *A. baumannii*

Generally, traits that enable *A. baumannii* to successfully inhabit nosocomial settings and colonise its host can be subdivided into two major groups: traits required for environmental persistence, and traits that directly influence infection (Harding *et al.*, 2018). The former includes such traits as multidrug-resistance, biofilm formation, motility, desiccation resistance, and ability to withstand oxidative stress. The traits that influence infection can be further subdivided into conventional virulence factors, secretion systems, nutrient acquisition systems, and bacterial community interactions (Harding *et al.*, 2018; Morris *et al.*, 2019).

1.3.1. *A. baumannii* traits required for environmental persistence

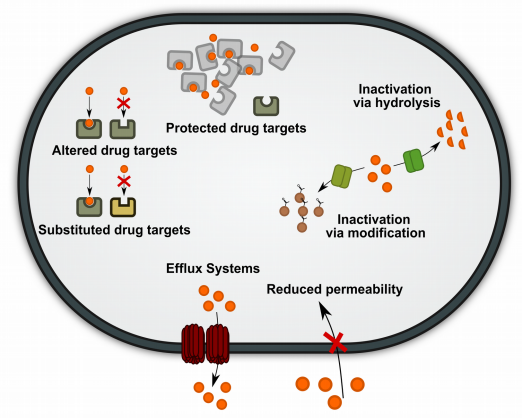

Fig. 1.2. Graphical schematic of main drug resistance mechanisms used by *A. baumannii*.

Antibiotic resistance represents one of the most important phenotypic traits that allow the persistence in nosocomial environments. It has been observed that nearly all known drug-resistance mechanisms are used by *A. baumannii* (Fig. 1.2) (Alekshun and Levy, 2007). These include resistance obtained through chromosomal mutation (mutated DNA gyrase or topoisomerase IV subunits); enzymatic drug inactivation via hydrolysis or modification (β-Lactamases, aminoglycoside-modifying enzymes); altered, substituted, or protected drug targets (altered penicillin binding proteins, Lipid A modifications); the use of efflux systems (at least four types of efflux pumps); and a reduced permeability (the loss of lipopolysaccharide

leads to increased resistance to colistin; the use of outer membrane porins with reduced permeability) (Lee *et al.*, 2017).

Biofilm formation is the ability of bacteria to regulate the aggregation of population into clumps that are wrapped in an extracellular polymeric matrix, which is composed of polysaccharides, proteins, lipids and extracellular DNA (Flemming *et al.*, 2016). These complexes are formed via multiple stages reaching a high cell density (10^8-10^{11} cells/g), and are characterized by some level of bacterial organization, where morphologically and/or genetically different cells signal or respond to nearby cells and surroundings (Flemming *et al.*, 2016; Flynn *et al.*, 2016; Poltak and Cooper, 2011). It is a highly regulated structure that allows bacteria to tolerate unfavourable environment conditions such as desiccation, increased concentrations of antimicrobials, disinfectants, and others (Flemming *et al.*, 2016).

Biofilm formation by *A. baumannii* is considered to be generally responsible for the ability to persist in the environment as the role of this phenotype in *in vivo* pathogenesis models is not well understood (Wong *et al.*, 2017). The pathogen forms biofilms on various surfaces including plastics and stainless steel (Harding *et al.*, 2018).

Currently, at least a dozen of factors are known that contribute to biofilm formation by *A. baumannii*. The best understood are the Csu Type 1 chaperone-usher pili, which allow the pathogen to adhere to abiotic surfaces. Each pilus is composed of CsuA/B pilins, minor subunits CsuA and CsuB, the chaperone CsuC, the usher CsuD, and the adhesive tip CsuE, which displays archaic finger-like loops to attach to the surface (Fig. 1.3) (Pakharukova *et al.*, 2018; Tomaras *et al.*, 2003).

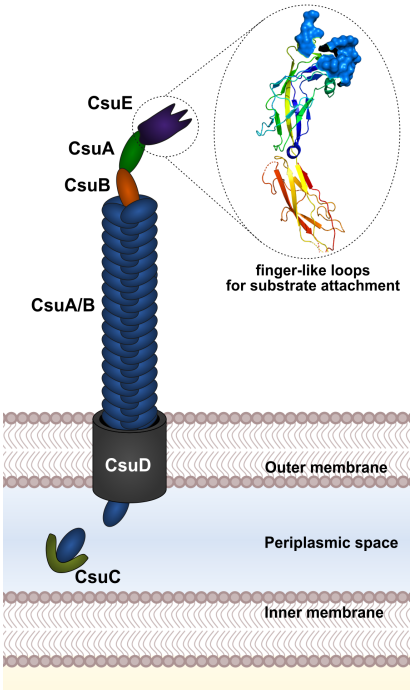

Fig. 1.3. Graphical schematic of *A. baumannii* Csu pilus. CsuE ribbon structure shows finger-like loops of the protein, which are displayed as a surface view. Experimental structure accessible in Protein Data Bank with the ID: 6FJY. The scheme is based on the proposition Harding *et al.*, (2018).

Aside from the Csu pili, there are three Type 1 pili gene clusters encoded in *A. baumannii* genomes, which in some cases contribute to biofilm formation. However, their exact role is currently unknown (Eijkelkamp *et al.*, 2014; Harding *et al.*, 2018; Wood *et al.*, 2018).

In addition to surface biofilms, some *A. baumannii* strains display a novel biofilm phenotype, termed pellicle (Armitano *et al.*, 2014; Marti *et al.*, 2011; Nait Chabane *et al.*, 2014). This structure is considered a type of biofilm, except it is not attached to surface. Instead, pellicle forming bacteria float on the surface of liquid, allowing the community to directly access high concentrations of oxygen above and nutrients from below (Armitano *et al.*, 2014). Similar to biofilms, the pellicle phenotype is also highly regulated and has a complex structure (Armitano *et al.*, 2014).

Motility of *A. baumannii*

While *Acinetobacter* genus initially was described to be a non-motile (George Garrity *et al.*, 2005), later it has been shown that *A. baumannii* indeed displays two forms of motility, namely, surface-associated motility and twitching motility (Clemmer *et al.*, 2011; Eijkelkamp *et al.*, 2011b; McQueary *et al.*, 2012; Mussi *et al.*, 2010; Skiebe *et al.*, 2012). The latter was shown recently to be mediated via Type IV pili (TFP). It is a multi-stage process involving assembly and export of TFP, pili attachment to the surface, followed by the retraction, resulting in the shift of the cell body towards the point of attachment (Harding *et al.*, 2013; Mattick, 2002). Interestingly, this type of motility contributes to natural DNA uptake as this molecule can be pulled into the cell during the retraction of the pili (Harding *et al.*, 2013).

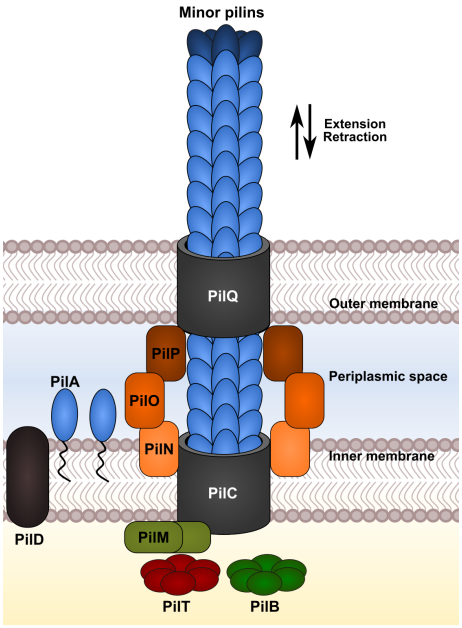

Fig. 1.4. Graphical schematic of the general structure of Type IV pilus. The scheme is based on the proposition by Craig *et al.*, (2019) and Harding *et al.*, (2013).

The twitching machinery consists of several proteins (Fig. 1.4) including cytoplasmic (PilB) and retraction (PilT) ATPases, which are required for the assembly and/or the disassembly

of a pilus; inner membrane platform (PilC) protein that mechanically moves a pilus; an outer membrane secretin protein (PilQ) that forms a channel; pilus filament, that extends throughout periplasmic space and outer membrane; minor pilins that prime the whole complex assembly and modulate the function of the assembled pilus, which itself is composed of multiple copies of the major pilin proteins PilA that were processed by PilD from pre-pilins. The complex is additionally secured and interconnected between the membranes by the supporting alignment proteins: PilM, PilN, PilO, PilP (Craig *et al.*, 2019).

Recently, it was observed that the PilA pilin displays a high sequence variability among *A. baumannii* strains (Eijkelkamp *et al.*, 2011b). Based on structural analysis observations, it was suggested that over time, *A. baumannii* Type IV pili diverged into two forms with different surface electrostatic properties that promote either biofilm formation or motility (Ronish *et al.*, 2019).

Contrary to twitching-motility, the mechanism of surface-associated motility is currently unknown. Visually, the locomotion is similar to the swarming motility of *P. aeruginosa*, however the underlying mechanism is different, since *A. baumannii* is not known to produce flagella (Harding *et al.*, 2018). It was shown that the genus specific polyamine – 1,3-diaminopropane is required for this type of locomotion (Skiebe *et al.*, 2012). Apparently, the motility is community and light controlled, as without auto-inducer synthesis and/or under blue light, the surface-associated motility of *A. baumannii* is inhibited (Clemmer *et al.*, 2011).

***A. baumannii* resistance to desiccation and oxidative stress** is one of the most pronounced features of the pathogen. It was observed that some *A. baumannii* isolates can remain viable for at least 100 days while desiccated (Harding *et al.*, 2018). Special adaptations are needed as water loss leads to the accumulation of free radicals (due to the inactivation of antioxidant mechanisms) and subsequent damage to DNA and proteins. Also, under these conditions, membrane damage and protein denaturation/destruction due to the cell shrinkage followed by molecular overcrowding is unavoidable (Laskowska and Kuczyńska-Wiśnik, 2019). While the exact molecular mechanisms of desiccation tolerance in *A. baumannii* have not been well understood, there were several observations indicating that the presence of capsule and the fatty acid lipid content of lipid A are two major factors contributing to the survival of *A. baumannii* (Boll *et al.*, 2015; Tipton *et al.*, 2018). Recently, it was also determined that the BfmR regulator protein contributes to the resistance

phenotype via the up-regulation of stress resistance proteins KatE and AbsA. The former encodes catalase, which detoxifies hydrogen peroxide, while the latter is a general stress-induced protein contributing to desiccation resistance (Farrow *et al.*, 2018).

A. baumannii strains living in the hospital environment regularly encounter various disinfectants in their surroundings. These conditions also generate reactive oxygen species from which the pathogen must defend. Recently, several genes were described contributing to this protection. It was determined that the RecA protein, which is involved in homologous genetic recombination and recombinational repair, contributes to the survival of *A. baumannii* under desiccative conditions (Aranda *et al.*, 2011). Additionally, the role of catalase genes in resistance to H_2O_2 was also described (Sun *et al.*, 2016).

1.3.2. *A. baumannii* virulence factors

While *A. baumannii* is considered as an opportunistic pathogen targeting humans with compromised immunity systems and lacking canonical toxins or determinants characteristic to known true pathogens (Harding *et al.*, 2018), it nevertheless has adaptations that facilitate host colonisation. These can be considered as potential virulence factors and the majority of them are summarised in Table 1.

Table 1. Summary of known *A. baumannii* virulence factors and their proposed functions.

Virulence factor	Role in pathogenesis/proposed function in virulence
Outer membrane proteins, porins	
OmpA (Omp38)	Biogenesis of outer-membrane vesicles (Moon *et al.*, 2012); attachment to eukaryotic cells, invasion, cytotoxicity (Choi *et al.*, 2008a, 2008b, 2005); binding to extracellular matrix, resistance to complement-mediated killing (Kim *et al.*, 2009; Smani *et al.*, 2012); virulence in nematode infection model, role in twitching motility, resistance to desiccation and serum-induced killing (Skerniškytė *et al.*, 2019b); contributes to biofilm formation (Gaddy *et al.*, 2009); antibacterial resistance (Sugawara and Nikaido, 2012).
Omp34	Released with outer-membrane vesicles (McConnell *et al.*, 2011); cytotoxic, induces apoptosis, and inhibits autophagy (Rumbo *et al.*, 2014); mounts a strong immune response (Jahangiri *et al.*, 2018); adhesion to extracellular matrix (Smani *et al.*, 2012).
OmpW	Contributes to transport of iron, hydrophobic and aromatic molecules across the outer membrane (Catel-Ferreira *et al.*, 2016; Nwugo *et al.*, 2011; Soojhawon *et al.*, 2017); mounts a strong immune response (Huang *et al.*, 2014).
CarO and OprD-like	Imipenem resistance and nutrient uptake (Mussi *et al.*, 2007; Zahn *et al.*, 2015); contributes to growth and cytotoxicity (Fernández-Cuenca

	et al., 2011).
AbuO	Contributes to resistance to oxidative stress, osmotic changes (Srinivasan *et al.*, 2015).
Bap and Bap-like (Blp) proteins	Affect adherence to surfaces (De Gregorio *et al.*, 2015; Loehfelm *et al.*, 2008; Skerniškytė *et al.*, 2019a); contributes to virulence against *Caenorhabditis elegans* and murine infection models (Skerniškytė *et al.*, 2019a).
TonB-copper receptor	Mediates adhesion to extracellular matrix (Smani *et al.*, 2012).
Capsule associated	
Capsule formation	Antimicrobial resistance (Geisinger and Isberg, 2015); protection from desiccation and complement mediated killing, and general aid in virulence (Harding *et al.*, 2018; Lees-Miller *et al.*, 2013).
LpxL and LpxM proteins	Modification of Lipid A, resulting in increased resistance to cationic antimicrobial peptides, desiccation resistance (Boll *et al.*, 2015).
gnaA gene	Required for cellular morphology, contributes to resistance to multiple drugs, and virulence in *Galleria mellonella* (Xu *et al.*, 2019).
Other	
CpaA protein	Metallo-endopeptidase deregulating the coagulation system of a host (Tilley *et al.*, 2014).
Phospholipases C and D	Required for cytolytic and haemolytic activity, contribute to virulence in *G. mellonella* (Fiester *et al.*, 2016); required for epithelial cell invasion and serum resistance (Jacobs *et al.*, 2010; Stahl *et al.*, 2015).
Thioredoxin-A protein	Contributes to twitching motility, virulence, and resistance to H_2O_2 (May *et al.*, 2019).
hisF gene	Required for virulence in mouse lung infection model and increased resistance to macrophages (Martínez-Guitián *et al.*, 2019).
A1S_0114 (gene)	Mediates virulence in *C. elegans*, *G. mellonella*, and mouse pneumonia models (Rumbo-Feal *et al.*, 2017); promotes biofilm formation and adherence (Rumbo-Feal *et al.*, 2017).
katG and *katE* genes	Required for resistance to H_2O_2 (Sun *et al.*, 2016).
Superoxide dismutase	Contributes to virulence in *G. mellonella*, surface associated motility, protection against reactive oxygen species, and resistance to antibiotics (Heindorf *et al.*, 2014).
Surface antigen protein 1	Participates in biofilm formation and contributes to virulence in *G. mellonella* (Liu *et al.*, 2016).
Response regulator PmrA (protein)	Increased resistance to colicin (Adams *et al.*, 2009; Beceiro *et al.*, 2011).

The most notable of these are outer membrane proteins, which modulate mainly the transport of various molecules across lipid bilayer membranes (Vila *et al.*, 2007). It was observed that *A. baumannii* resistance to antibiotics is partially provided by small size and low number of porins present in the outer membrane, which cause low cell permeability (Vila *et al.*, 2007). Recent data indicate that these proteins are essential in various phenotypic outcomes that enable the bacteria to persist in the environment and/or contribute to general virulence (Morris *et al.*, 2019). For instance, OmpA

porin participates in various cellular processes, such as adhesion to biotic and abiotic surfaces, outer membrane vesicle secretion, and complement resistance, to name a few (Wang *et al.*, 2014). Also, it was observed to significantly contribute to virulence in *in vivo* infection models (Wang *et al.*, 2014). Other porins, such as CarO, OprD-like, and OmpW, mediate nutrient uptake, which aid in the survival under limiting conditions (Wong *et al.*, 2017). It is worth noting that the majority of porins were determined to modulate adhesion to abiotic and/or biotic surfaces, promoting the persistence of bacteria.

Another important virulence mechanism of *A. baumannii* is the evasion of the immune system involving complement-mediated killing and phagocytosis (Harding *et al.*, 2018). Resistance is mediated by capsular polysaccharide (Russo *et al.*, 2010). In addition, it was suggested that the glycosylation of membrane-associated proteins might also protect *A. baumannii* from being recognised by the immune system (Harding *et al.*, 2018). It is worth noting that several bacterial type C and D phospholipases were observed to mediate hemolytic activity, serum resistance, epithelial cell invasion, and *in vivo* pathogenesis in general (Fiester *et al.*, 2016; Jacobs *et al.*, 2010; Stahl *et al.*, 2015).

1.3.2.1. *A. baumannii* capsular polysaccharides

The outer layer of *A. baumannii* is surrounded by a high molecular weight capsular polysaccharide composed of repeating oligosaccharide units (K units). This structure allows protection against various unfavourable environmental factors such as antimicrobials, desiccation, immune system and others (Geisinger and Isberg, 2015; Harding *et al.*, 2018; Lees-Miller *et al.*, 2013; Russo *et al.*, 2010). Nearly all genes required for *A. baumannii* capsule synthesis are clustered in a K locus, which can be divided into three parts: capsule export machinery, module of the synthesis of simple sugar substrates, and the region required for capsule production (Fig. 1.5) (Wyres *et al.*, 2020).

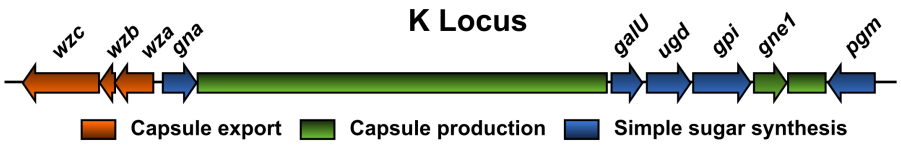

Fig. 1.5. Graphical schematic of capsule polysaccharide locus in *A. baumannii*. Genes are coloured based on the role they play in capsule polysaccharide production. The figure was adapted from Wyres *et al.*, 2020.

Capsule production regions are especially variable among strains and determine the final capsular polysaccharide structure. These regions contain genes required for repeat unit processing (*wzx*, *wzy*), specific glycosyl transferases and/or various other transferases such as acetylation proteins. they can also contain genes required for complex sugar synthesis (Singh *et al.*, 2018; Wyres *et al.*, 2020). Currently, there are more than 92 types of K locus gene clusters known (Wyres *et al.*, 2020). All this variability indicates that complete structures can only be determined experimentally.

A. baumannii capsule synthesis begins at the cytoplasmic side, where sugar oligomers consisting of 4-6 monosaccharides (K units) are assembled together with a carrier lipid undecaprenyl phosphate (und-P) by an initial transferase (Itr) (Fig. 1.6). Then, additional sugars are added by specific glycosyl transferases (Gtr), and the resulting product is transferred to the periplasm via the Wzx translocase. There, the repeat unit translocase Wzy starts polymerising the incoming oligomers onto a single und-P molecule. Finally, the export machinery composed of Wza, Wzb, and Wzc proteins, transport the assembled capsule polymer to the outside (Fig. 1.6) (Singh *et al.*, 2018).

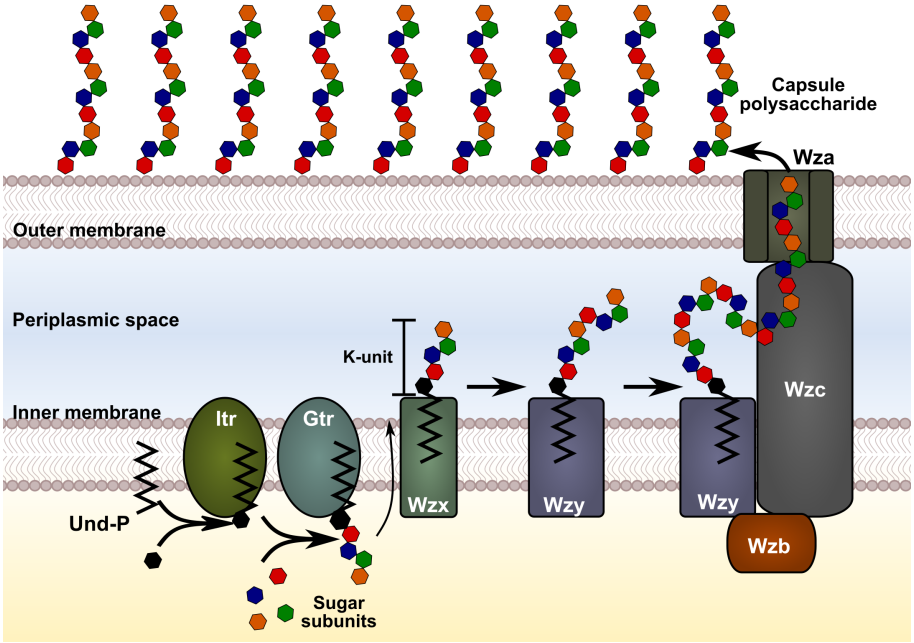

Fig. 1.6. Graphical schematic of the proposed mechanism of capsule polysaccharide synthesis and export in *A. baumannii*. Und-P, lipid undecaprenyl phosphate. The scheme is based on the proposition by Singh *et al.*, (2018).

It is worth noting that capsule synthesis machinery allows protein glycosylation. It has been described that oligo-saccharides from K units can be transferred onto various proteins via oligosaccharyl-transferases, potentially contributing to biofilm formation and survival in the mouse model of systemic infection (Weber *et al.*, 2015a). The glycosylation of Type IV pili and Lipid A were observed also. These modifications are suspected to mediate drug resistance and aid in the evasion from host recognition (Harding *et al.*, 2018).

There are also several other loci involved in the production of surface polysaccharides, which include poly-β-1-6-N-acetylglucosamine that is important for virulence and biofilm formation. Additionally, *A. baumannii* can synthesize lipooligosaccharide (LOS), which contains lipid A, anchoring LOS complex in the outer membrane, and an oligosaccharide. The LOS contributes to *A. baumannii* adherence, motility, and resistance to immune system or antimicrobials (Harding *et al.*, 2018).

1.4. Gene regulatory systems in *A. baumannii*

Prokaryotes use various regulatory systems to respond to environmental stimuli. This is essential for microorganisms, as it allows them to optimally balance energy utilization and rapidly respond to fluctuating environmental conditions and stresses. It has been observed that organisms that can thrive in a more diverse environments, possess a larger number of genes encoding regulatory elements (Bervoets and Charlier, 2019). Gene regulation mechanisms can be separated into a few large groups, which include DNA-binding transcription factors, alternative sigma (σ) factors, nucleoid-associated proteins, covalent DNA modifications and/or sequence variations, small effector binding to RNA polymerase, mRNA stability, RNA binding proteins, riboswitches, and small RNAs (Bervoets and Charlier, 2019).

1.4.1. Transcription factors of *A. baumannii*

The majority of genes in prokaryotes are regulated by proteins that bind DNA sequences and directly influence RNA polymerase binding capabilities to promoters or their functional activity. To bind, transcription factors use helix-turn-helix (HTH) or ribbon-helix-helix (β-ribbon) motifs. Depending on the effect, these factors might activate or repress transcription through various different mechanisms. It must be noted that the affinity of factors to DNA sequences is adjusted either by covalent modifications or reversible interactions with small molecules (Bervoets and Charlier, 2019). Transcription factors, based on their regulation mechanisms and/or proteins

involved, can be subdivided into one-component transcription factors, two-component systems, phosphorelay systems, and oxidation/reduction-regulated proteins, which change their regulatory properties depending on the oxidative state of the cell or its surroundings (Bervoets and Charlier, 2019; Sevilla *et al.*, 2019).

1.4.1.1. One-component transcription factors of *A. baumannii*

A. baumannii is able to survive in various different unfavourable environments, which require specific responses in order to successfully persist. Some of these systems in addition to regulating physiological responses to the environment, also modulate virulence phenotype of the pathogen, making them good targets for antimicrobial therapy (Tiwari *et al.*, 2017).

One of the responses that has been characterised in *A. baumannii*, allows it to cope with the changes of abundance of iron or zinc in the surroundings. Bacteria responds to these via Fur and Zur transcription factors. Iron is used in various metabolic processes and as a cofactor for many enzymes. Free iron is a limited resource in the environment because it can be insoluble (oxidised form), highly toxic (reduced form), or, as often is the case, sequestered by iron- and heme-carrier proteins. To evade limitation, bacteria can either directly bind and import iron ions, or can produce high-affinity molecules, termed iron chelating siderophores, which compete with the host cells (Wandersman and Delepelaire, 2004). In many bacteria, including *A. baumannii,* these genes are under the tight control of Fur or Zur response regulators, which, in the presence of high concentrations of metal, bind to DNA and repress transcription (Fig. 1.7). However, under the conditions of limited Fe or Zn, regulators de-repress the transcription of uptake genes (Fig. 1.7) (Eijkelkamp *et al.*, 2011a; Mortensen *et al.*, 2014). In addition to its role in iron uptake, *A. baumannii* Fur regulator has been shown to contribute to virulence phenotype in a mouse lung infection model (Eijkelkamp *et al.*, 2011a).

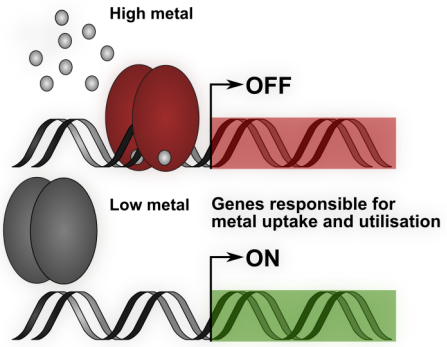

Fig. 1.7. Graphical schematic of the modulation of transcription due to direct metal binding.

It has been long observed that environmental and pathogenic chemotrophic non-phototrophic prokaryotes encode light-sensing

photoreceptors, but only recently, data regarding their role in bacteria physiology began to emerge. Mussi *et al.* reported that *A. baumannii* uses a 18.6-kDa single BLUF domain (sensors of **b**lue-**l**ight **u**sing **F**AD) containing photoreceptor protein to respond to blue light. Additionally, this protein regulates various physiological processes: cell motility, biofilm formation, iron uptake, and killing of fungal filaments (Mussi *et al.*, 2010; Tuttobene *et al.*, 2018). Interestingly, the regulation is temperature-dependent, as photo-regulation is lost at temperatures above 25°C (Golic *et al.*, 2019).

In 2015, Webber *et al*, described a peculiar regulatory mechanism of *A. baumannii* Type VI secretion system (T6SS), which encodes a puncturing device required for the killing of neighbouring bacteria (the in depth description of the system is provided in section 1.5.4.). They showed, that some *A. baumannii* strains carry a resistance conjugative plasmid, which encodes two transcriptional repressors, TetR1 and TetR2, that negatively regulate T6SS. This suppression results in the inability of the pathogen to out-compete other bacteria in a T6SS-dependent manner (Weber *et al.*, 2015b).

Recently, the *A. baumannii* isolate AB5075 was shown to produce colonies with two opacity phenotypes – opaque and translucent (Fig. 1.8), that display differences in terms of cell morphology, capsule thickness, motility, biofilm formation, antibiotic resistance, and virulence (Chin *et al.*, 2018; Tipton *et al.*, 2015). The gene ABUW_1645 was identified as the master TetR-type transcriptional regulator promoting the switch to translucent colony morphology (Chin *et al.*, 2018). The overexpression of the regulator reduced resistance to antimicrobials, disinfectants, and desiccation. Additionally, cells with overexpressed ABUW_1645 became less virulent in a mouse lung infection model (Chin *et al.*, 2018).

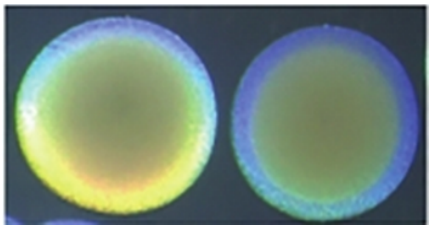

Fig. 1.8. Opaque (left) and translucent (right) *A. baumannii* colony phenotypes. The image was reproduced from Tipton *et al.* (2015).

1.4.1.2. Two-component regulatory systems.

While found in all domains of life, two-component systems play an exceptional role in gene regulation in bacteria (Groisman, 2016). These systems are widely distributed among prokaryotes allowing them to sense and respond to various environmental and internal stimuli such as cell

envelope stress, ion or electrochemical gradients, pH, osmolarity, presence of antimicrobial peptides and many other (Mascher *et al*., 2006). Canonical two-component systems are composed of a membrane anchored histidine kinase, which, via phosphoryl group transfer to a conserved aspartate on a cognate response regulator, modulates its activity (Fig. 1.9). Also, histidine kinases are bifunctional enzymes and, depending on stimulus or its presence, can act as kinases or as phosphatases to their cognate regulators (Zschiedrich *et al.*, 2016). It must be noted that the activating stimuli for the majority of two-component systems are unknown (Mascher *et al.*, 2006).

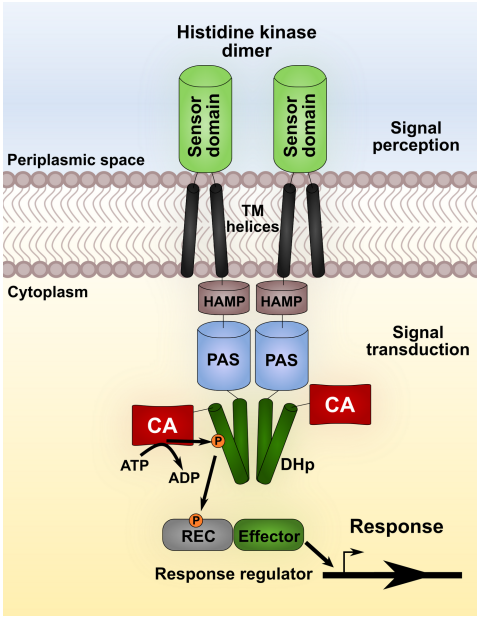

Fig. 1.9. Graphical schematic of domain structures and mechanism of signal transduction in two-component systems. TM, transmembrane helices; HAMP, transmembrane domain; PAS, extra-cytoplasmic sensor domain; DHp, histidine-phosphotransfer domain; CA, catalytic and ATP-binding domain; REC, receiver domain. The scheme is based on the proposition by Zschiedrich *et al.*, (2016) and Jacob-Dubuisson *et al.*, (2018).

Generally, histidine kinases and their response regulators are encoded in the same operon, allowing for an easy identification in genome. Also, it has been observed that the total number of two-component systems encoded by a specific bacteria species depend on the type of environment an organism lives in – the more diverse the inhabited environment, the more systems are encoded in genome (Capra and Laub, 2012). However, it is worth noting that despite multiple number of two-component systems encoded in genome, the specificity-determining residues at the binding interface of sensor and its cognate regulator allows to avoid cross-talk between different systems (Capra and Laub, 2012).

Two-component systems are absent in humans, making them a promising targets for antibiotic development. It has been suggested that a specific inhibition of these systems in bacterial pathogens would completely impair their ability to infect a host (Tiwari *et al.*, 2017). This is because these systems act globally on the pathogen's ability to respond to the environment,

limiting ways of how it can evade the inhibition. Additionally, two-component systems have been shown to regulate the expression of resistance genes. Therefore, the modulation of activity of these systems could render bacteria susceptible to conventional antimicrobials (Poole, 2012; Tiwari *et al.*, 2017).

Generally, response regulators are composed of two domains: a highly diverse receiver (REC) domain, which contains a site of phosphorylation with a conserved aspartate, and an effector domain, which is responsible for the output of the signalling pathway. The effector domain can be linked to REC either covalently or non-covalently (Gao *et al.*, 2019).

The majority of response regulators act as transcription factors, which regulate gene expression by binding to DNA via their effector domains. In addition, some response regulators can bind RNA molecules, proteins, or even display various enzymatic activities such as cyclic diguanylate monophosphate (c-di-GMP) synthesis, phosphodiesterases, and phosphatases (Zschiedrich *et al.*, 2016).

Signal sensing in two-component systems is mediated via the extra-cytoplasmic sensor domains (mainly periplasmic PAS-like or all α-helical) of membrane-associated homodimeric histidine kinase, which upon activation, induces conformational changes in the transmembrane (TM) helices. The signal is then transduced to the C-terminal extensions of transmembrane domain (dimeric HAMP or monomeric STAC domains), which act as connectors between transmembrane and cytoplasmic sensing domains (PAS or GAF). Finally, the signal reaches the C-terminal catalytic domains of a histidine kinase composed of dimerization and histidine-phosphotransfer (DHp), catalytic and ATP-binding (CA) domains (Fig. 1.9) (Zschiedrich *et al.*, 2016). These two domains, along with the REC domain, comprise the catalytic core of a two-component system, where three distinct enzymatic reactions (autophosphorylation, phosphotransfer and dephosphorylation) take place. Firstly, the histidine-phosphotransfer domain comes close to the catalytic and ATP-binding domain with bound ATP and auto-phosphorylates itself from the nucleotide. Then, the catalytic and ATP-binding domain moves away, allowing the binding and subsequent self-catalysed phosphoryl transfer from phosphohistidine on the histidine-phosphotransfer domain to its own conserved aspartyl (Jacob-Dubuisson *et al.*, 2018; Zschiedrich *et al.*, 2016). It is worth noting that the catalytic core of a two-component system is the place, where the specificity of a histidine kinase and response regulator is determined (Gao *et al.*, 2019).

The phosphorylation of response regulator mediates the switch between active and inactive conformations, which can relieve the REC domain mediated inhibition and/or activate an effector domain. For example, the phosphorylation of REC domains can promote dimerization and increased DNA binding affinity of response regulators (Fig. 1.10) (Gao *et al.*, 2019). It should be noted that histidine kinases are bifunctional enzymes and, depending on a stimulus, can act as kinases or as phosphatases towards the cognate regulator (Jacob-Dubuisson *et al.*, 2018).

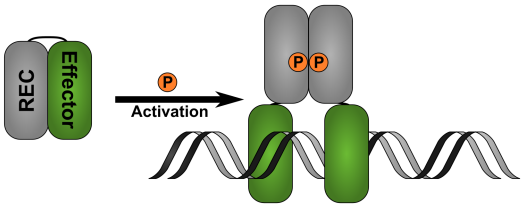

Fig. 1.10. Graphical schematic diagram of the activation of response regulator via phosphorylation. REC, receiver domain. The scheme is based on the proposition by Gao *et al.*, (2019).

1.4.1.2.1. Two-component systems of *A. baumannii*

Bioinformatic analyses of *A. baumannii* genomes have predicted nearly 20 two-component systems. However, only six have been studied in *Acinetobacter* (De Silva and Kumar, 2019). These are BfmRS, GacSA, PmrAB, orphan sensor kinase A1S_2811, BaeSR, AdeRS, and ompR-envZ.

BfmRS system in *A. baumannii* is responsible for the regulation of *csuA/BABCD* pili operon, which mediates biofilm formation on abiotic surfaces (Tomaras *et al.*, 2008, 2003). The system is highly conserved among *A. baumannii* genomes (Russo et al., 2016; Tomaras et al., 2008; also our observations). The chromosomal region encoding the *bfmRS* system is surrounded by a ribonucleotide reductase subunit (*nrdA*) encoding gene upstream and a hypothetical protein along with GGDEF domain containing diguanylate cyclase encoding genes downstream (Fig. 1.11) (Ahmad *et al.*, 2020; Tomaras *et al.*, 2008). The *bfmR* gene is 714 nucleotides long with a predicted 27.1 kDa cytoplasmic protein containing receiver and winged-helix DNA-binding domains (Geisinger and Isberg, 2015; Tomaras *et al.*, 2008). The BfmS sensor is encoded by a 1649 nucleotides long sequence, which produces a predicted 62.4 kDa transmembrane protein (Tomaras *et al.*, 2008). Domain organization includes all domains that are conserved to histidine kinases (Geisinger and Isberg, 2015; Tomaras et al., 2008; also please see section 1.4.1.2.). Currently, the activating signal of the BfmS sensor is unknown.

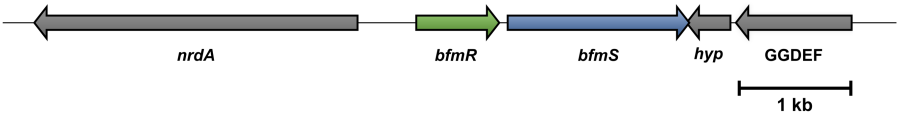

Fig. 1.11. Graphical schematic of *A. baumannii* chromosomal region encoding the *bfmRS* system. The *bfmRS* system is surrounded by the following genes: ribonucleotide reductase subunit (nrdA), hypothetical (*hyp*) and GGDEF domain containing diguanylate cyclase. kb, kilobase. The part of the scheme was adapted from Tomaras *et al.*, 2008.

Recently solved crystal structure by coupling X-ray crystallography, solution nuclear magnetic resonance, chemical crosslinking, and mass spectrometry, indicated that BfmR binds an inverted repeat within the *bfmRS* promoter in both forms – phosphorylated and non-phosphorylated. The latter form binds to DNA with a higher affinity despite the negative impact of dephosphorylation on dimer formation, which in other response regulators increases binding affinity. This phenotype suggests a novel mechanism of self-regulation (Draughn *et al.*, 2018). Other studies also implicate BfmRS in the regulation of various virulence phenotypes, such as surface-associated motility (Clemmer *et al.*, 2011), tolerance to desiccation and oxidative stress (Farrow *et al.*, 2018), physiological modulation of cell envelope, capsular exopolysaccharide expression, resistance to β-lactams and serum (Geisinger *et al.*, 2018; Geisinger and Isberg, 2015; Russo *et al.*, 2016). It has also been observed that BfmRS contributes to *A. baumannii* persistence in murine lung and virulence in *Galleria mellonella* model system (Gebhardt *et al.*, 2015; Wang *et al.*, 2014). Lastly, recent observations indicate that the system modulates outer membrane vesicle secretion (Kim *et al.*, 2019).

GacSA two-component system is composed of the hybrid sensor kinase GacS, which contains both histidine kinase and response regulator domains, suggesting that it can act as a hybrid two-component system. The system also includes additional response regulator, GacA, encoded on a different genome locus (Cerqueira *et al.*, 2014). While the initial role of GacSA was proposed to be citrate utilization, later it was shown that GacSA regulates various additional phenotypes such as aromatic compound metabolism, attachment and biofilm formation, motility, serum resistance, and virulence (Bhuiyan *et al.*, 2016; Cerqueira *et al.*, 2014; Kentache *et al.*, 2017).

PmrAB two-component system along with the phosphoethanolamine transferase gene *pmrC*, is encoded on a single locus *pmrCAB* and in various pathogens has been described to be responsible for colistin resistance (De Silva and Kumar, 2019). Mutations in *A. baumannii pmrAB* also causes resistance to colistin (Adams *et al.*, 2009). While the exact mechanism is still unknown, it is assumed that mutations lead to the up-regulation of the two-

component system, followed by the PmrC-mediated addition of phosphoethanolamine to hepta-acylated lipid A, resulting in resistance to cationic colistin due to positively charged lipid A (Da Silva and Domingues, 2017).

A recently characterized histidine kinase **A1S_2811** has four histidine-containing phosphotransfer domains, a CheA-like regulatory domain, and a CheY-like receiver domain at its C-terminus, therefore making it a hybrid two-component system. It has been suggested that the kinase regulates surface-associated motility, biofilm, and pellicle formation. The latter was proposed to be mediated via the regulation of *csuA/BABCDE* operon. Interestingly, the phenotype of A1S_2811 mutant, when supplemented with synthetic N-acyl-homoserine lactone (quorum sensing molecule) was reinstated, indicating that the kinase participates in quorum sensing pathway (Chen *et al.*, 2017).

BaeSR two-component system was found to modulate the expression of AdeABC efflux pump and respond to osmotic stress (Lin *et al.*, 2014). Additionally, a subsequent study indicated that BaeSR also regulates AdeIJK and MacAB-TolC transport systems (Lin *et al.*, 2015). The AdeIJK efflux pump was determined to transport not only various antibiotics but also contribute to virulence in a mouse lung infection model (Wang *et al.*, 2014).

AdeRS two-component system regulates one of the most in depth described resistance-nodulation-division family-type efflux pump AdeABC (Marchand *et al.*, 2004). Its substrate profile includes aminoglycosides, tigecycline, erythromycin, chloramphenicol, tetracyclines, fluoroquinolones, trimethoprim, and ethidium bromide (Lin *et al.*, 2014; Peleg *et al.*, 2008). Additionally, this pump was suggested to contribute to virulence in a mouse infection model (Yoon *et al.*, 2016). The AdeRS two-component system itself was implicated in the control of virulence phenotypes such as surface-associated motility, biofilm formation, resistance to salinity (De Silva and Kumar, 2018; Richmond *et al.*, 2016). While AdeABC is regulated by the two-component system, the other two well-known *A. baumannii* efflux pumps, namely AdeFHG and AdeIJK, are regulated by LysR-type AdeL and TetR-type AdeN transcription factors, respectively (Coyne *et al.*, 2010; Rosenfeld *et al.*, 2012). These regulators act as repressors of the pumps, subsequently leading to the reduced resistance of strains to antimicrobials. Interestingly, it seems that at least the AdeN regulator can also play a role in *A. baumannii* virulence phenotype as strains with disrupted *adeN* not only displayed a greatly reduced biofilm formation, but also showed an increased virulence towards *G. mellonella* (Saranathan *et al.*, 2017).

OmpR-EnvZ two-component system regulates switching frequency of phase-variable colony opacity phenotype and modulates *A. baumannii* motility, response to osmotic stress, and virulence in the *G. mellonella* infection model (Tipton *et al.*, 2018).

1.4.1.3. Oxidation/reduction-regulated proteins

OxyR is a conserved bacterial transcriptional regulator that responds to the oxidation state of the cell by undergoing a conformational change due to the oxidation of cysteine residues, followed by disulphide formation (Sevilla *et al.*, 2019). *A. baumannii* OxyR was confirmed recently to be required for growth in the presence of hydrogen peroxide. Also, it was found to mediate global transcription response to peroxide induced stress, as well as to contribute to *A. baumannii* survival in murine model of pneumonia (Juttukonda *et al.*, 2019).

1.4.2. Gene regulation by alternative sigma factors

The first step in gene expression involves RNA polymerase mediated transcription of DNA into messenger RNA. The core of this enzyme is composed of two identical α subunits, a single β subunit, and a catalytic β′ subunit (Lodish *et al.*, 2000). For full functionality, RNA polymerase also needs to bind a σ factor, which is essential for promoter recognition. These factors are grouped into two protein families, which are further subdivided into either essential for housekeeping gene expression or alternative factors. The latter are responsible for the regulation of genes required for various cellular processes under different conditions (Pinto *et al.*, 2019). All σ factors in a cell compete for binding to RNA polymerases, and under various conditions their ratio and/or concentration fluctuates, resulting in the modulation of gene expression (Bervoets and Charlier, 2019).

While sigma factors are conserved among bacteria, a lot is still unknown about the mechanisms of how they are regulated in *A. baumannii*. Previously, two chromosome encoded genes *gigA*/*gigB* were proposed to globally modulate the response to multiple stressors such as acidic pH, exposure to increased concentrations of Zn^{2+}, elevated growth temperatures. Sequence analysis of these proteins show that GigA contains a N-terminal receiver and a C-terminal protein phosphatase domains, while the GigB protein contains a sulphate transport and anti-sigma factor antagonist domains. Subsequent experiments led to a proposed model suggesting that GigB is able to sequester phosphate groups from the phosphorylated anti-sigma factor Npr-P, which suppresses sigma factor σ^E, thereby allowing the

σ^E activated transcription of stress response genes. Unphosphorylated NPr can then acquire a new phosphate group from phosphoenolpyruvate (PEP), under normal growth conditions. The phosphates from GigB are removed by the phosphatase activity of GigA via a yet unidentified GigA activation mechanism (Gebhardt and Shuman, 2017).

1.4.3. Gene regulation by nucleoid-associated proteins

Nucleoid-associated proteins introduce an additional level of gene regulation. These proteins affect bacterial chromatin organisation by influencing transcription from exposed or hidden regions via non-specific binding to DNA (Dame and Tark-Dame, 2016). Currently, only one nucleoid-associated protein has been characterised in *A. baumannii*. It was shown that *hns*-like gene acts as the suppressor of motility but promotes pellicle formation. Additionally, the gene mutants displayed an increased adherence to A549 eukaryotic cells and increased virulence against *Caenorhabditis elegans,* suggesting a global role of H-NS in *A. baumannii* pathobiology (Eijkelkamp *et al.*, 2013).

1.4.4. Other *A. baumannii* gene regulation mechanisms

Some genes in bacteria can also be regulated via chemical modification of bases, such as adenine methylation, which modulates the affinity of transcription factors or RNA polymerase to promoters. Moreover, there were observations of changes in DNA sequence, directly impacting transcription such as variable numbers of binding repeats or site-specific recombination of promoter regions (Bervoets and Charlier, 2019). *A. baumannii* is frequently observed to contain various insertion sequences, which promote the expression of resistance genes by either providing a novel promoter or better positioning the existing -35 sequence. In some cases, insertion sequences inactivate genes leading to increased resistance to antibiotics or virulence (Vandecraen *et al.*, 2017).

Mechanisms that regulate gene expression can act via RNA molecules or target them. Specifically, RNA binding proteins can modulate the stability and function of RNA by facilitating their correct secondary and ternary structures, susceptibility to RNases, affinity to ribosomes, and, finally, promote interaction with other effectors (Duval *et al.*, 2015). One of the examples is the Hfq chaperone. This protein usually binds RNA molecules and protects them from degradation. Moreover, it is known to promote interaction between small RNAs and their targets (Bervoets and Charlier, 2019). A recent analysis of RNA chaperone Hfq in *A. baumannii* has

demonstrated that the gene deletion causes multiple defects in *A. baumannii* physiology including growth defects, increased susceptibility to various stresses and to killing by microphages, impairments in biofilm formation, adhesion, and invasion (Kuo *et al.*, 2017). This shows that regulation via RNA molecules is just as important for *A. baumannii* as via transcription factors.

Finally, the regulation of gene expression can be enacted via highly specific mechanisms, which include riboswitches and small RNAs. The former are mRNA molecules with sequences that, depending on physical conditions or the presence of a small metabolite, can fold into a ternary complex and modulate gene expression at transcriptional or translational levels. The latter are small regulatory antisense RNA molecules that when produced, form RNA-RNA interactions with mRNA, influencing gene expression (Saberi *et al.*, 2016). Recent studies identified nearly 300 sRNAs expressed in *A. baumannii* under various stress conditions (Álvarez-Fraga *et al.*, 2017; Cafiso *et al.*, 2020; Sharma *et al.*, 2014; Weiss *et al.*, 2016). However, only some of them were directly associated with a specific *A. baumannii* phenotype, while the vast majority still awaits more detailed characterisation (Álvarez-Fraga *et al.*, 2017).

1.5. Secretion systems in *A. baumannii*

Protein secretion is an essential feature of all bacteria, allowing them to transport proteins from the cell cytoplasm to other compartments of the cell, the environment, other bacteria or target eukaryotes (Green and Mecsas, 2016). In Gram-negative bacteria, protein secretion to the environment is problematic due to the two membranes that cargo must cross. There are two general mechanisms required for solute transport across membranes: secretion (Sec)-dependent and twin

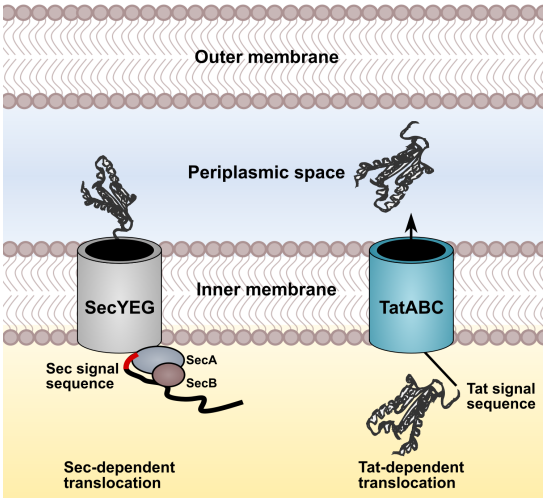

Fig. 1.12. Graphical schematic of export through the Sec-dependent and Tat-dependent translocation pathways in Gram-negative bacteria. The scheme is based on the proposition by Green and Mecsas (2016).

arginine translocation (Tat)-dependent protein secretion mechanisms (Fig. 1.12) (Green and Mecsas, 2016).

The Sec and Tat pathways transport proteins that are destined to remain inside a cell (periplasm). In cases where a protein is to be exported outside, Type I and V secretion systems take over (please see the description below). The main difference between the Sec- and Tat-dependent transport pathways is that the former transports only unfolded proteins, while the latter transports folded substrate. Proteins to be secreted via the Sec pathway contain a ~20 aa long hydrophobic signal sequence at the N-terminus. They are bound by SecB protein, and via SecA are then delivered to the SecYEG channel (Fig. 1.12). If a protein is to be integrated into the membrane, it co-translationally binds SRP protein and a docking protein FtsY. Similarly, the Tat secretion pathway includes proteins TatB and TatC, which bind Tat signal sequence via two arginines of the target protein, and direct it to the membrane channel TatA (Fig. 1.12) (Green and Mecsas, 2016).

Sec- and Tat-independent protein secretion systems are numbered from Type I through Type VI, each with their specific substrates and/or functions. It has been determined that *A. baumannii* has at least four distinct functional secretion systems: Type I (T1SS), Type II (T2SS), Type V (T5SS), Type VI (T6SS).

1.5.1. T1SS

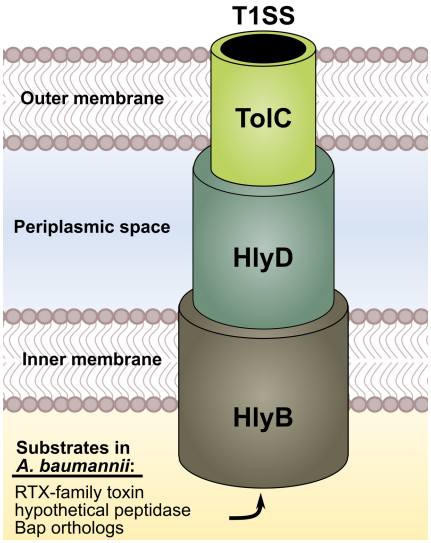

Fig. 1.13. Graphical schematic of structural organization of a Type I secretion system. The scheme is based on the proposition by Harding *et al.*, (2017).

T1SS are found in the majority of Gram-negative bacteria, facilitating the transport of various substrates (in terms of size and function) through both membranes (Fig. 1.13). These include haeme-binding proteins, proteases, lipases, adhesins, and RTX-family toxins. The size of transferred proteins varies from 20 kDa to 900 kDa. The T1SS complex is composed of three proteins: ABC-transporter (HlyB), membrane fusion protein (MFP/HlyD), and outer membrane protein (OMP/TolC). The transporter via the hydrolysis of ATP provides the required energy, TolC forms a channel in the outer

membrane, and HlyD in addition to performing a substrate recognition role, acts as a connector between the transporter and TolC in the periplasm (Fig. 1.13) (Kanonenberg *et al.*, 2013). Recent data indicate that *A. baumannii* possesses a functional T1SS. It has been determined that this system is required for the secretion of Bap orthologs, RTX-family toxin, and a hypothetical peptidase M10 serralysin. This was supported by the fact that T1SS mutants were impaired in both biofilm formation and ability to cause infection in *G. mellonella*. Interestingly, the system cross-talks and negatively regulates the activity of other secretion systems of *A. baumannii* such as T6SS and T2SS, suggesting the global integration of T1SS in *A. baumannii* physiology (Harding *et al.*, 2017).

1.5.2. T2SS

T2SS are also widespread among Gram-negative bacteria. These systems transport folded proteins from the periplasm that were transported there via either Sec- or Tat-dependent secretion mechanisms (Green and Mecsas, 2016). T2SS are highly complex machineries, spanning both membranes and involving 40–70 proteins of 12–15 different types (Fig. 1.14) (Korotkov *et al.*, 2012). These proteins form the following sub-assemblies: pseudopilus, outer-membrane, inner-membrane, and secretion ATPase. The cytoplasmic ATPase GspE provides energy for the whole complex and interacts with the inner-membrane complex proteins GspL and GspF. The complex also include proteins GspN, GspM, and GspC. The latter, interacts with the outer-membrane complex secretin GspD, and possibly determines the recognition of substrates. Finally, in the periplasm, a pseudopilus is formed from at least five proteins. The assembled complex is then ready to secrete substrates. One of the generally accepted models of secretion, the

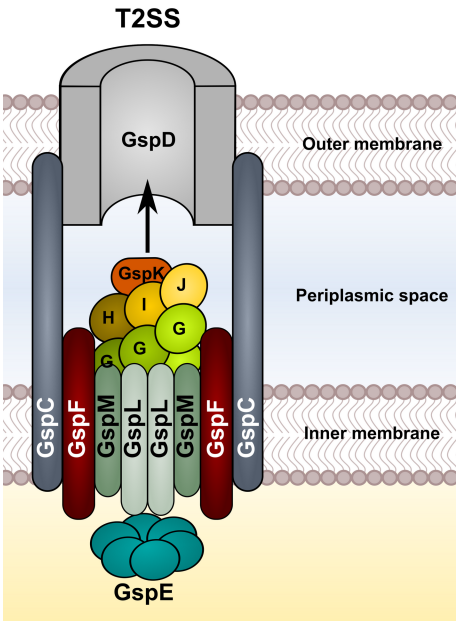

Fig. 1.14. Graphical schematic of structural organization of a Type II secretion system. The scheme is based on the proposition by Korotkov *et al.*, (2012) and Korotkov and Sandkvist (2019).

piston model, suggests that the pseudopilus tip is used to push substrates through the secretin channel to the outside (Korotkov and Sandkvist, 2019). However, the exact mechanism of secretion has not been fully elucidated.

Many bacterial pathogens, including *A. baumannii*, employ T2SS to secret various virulence factors outside of the cell. The substrates include toxins, proteases, lipid-modifying enzymes, carbohydrate-active enzymes, phosphatases, nucleases, and other (Korotkov and Sandkvist, 2019). In the case of *Acinetobacter*, it was found that the T2SS of *A. nosocomialis* was required for secretion of CpdA metallo-peptidase, LipA, and LipH lipases. It also contributed to the virulence against mouse and *G. mellonella* (Harding *et al.*, 2016; Johnson *et al.*, 2015). It must be noted, that various T2SS secreted proteins promote the formation and stability of biofilm (Korotkov and Sandkvist, 2019).

1.5.3. T5SS

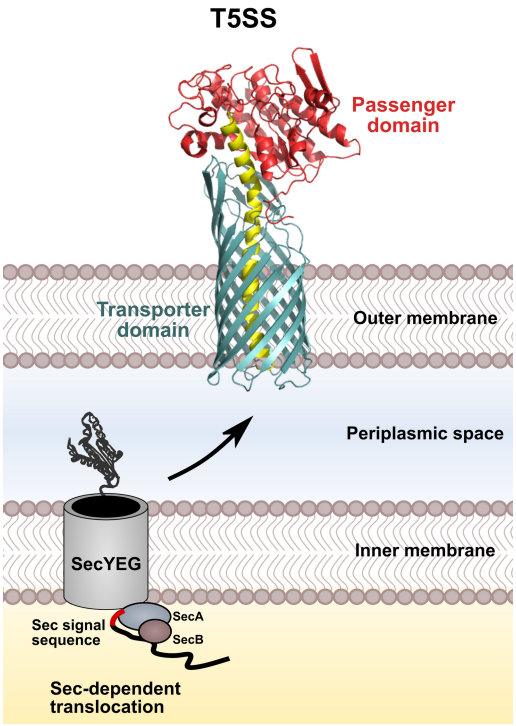

Fig. 1.15. Graphical schematic of structural organization and transport and of a Type V secretion system (Experimental structure accessible in Protein Data Bank with the ID: 3KVN). Transporter and passenger domains are coloured cyan and red, respectively. The scheme is based on the proposition by Fan *et al.*, (2016).

T5SS are wide-spread among Gram-negative bacteria and due to their variability are separated into subtypes a-e. Generally, T5SS are simple systems as they require one or two-components to mediate transport. Also, as mentioned above, protein substrates in order to be transported via T5SS require the Sec machinery that transports them into the periplasm (Fig. 1.15) (Fan *et al.*, 2016). Depending on the number of components required for secretion, T5SS can be separated into three categories: auto-transporter secretion, two-partner secretion, and chaperone-usher secretion (Green and Mecsas, 2016).

The auto-transporter secretion requires only a single polypeptide containing a translocation domain fused to effector/passenger domain. In some instances, where an effector needs to be released, a protease domain allowing the cleavage of effector domain is present. This mechanism is used in Va, Vc, Vd, Ve subtypes (Green and Mecsas, 2016).

A. baumannii was recently found to encode a functional subtype Vc trimeric auto-transporter, termed Ata (Bentancor *et al.*, 2012). This subtype is unique among other auto-transporters due to the fact that it forms a trimeric outer membrane pore. These transporters generally contribute to biofilm formation (Guérin *et al.*, 2017). Accordingly, it has been shown that Ata auto-transporter mediates *A. baumannii* biofilm formation and adhesion to extracellular matrix components (Bentancor *et al.*, 2012). Additionally, the auto-transporter is required for adhesion and invasion to human endothelial and epithelial cells, induces inflammatory signals, and mediates virulence in *G. mellonella* and in murine pneumonia models (Bentancor *et al.*, 2012; Weidensdorfer *et al.*, 2019). There were also observations that among different *A. baumannii* strains Ata auto-transporter expression varies, suggesting that it is tightly regulated (Bentancor *et al.*, 2012).

In the two-partner secretion class (subtype Vb), passenger and translocation domains are two different proteins, TpsA and TpsB, respectively. However, the majority of cases show that TpsA after the secretion, is retained on the surface of TpsB (Fan *et al.*, 2016). It is worth noting that sometimes TpsB can mediate the secretion of different TpsA (Fan *et al.*, 2016; Guérin *et al.*, 2017). The Vb subtype, depending on the functions performed, can be further separated into two major groups: cytolysin/hemolysin secretion and contact-dependent growth inhibition (CDI) systems. However, there have been observations that some TPS can perform adhesion, iron acquisition or proteolysis functions (Guérin *et al.*, 2017).

Previous studies have identified two adhesins in the *A. baumannii*: FhaB/FhaC-like 2-partner secretion system and filamentous hemagglutinin adhesin FhaB1/FhaC1 in AbH12O-A2 and ATCC19606 strains, respectively. Both systems seem to contribute to biofilm formation and adhesion to epithelial cells (Darvish Alipour Astaneh *et al.*, 2014; Pérez *et al.*, 2017). In addition, the FhaB/FhaC system has been further demonstrated to mediate adhesion to extracellular matrix, and contribute to virulence in mouse or *C. elegans* infection models (Pérez *et al.*, 2017). Recently, these adhesins were suggested to also mediate bacterial contact-dependent growth inhibition (Roussin *et al.*, 2019).

1.5.3.1. Contact-dependent growth inhibition (CDI) systems

CDI systems were first identified and described in the *E. coli* EC93 isolate in 2005 (Aoki *et al.*, 2005). The term was coined because growth inhibition requires a cell-cell contact (Aoki *et al.*, 2005; Hayes *et al.*, 2014). These systems are able to transfer a toxic compound to a nearby competitor cell and arrest their growth (Hayes *et al.*, 2014).

Contact-dependent growth inhibition systems consist of three components – outer membrane transporter (CdiB), toxin encoding exoprotein CdiA, and immunity protein CdiI, which prevents bacteria from autoinhibition (Hayes *et al.*, 2014). The genetic organisation of CDI loci depends on the strain, but generally they can be classified into three main types: 1) *E. coli* type with a three gene locus *cdiBAI*, 2) *Burkholderia* type with an analogous *bcpAIB* locus along with an accessory *bcpO* gene between *bcpI* and *bcpB*, and 3) *cdiBCAI*-type with *cdiC* encoding a hypothetical protein potentially involved in CdiB or CdiA biogenesis (Guérin *et al.*, 2017).

It has been observed that CDI systems are found among different α-, β- and γ-proteobacteria species. However, due to their localisation within genomic or pathogenicity islands not all strains from a given species have these systems (Ruhe *et al.*, 2013a). Therefore, it has been suggested that CDI coding regions provide stability to the genetic elements that encode them as the loss would render the bearer to be susceptible to the inhibition (Ruhe *et al.*, 2016).

Toxin translocation requires a specific receptor on target bacteria to be recognized. Also, the mechanism seems to recognise only highly conserved sequences. This requirement results in a very limited target cell range composed of only bacteria within the same species (Ruhe *et al.*, 2013b). A recent proposition indicates that due to the nature of CDI systems to encode variable toxin-immunity pairs they can be used as cues to distinguish "self" from "non-self" neighbours and selectively exclude the latter from the population (Danka *et al.*, 2017).

Currently, the exact role of CDI systems in bacterial physiology is unclear. A proposed model suggests that bacteria use them to compete for a specific niche environments. Additionally, it has been suggested that it could be used as a policing mechanism for non-cooperators in a population (Garcia, 2018). Lastly, a recent observation indicates that contact-dependent growth inhibition is responsible for persister cell creation, which aid in the increased survival chances of population (Ghosh *et al.*, 2018).

1.5.3.1.1. Domain architecture and mechanism of action of CDI systems

Contact-dependent growth inhibition is mediated via the two-partner secretion proteins CdiB and CdiA (Guérin *et al.*, 2017). CdiB is an outer-membrane β-barrel protein that is required to export the toxic CdiA protein/effector onto the cell surface. CdiA proteins are large molecules with sizes starting from as low as 180 kDa and reaching up to 640 kDa. The domain and structural organisation of CdiA is displayed in Figure 1.16 A and B. At the N-terminus CdiA contains a Sec-dependent secretion signal sequence, which allows transport into the periplasm. The additional two-partner secretion (TPS) domain is recognised by CdiB, thereby allowing further transport through the outer membrane. The majority of CdiA protein is composed of filamentous hemagglutinin adhesin domains FHA-1 and FHA-2, which are themselves composed of a degenerate 20-residue sequences of polar and non-polar residues (Willett *et al.*, 2015b). Recent data show that between these regions, there is a ~300 residue-long sequence involved in the recognition of a target (receptor binding domain (RBD)) and cell-surface presentation (YP domain) (Ruhe *et al.*, 2018, 2017). Approximately 200-300 aa long C-terminal region of

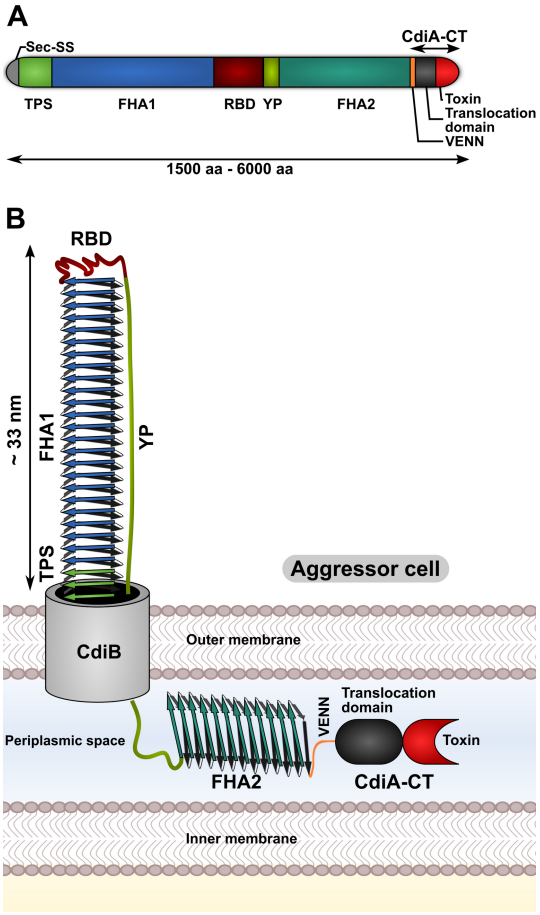

Fig. 1.16. Graphical schematic of the proposed (**A**) domain organisation and (**B**) structural organization of contact-dependent inhibition system. Sec-SS, Sec-dependent secretion signal; TPS, two-partner secretion domain; FHA-1 and FHA-2, filamentous hemagglutinin adhesin domains; RBD, receptor binding domain; YP, cell-surface presentation domain; CdiA-CT, C-terminal region of CdiA. The scheme is based on the proposition by Ruhe *et al.*, (2018, 2017).

CdiA has been named CdiA-CT and is the part of the protein responsible for toxic activity. In some CDI systems this region is easily identifiable due to the presence of VENN or (E/Q)LYN motif. In other CDI systems CdiA-CT can be identified by a high sequence variability.

The last component of CDI systems, immunity protein CdiI, directly binds and neutralises CdiA-CT, preventing bacterial cell from auto-toxicity (Willett *et al.*, 2015b). Some CDI systems contain functional orphan *cdiA*-CT/*cdiI* toxin-immunity modules in their genomes. These modules require a full length CdiA to be delivered to the target cell. It is speculated that due to the repeat regions upstream of these modules, homologous recombination could create a novel effector-immunity pairs not only increasing toxin diversity but also yielding a competitive advantage to the host (Hayes *et al.*, 2014).

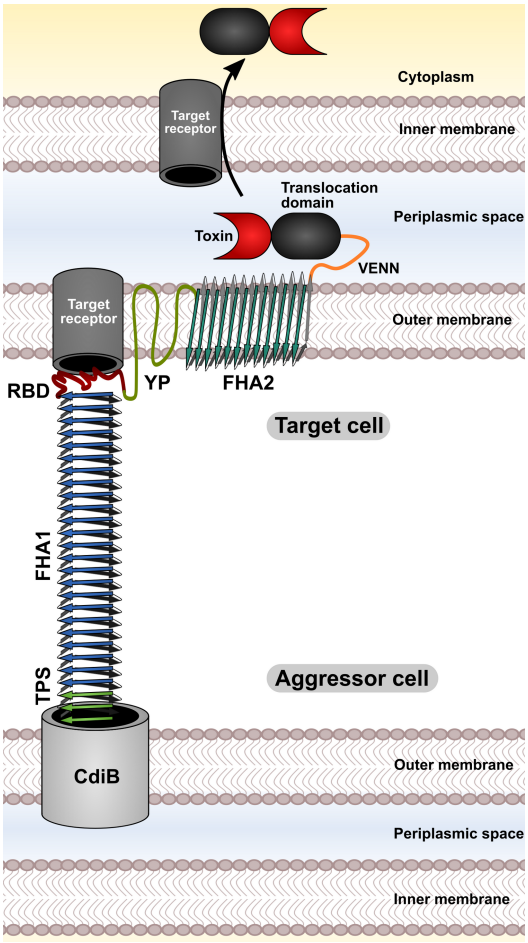

Fig. 1.17. Graphical schematic of the proposed mechanism of action of contact-dependent growth inhibition. TPS, two-partner secretion domain; FHA-1 and FHA-2, filamentous hemagglutinin adhesin domains; RBD, receptor binding domain; YP, cell-surface presentation domain; CdiA-CT, C-terminal region of CdiA. The scheme is based on the proposition by Ruhe *et al.*, (2018).

The mechanism of CDI activity based on the ultrastructural images of CdiA was proposed recently. The model suggests that before target binding, the full CdiA secretion out of the cell is inhibited. This results in a ~33 nm long extracellular filament composed of the following domains: filamentous hemagglutinin adhesin (FHA1), receptor binding (RBD), and N-terminus of YP (Fig. 1.16 B). The rest of CdiA remains localised in the periplasm. After binding a receptor with the receptor

binding domain, the C-terminal half of CdiA is exported, leading to filamentous hemagglutinin adhesin domain 2 interaction and subsequent integration into the outer membrane of the target cell (Fig. 1.17). This leads to the subsequent translocation of CdiA-CT into the periplasm, cleavage, and, depending on the mode of toxicity, integration into the inner membrane or translocation into the cytoplasm of the target cell (Fig. 1.17) (Ruhe *et al.*, 2018).

1.5.3.1.2. Contact-dependent growth inhibition receptors

To date, only three outer membrane receptors that are recognised by CDI have been determined: the outer membrane protein BamA, heterotrimers of the outer membrane proteins OmpC and OmpF, and the bacterial nucleoside transporter Tsx. These are recognised by $CdiA^{EC93}$, $CdiA^{EC536}$, and $CdiA^{STECO31}$, respectively. (Aoki et al., 2008; Beck et al., 2016; Ruhe et al., 2017, 2013b). One of the best studied examples is the BamA receptor, which is highly conserved among γ-proteobacteria (Ruhe et al., 2013b). Despite conservation, it was observed that *E. coli* EC93 targets only other *E. coli* strains, but not related species. A subsequent analysis has found that $CdiA^{EC93}$ binds highly variable extracellular loops 4, 6, and 7, thereby restricting CDI-mediated activity to a narrow target range (Ruhe et al., 2013b). This highly specific targeting was also confirmed for the remaining receptors (Beck *et al.*, 2016; Ruhe *et al.*, 2017). Once inside the periplasm, $CdiA\text{-}CT^{EC93}$ integrates into the inner membrane and via the pore formation activity causes dissipation of proton gradient, leading to decreased ATP and respiration (Hayes *et al.*, 2014). Other CdiA-CT proteins can translocate into the cytoplasm of a target cell, where they execute their activity. For the translocation, the N-terminal domain of CdiA-CT and proton motive force are required. It was observed that N-terminal domains recognize and target different membrane proteins, which usually are metabolite transporters (Willett *et al.*, 2015b, 2015a).

Although the translocation mechanism is currently unknown, it has been suggested that instead of exploiting transport mechanism of transporters, toxins use receptors to bring toxin domains together. This clustering allows the integration into the inner-membrane, and, subsequently, proton-motive force facilitated transport into the cytosol (Willett *et al.*, 2015a).

1.5.3.1.3. CdiA functional activities

Based on the functional activity, CdiA-CT domains can be separated into several groups: toxins with pore-forming activity; nuclease activity,

deaminase activity, and peptidase activity. However, the functions of the majority of CdiA-CTs are unknown (Willett *et al.*, 2015b). There also have been suggestions, that predictions regarding the functional activity of CdiA-CTs can be unreliable due to the high variability of these domains (Beck *et al.*, 2014).

It is worth noting the multiple observations of CDI-mediated roles beyond bacterial competition. These include biofilm formation and virulence (Allen *et al.*, 2020; Garcia *et al.*, 2013; Ruhe *et al.*, 2015). Recently, it was shown that *Burkholderia thailandensis* CDI effectors are required for biofilm formation (Garcia *et al.*, 2013). Subsequent work has found that *B. thailandensis* cells in a population can sense and respond to each other via a CDI system. Specifically, the delivery of CdiA-CT into immune bacteria resulted in gene expression and phenotypic changes such as biofilm formation, pigment production, and cell aggregation (Garcia *et al.*, 2016).

CdiA-mediated virulence was also reported. The majority of microorganisms that use contact-dependent growth inhibition for virulence include bacterial phytopathogens (Guérin *et al.*, 2017). CDI contribution to virulence in eukaryotic models was observed in a few studies such as CdiA-mediated survival and escape of *Neisseria meningitidis* from the intracellular vacuoles of HeLa cells (Talà *et al.*, 2008). Interesting results were obtained recently, indicating that CDI systems in virulent *Pseudomonas aeruginosa* isolates directly influence virulence in mouse infection models (Allen *et al.*, 2020).

It has been determined that *Acinetobacter* sp. harbour up to two functional CDI systems. These can be divided into two classes based on the size – type I and type II (De Gregorio *et al.*, 2019). Interestingly, while many CDI systems in other bacteria were determined to contribute to biofilm formation, they do not seem to be required for this phenotype in *Acinetobacter* sp., and therefore, it has been proposed that their main role is competition with neighbouring bacteria (De Gregorio *et al.*, 2018; Harding *et al.*, 2017; Roussin *et al.*, 2019). Some researchers even found that expression of at least one *A. baumannii* CDI system decrease biofilm formation and adhesion to epithelial cells (Roussin *et al.*, 2019).

1.5.4. T6SS

Type VI secretion systems are encoded in the genomes of a quarter of all proteobacteria, and used mainly as a killing mechanism for competing bacteria (Coulthurst, 2019). These large complexes, structurally homologous to T4 bacteriophage injectosome, are composed of at least 13 proteins and

span both membranes (Fig. 1.18) (Pukatzki *et al.*, 2009). Based on structural similarities, these systems are split into six types. However, the general mechanism of action is similar – the assembled apparatus uses contractile ejection machinery to deliver effectors straight into target cell (Fig. 1.18). The expression of immunity proteins prevents from self-inhibition by the cognate effectors (Coulthurst, 2019).

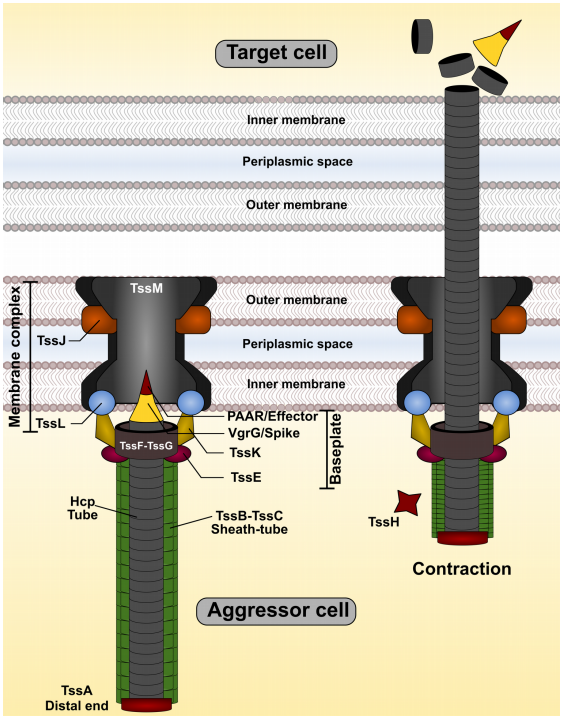

Fig. 1.18. Graphical schematic of structural organization and proposed mechanism of action of a Type VI secretion system. The left and right parts of the image show assembled/extended and contracted states of the system, respectively. The scheme is based on the proposition by Pukatzki *et al.* (2009) and Ho *et al.* (2014).

The structure of the whole apparatus can be split into four parts (Fig. 1.18): membrane complex, cytoplasmic baseplate, cytoplasmic contractile sheath, and puncturing device. Firstly, the membrane complex composed of TssJLM proteins, is assembled. This structure then connects with the baseplate from the cytoplasmic side, that is composed of TssEFGK. The baseplate also contains central VgrG trimer with a PAAR-repeat protein tip, which places themselves on the top of VgrG proteins and mediates cell puncturing (in some cases, VgrG proteins contain additional domains encoding effector functions). Then, Hcp proteins start to polymerise from the VgrG protein base, forming a hollow tube, made up of hexameric Hcp rings, which along with VgrG and PAAR-repeat proteins form a puncturing device. At the same time, the TssBC sheath proteins polymerise around the Hcp tube. This structure is capped by TssA and acts as a contraction machinery that pushes the assembled puncturing device out of the cell (Coulthurst, 2019). The presence of Hcp and VgrG in the growth media is a reliable indicator of a fuctional T6SS (Pukatzki *et al.*, 2009). After

the contraction, ATPase TssH depolymerises sheath structure, which can readily re-polymerase and contract again.

Fully assembled T6SS can extend across the diameter of the cell. It was suggested that after contraction, the puncturing device can extend up to 500 nm outside the cell (Ho *et al.*, 2014) (Fig. 1.19). Interestingly, due to the extension across the whole cell, T6SS can fire in both sides. In this case, TssA protein acts both as a cap for the distal end and, along with additional proteins, might form alternative baseplate at the proximal end (Szwedziak and Pilhofer, 2019). It has been calculated that T6SS sheath assembly takes 20–30 s, contraction – less than 5 ms, and disassembly – several tens of seconds. Also, a single contraction release energy equivalent to hydrolysis of 1600 molecules of ATP and allows the puncturing device to reach the speed of ~100 μm/s, meaning that T6SS can effectively puncture a target cell membrane (Basler, 2015).

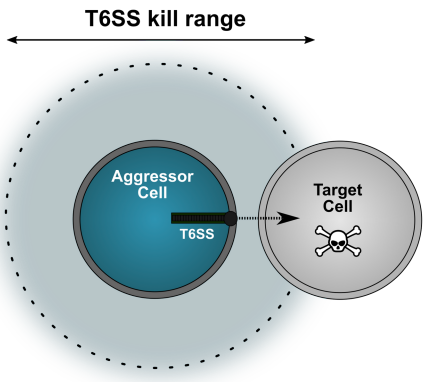

Fig. 1.19. Proposed spatial geometry of Type VI secretion system (T6SS) attack range (area marked as a ticked circle). The figure was adapted from Basler (2015).

A recent in depth bioinformatic analysis of *Acinetobacter* sp. T6SS secretion systems has identified at least two clusters that display differences in the organisation of T6SS encoding loci. The majority of bacteria including pathogenic *Acinetobacter* species contain T6SS type I cluster, which is unique in terms that no *vgrG* genes are encoded within it, in contrast to the observations made in other bacteria (Repizo *et al.*, 2019). Another analysis have predicted that around half of all *A. baumannii* strains encode functional T6SS loci with two or three effectors per genome. Interestingly, the analysis have found at least 30 distinct effector families with approximately half of them performing an unknown function (Lewis *et al.*, 2019). It has been previously observed that there is a great heterogeneity among clinical *A. baumannii* strains in their ability to display an active T6SS system and pathogenesis phenotype (Repizo *et al.*, 2019; Weber *et al.*, 2015b, 2013). These results, along with the bioinformatic data showing that *A. baumannii* genomes do not encode effectors with a known anti-eukaryotic function (Lewis *et al.*, 2019), indicate that the pathogen might use T6SS mainly for antibacterial purposes.

2. MATERIALS AND METHODS

2.1. Materials

In this work, strains from the previously characterized collection of clinical *A. baumannii* isolates were used (Povilonis *et al.*, 2013). The isolates were collected in the period from July 2010 to November 2011 in: Lithuanian University of Health Sciences Kauno Klinikos Hospital, Vilnius University Emergency Hospital, Republican Šiauliai County Hospital. Identification of *A. baumannii* strains was performed in the respective hospital laboratories, using an automated microbiology system Phoenix TM (BD). Additionally, isolates were confirmed using *A. baumannii*-specific identification primers (Chen *et al.*, 2007). *A. baumannii* strains used in this work and their characteristics are listed in Table 2.1. Other bacterial strains and plasmids are listed in Tables 2.2 and 2.3, respectively. Oligonucleotide primers were obtained from Metabion or Thermo Fisher Scientific and are listed in Table 2.4.

Microbial growth media used in the work (g/L volume):

- LB (Lysogeny Broth) – 10 g tryptone, 5 g yeast extract, 5 g NaCl, 15 g agar (omited for liquid media).
- TSB (Tryptic Soy Broth) – 17 g Pancreatic digest of casein, 3 g Enzymatic digest of soya bean, 5 g NaCl, 2.5 g K_2HPO_4, 2.5 g glucose, 15 g agar (omited for liquid media). The dehydrated culture media was obtained from Oxoid.

Table 2.1. Origin of *A. baumannii* clinical isolates used in this work. The list of representative clones was compiled by Skerniškytė *et al.*, (2019c).

Isolate	Place of origin[a]	Ward/unit	Clinical specimen	Date of isolation
Isolates selected for genetic manipulations				
AbV15	A	Toxicology	n.d.	n.d.
II-a	A	Gastroenterology	Sputum	2010-08-02
II-a1	B	Intensive care	Sputum	n.d.
II-c	A	Intensive care	Bronchi	2010-10-07
Remaining representative isolates				
I-a	A	Heart surgery	n.d.	2010-10-05
I-aC	C	Trauma center	Joint	n.d.
I-b	A	Head injury	Blood	2010-07-03
I-c	A	Burn	Wound	2010-10-06
I-d	A	Trauma center	Joint	2010-07-13
I-dB	B	Intensive care	Sputum	n.d.
I-e	A	Intensive care	Bronchi	2010-10-11
I-f	A	Intensive care	Bronchi	2010-07-16
I-g	A	Intensive care	Bronchi	2010-07-13
I-gB	B	Intensive care	Wound	n.d.
I-h	A	Neurosurgery	n.d.	2010-06-22
I-i	A	Intensive care	Bronchi	2010-10-28
I-j	A	Urology	Urine	2010-10-28
I-k	A	Burn	Wound	2010-10-12

I-m	A	Intensive care	Bronchi	2010-07-02
I-n	A	Intensive care	n.d.	2010-06-29
I-o	A	Intensive care	n.d.	2010-06-29
I-p	B	Nefrology	n.d.	2010-11-10
I-u1	B	Intensive care	n.d.	n.d.
I-v	A	Intensive care	n.d.	n.d.
II-a1C	C	n.d.	n.d.	n.d.
II-a2	B	Neurosurgery	n.d.	n.d.
II-a3	C	n.d.	Intubation tube	n.d.
II-b	A	Head injury	n.d.	2010-06-29
II-d	A	Neurosurgery	Bronchi	n.d.
II-dB	B	Intensive care	n.d.	n.d.
II-e	A	Intensive care	Bronchi	n.d.
II-e	A	Neurosurgery	Trachea	2010-10-13
II-f	A	Intensive care	Bronchi	2010-10-14
II-g	A	Neurosurgery	n.d.	2010-11-09
II-h	A	n.d.	n.d.	2010-11-09
II-j2	A	Head injury	Blood	n.d.
II-j4	A	Child intensive care	Trachea	n.d.

[a] – (A) Lithuanian University of Health Sciences Kauno Klinikos Hospital; (B) Vilnius University Emergency Hospital; (C) Republican Šiauliai County Hospital. Roman numerals (I or II) indicate clonal lineage; letters indicate pulso-type as determined by Povilonis *et al.* (2013).

Table 2.2. Bacterial strains used in the study.

Bacterial strain	Description and/or genotype	Reference
Escherichia coli JM107	*endA1*, *glnV44*, *thi*$^-$, *relA1*, *gyrA96*, *Δ(lac-proAB)* [F', *traD36*, *proAB*$^+$, *lacI*^{q}*ZΔM15*], *hsdR17*(R_K^- m_K^+), λ^-	Yanisch-Perron *et al.* (1985)
Escherichia coli DH5α	*F-, Δ(argF-lac)169, φ80dlacZ58(M15), ΔphoA8, glnX44(AS), λ-, deoR481, rfbC1, gyrA96(NalR), recA1, endA1, thiE1, hsdR17*	Woodcock *et al.* (1989)
Escherichia coli MC4100	F-, [*araD139*]$_{B/r}$, *Δ(argF-lac)169*, *λ-*, *e14-*, *flhD5301*, *Δ(fruK-yeiR)725(fruA25)*, *relA1*, *rpsL150(strR)*, *rbsR22*, *Δ(fimB-fimE)632(::IS1)*, *deoC1*	Casadaban and Cohen (1979)
Escherichia coli BL21(DE3)	F-, *lon-11*, *Δ(ompT-nfrA)885*, *Δ(galM-ybhJ)884*, *λDE3 [lacI, lacUV5-T7 gene 1, ind1, sam7, nin5]*, *Δ46*, *[mal*$^+$*]*$_{K-12}$(λ^S), *hsdS10*	Wood (1966)
Bacillus subtilis	Wild-type. Used for the amplification of the *sacB* gene	Gift from Audrius Gegeckas
Acinetobacter baylyi ADP1	Wild-type.	ATCC 33305
A. baylyi ADP1 *pcdiI*	*A. baylyi* ADP1 strain complemented with pUC_AcORI_*Ptac_cdiI*_TER_*lacI*^{q}*2*_gm	This work
*Ab*V15 *ΔbfmRS*	*Ab*V15 derivative with the *bfmRS* operon deletion	This work
*Ab*V15 *ΔbfmR*	*Ab*V15 derivative with the in-frame *bfmS* deletion	This work
*Ab*V15 *ΔbfmS*	*Ab*V15 derivative with the in-frame *bfmR* deletion	This work
*Ab*V15 *ΔbfmRS pbfmRS*	*Ab*V15 *ΔbfmRS* complemented with pUC_AcORI_*Ptac_bfmRS*_TER_*lacI*^{q}*2*	This work
*Ab*V15 *ΔbfmRS pbfmR*	*Ab*V15 *ΔbfmRS* complemented with pUC_AcORI_*Ptac_bfmR*_TER_*lacI*^{q}*2*	This work
*Ab*V15 *ΔbfmRS pbfmS*	*Ab*V15 *ΔbfmRS* complemented with pUC_AcORI_*Ptac_bfmS*_TER_*lacI*^{q}*2*	This work
*Ab*V15 *ΔbfmS pbfmS*	*Ab*V15 *ΔbfmS* complemented with pUC_AcORI_*Ptac_bfmS*_TER_*lacI*^{q}*2*	This work
*Ab*V15 *Δhcp*	*Ab*V15 derivative with the *hcp* gene deletion	This work
*Ab*V15 *Δhcp phcp*	*Ab*V15 *Δhcp* complemented with pUC_AcORI_*Ptac_hcp*_TER_*lacI*^{q}*2*	This work
*Ab*V15 *ΔbfmRSΔhcp*	*Ab*V15 *ΔbfmRS* derivative with the *hcp* gene deletion	This work
*Ab*V15 *ΔbfmRSΔhcp pbfmRS*	*Ab*V15 *ΔbfmRSΔhcp* complemented with pUC_AcORI_*Ptac_bfmRS*_TER_*lacI*^{q}*2*	This work
*Ab*V15 *ΔbfmRSΔhcp pbfmR*	*Ab*V15 *ΔbfmRSΔhcp* complemented with pUC_AcORI_*Ptac_bfmR*_TER_*lacI*^{q}*2*	This work
*Ab*V15 *ΔbfmRSΔhcp phcp*	*Ab*V15 *ΔbfmRSΔhcp* complemented with pUC_AcORI_*Ptac_hcp*_TER_*lacI*^{q}*2*	This work
*Ab*V15 *Δcdi*	*Ab*V15 derivative with a partial *cdiBAI* operon deletion	This work
*Ab*V15 *ΔbfmRSΔcdi*	*Ab*V15 *ΔbfmRS* derivative with a partial *cdiBAI* operon deletion	This work
*Ab*V15 *ΔbfmRSΔhcpΔcdi*	*Ab*V15 *ΔbfmRSΔhcp* derivative with a partial *cdiBAI* operon deletion	This work
*Ab*V15 *ΔbfmRSΔcdi pbfmRS*	*Ab*V15 *ΔbfmRSΔcdi* complemented with pUC_AcORI_*Ptac_bfmRS*_TER_*lacI*^{q}*2*	This work
*Ab*V15 *ΔbfmRSΔcdi pbfmR*	*Ab*V15 *ΔbfmRSΔcdi* complemented with	This work

	pUC_AcORI_*Ptac_bfmR*_TER_*lacI^{q}2*	
*Ab*V15 *ΔbfmRSΔhcpΔcdi pbfmRS*	*Ab*V15 *ΔbfmRSΔhcpΔcdi* complemented with pUC_AcORI_*Ptac_bfmRS*_TER_*lacI^{q}2*	This work
*Ab*V15 *ΔbfmRSΔhcpΔcdi pbfmR*	*Ab*V15 *ΔbfmRSΔhcpΔcdi* complemented with pUC_AcORI_*Ptac_bfmR*_TER_*lacI^{q}2*	This work
II-a1 *ΔgalU*	II-a1with the *galU* gene deletion	This work
II-a *ΔgalU*	II-a with the *galU* gene deletion	This work
II-c *ΔgalU*	II-c with the *galU* gene deletion	This work
II-a1 *ΔgalU* p*galU*	II-a1*ΔgalU* complemented with pUC_AcORI_*Ptac_galU*$^{II\text{-}a1}$_TER_*lacI^{q}2*_gm	This work
II-a *ΔgalU* p*galU*	II-a *ΔgalU* complemented with pUC_AcORI_*Ptac_galU*$^{II\text{-}a}$_TER_*lacI^{q}2*_gm	This work
II-c *ΔgalU* p*galU*	II-c *ΔgalU* complemented with pUC_AcORI_*Ptac_galU*$^{II\text{-}c}$_TER_*lacI^{q}2*_gm	This work
II-a1 *ΔgalU* p*cdiI*	II-a1 *ΔgalU* complemented with pUC_AcORI_*Ptac_cdiI^{AbV15}*_TER_*lacI^{q}2*_gm	This work
II-a *ΔgalU* p*cdiI*	II-a *ΔgalU* complemented with pUC_AcORI_*Ptac_cdiI^{AbV15}*_TER_*lacI^{q}2*_gm	This work
II-c *ΔgalU* p*cdiI*	II-c *ΔgalU* complemented with pUC_AcORI_*Ptac_cdiI^{AbV15}* _TER_*lacI^{q}2*_gm	This work
II-a1 *ΔbfmRS*	II-a1 with the *bfmRS* operon deletion	This work
II-a *ΔbfmRS*	II-a with the *bfmRS* operon deletion	This work
II-c *ΔbfmRS*	II-c with the *bfmRS* operon deletion	This work
II-a1 *ΔbfmRS* p*bfmRS*	II-a1 *ΔbfmRS* complemented with pUC_AcORI_*Ptac_bfmRS*$^{Ab\text{V}15}$_TER_*lacI^{q}2*_gm	This work
II-a *ΔbfmRS* p*bfmRS*	II-a *ΔbfmRS* complemented with pUC_AcORI_*Ptac_bfmRS*$^{Ab\text{V}15}$_TER_*lacI^{q}2*_gm	This work
II-c *ΔbfmRS* p*bfmRS*	II-c *ΔbfmRS*complemented with pUC_AcORI_*Ptac_bfmRS*$^{Ab\text{V}15}$_TER_*lacI^{q}2*_gm	This work
II-a1 *ΔbfmRS* p*cdiI*	II-a1 *ΔbfmRS* complemented with pUC_AcORI_*Ptac_cdiI*$^{Ab\text{V}15}$ _TER_*lacI^{q}2*_gm	This work
II-a *ΔbfmRS* p*cdiI*	II-a *ΔbfmRS* complemented with pUC_AcORI_*Ptac_cdiI*$^{Ab\text{V}15}$ _TER_*lacI^{q}2*_gm	This work
II-c *ΔbfmRS* p*cdiI*	II-c *ΔbfmRS* complemented with pUC_AcORI_*Ptac_cdiI*$^{Ab\text{V}15}$ _TER_*lacI^{q}2*_gm	This work
Pseudomonas aeruginosa P16	Clinical isolate	Krasauskas *et al.*, (2015)
Klebsiella pneumoniae K39	Clinical isolate	Seputiene *et al.*, (2010)

Table 2.3. Plasmids used in the study.

Plasmids	Description and/or genotype	Reference
pUC19	Used as the scaffold for the construction of suicide plasmid pUC19_*sacB*; Amp^R	Norrander *et al.* (1983)
pWH1266	*Acinetobacter calcoaceticus* plasmid fragment containing *ori* cloned to pBR322	Hunger *et al.* (1990)
pAcGFP1-C3	Used as the source for *gfp* gene; Kan^R	Clonetech laboratories Inc
pKK223-3	Used as the source for *Ptac* promoter and termination sites; Amp^R	Cloning Vector from PL-Pharmacia, GenBank:M77749.1
pUC19_*sacB*	*A. baumannii* suicide vector containing *sacB* gene from *Bacillus* spp. cloned via *Xba*I and *Pae*I; Amp^R	This work
pUC19_*sacB_bfmRS*UPDwn_gmR	pUC19_*sacB* derivative with *ΔbfmRS*::*aac3I*; Amp^R; Gm^R	This work
pUC19_*sacB_hcp*UPDwn_gmR	pUC19_*sacB* derivative with *Δhcp*::*aac3I*; Amp^R; Gm^R	This work
pUC19_*sacB_cdi*UPDwn_gmR	pUC19_*sacB* derivative with *ΔcdiAI*::*aac3I*; Amp^R; Gm^R	This work
pUC19_*sacB_galU*$^{II\text{-}a1}$UPDwn_gmR	pUC19_*sacB* derivative with *ΔgalU*$^{II\text{-}a1}$::aac3I; Amp^R; Gm^R	This work
pUC19_*sacB_galU*$^{II\text{-}a}$UPDwn_gmR	pUC19_*sacB* derivative with *ΔgalU*$^{II\text{-}a}$::aac3I; Amp^R; Gm^R	This work
pUC19_*sacB_galU*$^{II\text{-}c}$UPDwn_gmR	pUC19_*sacB* derivative with *ΔgalU*$^{II\text{-}c}$::aac3I; Amp^R; Gm^R	This work
pUC19_*sacB_bfmRS*$^{II\text{-}a1}$UPDwn_gmR	pUC19_*sacB* derivative with *ΔbfmRS*$^{II\text{-}a1}$::aac3I; Amp^R; Gm^R	This work
pUC19_*sacB_bfmRS*$^{II\text{-}a}$UPDwn_gmR	pUC19_*sacB* derivative with *ΔbfmRS*$^{II\text{-}a}$::aac3I; Amp^R; Gm^R	This work
pUC19_*sacB_bfmRS*$^{II\text{-}c}$	pUC19_*sacB* derivative with *ΔbfmRS*$^{II\text{-}c}$::aac3I; Amp^R;	This work

[c]UPDwn_gmR	Gm^R	
pUC_gm	pUC19 derivative with the *aac3I* gene; Amp^R; Gm^R	Laboratory collection
pUC_gm_AcORI	pUC19_gm derivative with the *Acinetobacter sp. ori*; Amp^R; Gm^R	Laboratory collection
pUC_gm_AcORI_*gfp*	pUC_gm_AcORI derivative with the *gfp* gene from pAcGFP1-C3 cloned downstream to *Acinetobacter sp. ori*; Amp^R, Gm^R	Laboratory collection
pUC_gm_AcORI_*Ptac_gfp*	pUC_gm_AcORI_*gfp* derivative with the *Ptac* promoter from pKK223-3 cloned downstream to *Acinetobacter sp.* ori; Amp^R; Gm^R	Laboratory collection
pUC_gm_AcORI_*Ptac_gfp_TER*	pUC_gm_AcORI_*Ptac_gfp* derivative with the terminator (TER) sequence from pKK223-3 cloned downstream to *gfp* gene; Amp^R; Gm^R	This work
pUC_AcORI_*Ptac_gfp*_TER_*lacI^{q}2*	pUC_gm_AcORI_*Ptac_gfp_TER* derivative with the *lacI^q* gene cloned downstream to terminator sequence, replacing *aac3I*; Amp^R	This work
pUC_AcORI_*Ptac_gfp*_TER_lacIq2_gm	pUC_AcORI_Ptac_*gfp*_TER_lacIq2 derivative, where the *bla* gene is replaced with the *aac3I* gene; Gm^R	This work
pUC_AcORI_*Ptac*_TER_*lacI^{q}2*	pUC_AcORI_*Ptac_gfp*_TER_*lacI^{q}2* derivative where the *gfp* gene is removed; Amp^R	This work
pUC_AcORI_*Ptac_bfmRS*_TER_*lacI^{q}2*	pUC_AcORI_*Ptac_gfp*_TER_*lacI^{q}2* derivative where the *gfp* gene is replaced with the *bfmRS* operon; Amp^R	This work
pUC_AcORI_*Ptac_bfmR*_TER_*lacI^{q}2*	pUC_AcORI_*Ptac_gfp*_TER_*lacI^{q}2* derivative where the *gfp* gene is replaced with the wild-type *bfmR* allele; Amp^R	This work
pUC_AcORI_*Ptac_bfmRS*_TER_*lacI^{q}2*	pUC_AcORI_*Ptac_gfp*_TER_*lacI^{q}2* derivative where the *gfp* gene is replaced with the wild-type *bfmRS* operon; Amp^R	This work
pUC_AcORI_*Ptac_bfmS*_TER_*lacI^{q}2*	pUC_AcORI_*Ptac_gfp*_TER_*lacI^{q}2* derivative where the *gfp* gene is replaced with the wild-type *bfmS* allele; Amp^R	This work
pUC_AcORI_*Ptac_hcp*_TER_*lacI^{q}2*	pUC_AcORI_*Ptac_gfp*_TER_*lacI^{q}2* derivative where the *gfp* gene is replaced with the *hcp* gene; Amp^R	This work
pUC_AcORI_*Ptac_cdiI*_TER_*lacI^{q}2*	pUC_AcORI_*Ptac_gfp*_TER_*lacI^{q}2* derivative where the *gfp* gene is replaced with the *cdiI* gene; Amp^R	This work
pUC_AcORI_*Ptac_cdiI*_TER_*lacI^{q}2*_gm	pUC_AcORI_*Ptac_imm^{V15}*_TER_*lacI^{q}2* derivative where the *bla* gene is replaced with the *aac3I* gene*;* Gm^R	This work
pUC_AcORI_*Ptac_galU*$^{fl\text{-}a1}$_TER_*lacI^{q}2*_gm	pUC_AcORI_*Ptac_gfp*_TER_*lacI^{q}2*_gm derivative, where the *gfp* gene is replaced with the wild-type *galU* gene from II-a1;Gm^R	This work
pUC_AcORI_*Ptac_galU*$^{fl\text{-}a}$_TER_*lacI^{q}2*_gm	pUC_AcORI_*Ptac_gfp*_TER_*lacI^{q}2*_gm derivative, where the *gfp* gene is replaced with the wild-type *galU* gene from II-a; Gm^R	This work
pUC_AcORI_Ptac_*galU*$^{fl\text{-}c}$_TER_*lacI^{q}2*_gm	pUC_AcORI_*Ptac_gfp*_TER_*lacI^{q}2*_gm derivative, where the *gfp* gene is replaced with the wild-type *galU* gene from II-c; Gm^R	This work
pUC_AcORI_Ptac_*bfmRS*^{4bV15}_TER_*lacI^{q}2*_gm	pUC_AcORI_*Ptac_bfmRS^{V15}*_TER_*lacI^{q}2* derivative, where the *bla* gene is replaced with the *aac3I* gene; Gm^R	This work

Amp^R – resistance to ampicillin; Gm^R – resistance to gentamicin

Table 2.4. Oligonucleotides used in the study

Oligonucleotide	Oligonucleotide sequence (5'→3')	Purpose	Reference
P-Ab-ITSF P-Ab-ITSB	CATTATCACGGTAATTAGTG AGAGCACTGTGCACTTAAG	*A. baumannii* specific identification primers	Chen *et al.* (2007)
sacB_F sacB_R	GTTGTCTAGAGATCCTTTTTAACCCATCAC GTTGGCATGCTGGGATTCACCTTTATGTTG	Amplification of the *sacB* gene	This work
BfmR_Ptac_F BfmR_Ptac_R	CATGAGCCAAGAAGAAAAGTTACC TTACAATCCATTGGTTTCTTTAAC	Amplification of the *bfmRS* operon and wild-type *bfmR*; cloning into inducible vector	This work
BfmS_Ptac_R	GAACCTGATGCAACTCAG	Amplification of the *bfmS* gene or the *bfmRS* operon; cloning into inducible vector	This work
BfmS_Ptac_F	CGTGTTTAAACACAGTATATTCCTGC	Amplification of the *bfmS* gene and cloning into inducible vector	This work
hcp_compl_F hcp_compl_R	CATGAAAGATATATACGTTGAGTTTCGC CTTTATGTCAGCCTCCACCAA	Amplification of the *hcp* gene and cloning into inducible vector	This work

BfmR_F	GTTGAAGCTTAAATGCAGCAACATCTCC	Verification of the *bfmRS* operon deletion	Tomaras *et al.* (2008)
ter_F ter_R	GGGCCATGGGCATGCGGTACCCTGTTTTGGC GGATGAGAG GTTGGAGCTCTTTGTAGAAACGCAAAAAGG C	Amplification of the transcription termination site	This work
M13_rwd Aac3I_seqR	ACTGGCCGTCGTTTTAC CGAAGTCGAGGCATTTCTGT	Inverted amplification of the plasmid pUC_gm_AcORI_Ptac_AcG FP_TER to remove Gm^R	This work
LacIq2_R LacIq2_F	CTCACTGCCCGCTTTCCA ATCGAATGGTGCAAAAC	Amplification of the *lacI*^{q} gene	This work
BfmR01F BfmRS01R	TCACGCATTGCACCATAA GGAACCTGATGCAACTCAGTTATAAATCATTG CCCCTATAAATCTC	Amplification of the *bfmRS* operon upstream region	This work
BfmS02F BfmS02Rgm	TTATAACTGAGTTGCATCAGG CGTTCAAGCCGAGATGAATTCGATCGGCCGA ATTTGGTTATTG	Amplification of the *bfmRS* operon downstream region	This work
5_hcpFwd 5_hcpRev	TCAGGAAACGCCTTCAAATC CTTTATGTCAGCCTCCACCAAGCTGACCTTG ATTAATTTGAGG	Amplification of the *hcp* gene upstream region	This work
3_hcpFwd 3_hcpRev	TTGGTGGAGGCTGACATAAAG CGTTCAAGCCGAGATGAATTCGATCGCTCAA ATTCGGATACATGCTG	Amplification of the *hcp* gene downstream region	This work
GentR_F GentR_R	GATCGAGCTCAGGACAGAAATGCCTCGACT GATCGAATTCATCTCGGCTTGAACGAATTG	Amplification of the *aac3I* gene	This work
Bfm_check_F Bfm_check_R	CAACACCCTGAGATTTACCG CAGCAACTTTTGTGCCTATG	Verification of the *bfmRS* operon deletion	This work
hcp_checkF hcp_checkR	GTCAACTTGGCGTGGTCTTT TGGGGTTCAGCATATTTTTCA	Verification of the *hcp* gene deletion	This work
Hcp_seq_chk	TGCTTCTGCTGGAAATGTTG	Verification of the *hcp* gene deletion	This work
rpoB_qF rpoB_qR	CGATTCGTACAGAACATTCTT TAAAGCAGCATTGCCAGAATA	qPCR house-keeping gene primer	This work
T6hcF T6hcR	ACTTCAAGTAGTGTGGGCGG AAGTCCACTCAACAGCAGCA	qPCR primer for quantification of the *hcp* gene expression	This work
TssMF TssMR	TGCTTTGGCGCAGTAAGACA CTTGCTGTGCGGATACAACG	qPCR primer for quantification of the *tssM* gene expression	This work
CDI_5Fwd_XH858 CDI1R CDIF CDI_3Rev_XH858 CDI_seq_2_F CDI_seq_2_R CDI_compl_F CDI_seq4_F CDI_seq4_R CDI_seq5_R CDI_seq_7F CDI_seq_7R	TTGTCGGTACGACTGCTGCT TGCTGTCAGGTGCAATCAGC GGTAAATGGCCGCAATAGCATAC TGGCCGTGGAGCTTTTAACT GGGGCGAATAATGTCAGTGC CTCAACACGGCAAGCAGATA CATGTTAACTAAGAACTTTATAACTTCTTC AATATCAATCTTGGGGAAGGTC TCACTGGCATAGATTTGACTC CTTAAGCCAATATTCTGAGCA TTCAAGTGGTGGTTTAGTGCTC CAGAAGGATTAGGACCATCACC	Sequencing of the *cdiBAI* operon from *A. baumannii* V15	This work
CDI_5Fwd_final_short CDI_5Rev_final_short	GCTGATTGCACCTGACAGCA TAAACGACCTGTAATAGACCGCACTGACATT ATTCGCCCC	Amplification of the *cdiBAI* operon upstream region; sequencing of the *cdiBAI* locus from *A. baumannii* V15	This work
CDI_3Fwd_final CDI_3Rev_final_gm	GGTCTATTACAGGTCGTTTACTTTAAATAG CGTTCAAGCCGAGATGAATTCGATCACCCCA AATCTTACTCCAATCG	Amplification of the *cdiBAI* operon downstream region	This work
Cdi_Imm_F Cdi_Imm_R	TTAAAGTAAACGACCTGTAATAGACC CATGATCGATTTTGTTAAAGAATTATCTGC	Amplification of the *cdiI* gene; cloning into inducible vector; check for the presence of the gene in a genome.	This work
CDI1F CDI1R	GGTAAATGGCCGCAATAGCATAC TGCTGTCAGGTGCAATCAGC	Detection of the type I CDI systems among *A. baumannii*; quantification of the *cdiBAI* operon expression	This work
CDI2F CDI2R	TTTATGCTTCGGGCAATCTGG GCACACCAAGTCGCAAAGAA	Detection of the type I CDI systems among *A. baumannii*	This work
F_CDI_cluster3_4	CGGAGAGGTTGGTGGAAAAACTGC	Detection of the type II CDI	This work

R_CDI_cluster3_4	CAAAGGCGCACCCACAAAAGC	system among *A. baumannii*	
galu_Up_F galu_Up_R	GTCCGTAAAAATTTAGGTTC CAAATAGTTAAGCAGAGCTACGTAGAACTGC TTTTTTAATCAT	Amplification of the *galU* gene upstream region	This work
galu_Dwn_F galu_Dwn_R_gmR	GTAGCTCTGCTTAACTATTTG CGTTCAAGCCGAGATGAATTCGATCCGGAAT AAAATTTCTTTTTGTTG	Amplification of the *galU* gene downstream region	This work
galu_check galu_check2	CTGCTTCCATGCCGTAACTA TTGTTTCCATGCGGTTACTA	Verification of the *galU* gene deletion	This work
galU_compl_F galU_compl_R	CATGATTAAAAAGGCAGTTTTACCT CAAATACTTAAGCAGAGCTAC	Amplification of the *galU* gene; cloning the gene into inducible vector	This work

2.2. Methods

2.2.1. Bacterial growth conditions

All bacteria were grown aerobically at 37°C or 30°C. Growth media were supplemented with antibiotics where appropriate: ampicillin 100 μg/mL, gentamicin 10 μg/mL, ceftazidime 10 μg/mL. *A. baumannii*, *P. aeruginosa*, *K. pneumoniae*, are second level biosafety agents and were handled in a laboratory with a laminar flow hood. Workplace was disinfected with either UV irradiation or cleaning with 70% ethanol. All waste or contaminated accessories were neutralised by autoclaving where appropriate.

2.2.2. Bacterial DNA extraction

Bacterial genomic and plasmid DNA was extracted using GeneJET Genomic DNA Purification and GeneJET Plasmid Miniprep kits (Thermo Fisher Scientific), respectively. The DNA from electrophoresis gels was purified using GeneJET Gel Extraction Kit (Thermo Fisher Scientific). The concentration and purity of the extracted DNA was evaluated using a NanoDrop spectrophotometer (Thermo Fisher Scientific).

2.2.3. PCR

The amplicons for cloning and/or sequencing were generated using Phusion polymerase (Thermo Fisher Scientific). For routine PCR reactions DreamTaq polymerase was used (Thermo Fisher Scientific). Oligonucleotides used in the work are listed in Table 2.4. Annealing temperatures for oligonucleotides were calculated using Thermo Fisher Scientific online T_m calculator.

2.2.4. Plasmid construction

Plasmids and oligonucleotides used in the work are listed in Tables 2.3 and 2.4, respectively. All resulting final constructs were verified by sequencing at BaseClear.

***A. baumannii*/*E. coli* shuttle expression plasmid construction.**

pUC_gm_AcORI plasmid containing *Acinetobacter* sp. origin of replication (*ori*) from pWH1266 and the *aac3I* gentamicin resistance cassette (Armalytė *et al.*, 2018) was used as a scaffold for the construction of expression plasmid. The plasmid pKK223-3 was used as a source for P*tac* promoter and terminator sites (TER). The *gfp* gene was obtained from the plasmid pAcGFP1-C3. BL21(DE3) strain genomic DNA was used as a source for the amplification of the *lacI*^{q} gene, encoding the Lac repressor. The *A. baumannii*/*E. coli* shuttle expression plasmid was obtained by cloning the *gfp* gene, P*tac* promoter, TER sites into the plasmid pUC_gm_AcORI to obtain the plasmid pUC_gm_AcORI_*Ptac_gfp*_TER. Then, this plasmid was inverse amplified with the primer pair M13_rwd/Aac3I_seqR to remove the *aac3I* gene, and blunt ligated with the *lacI*^{q} gene to generate a final *A. baumannii*/*E. coli* shuttle expression plasmid pUC_AcORI_*Ptac_gfp*_TER_*lacI*^{q}*2* (Fig. 2.1). The alternative shuttle plasmid, containing the *aac3I* gentamicin resistance cassette was generated by removing the *bla* ampicillin resistance gene with *Eam*1105I restriction endonuclease, followed by blunt ligation of the *aac3I* gene, which was amplified from the plasmid pUC_gm_AcORI. Control plasmids were obtained by removing the *gfp* gene from each shuttle plasmid by digestion with *Pae*I and *Kpn*I, and blunt ligating the remaining fragments (Fig. 2.1). Control plasmids in figures and throughout the text are denoted as "p", where relevant.

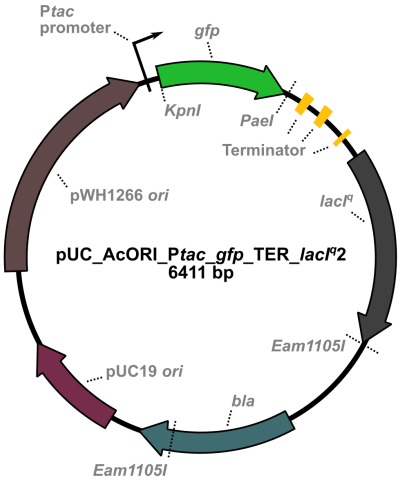

Fig. 2.1. *A. baumannii/E. coli* shuttle expression plasmid map. pUC19 *ori*, *E. coli* replication origin; pWH *ori*, *Acinetobacter* sp. origin of replication; *bla*, ampicillin resistance gene; *lacI*^{q}, Lac repressor encoding gene; *gfp*, green fluorescent protein gene; bpm base pair; restriction enzyme sites for *Kpn*I, *Pae*I, *Eam*1105I are also displayed.

Plasmids for complementation were constructed by substituting the *gfp* gene in the shuttle plasmid with the required gene via blunted *Pae*I and *Kpn*I sites (Fig. 2.1). These plasmids were used to complement the relevant strains (Table 2.2).

For the construction of suicide plasmid, *B. subtilis* gene *sacB*, encoding levansucrase, was amplified with the primer pair sacB_F/sacB_R and subsequently cloned into the plasmid pUC19 via *Xba*I and *Pae*I, resulting in the plasmid pUC19_*sacB*. Suicide plasmids for gene deletions were constructed by amplifying the *aac3I* gentamicin resistance cassette and approximately 1 kb long upstream and downstream regions of a gene of interest, containing overlap sequences with each other and the cassette. All three amplicons were then joined into a single fragment using overlap extension PCR and blunt-end ligated into the plasmid pUC19_*sacB*.

2.2.5. Preparation of electrocompetent cells

A. baumannii electrocompetent cells were prepared from overnight culture grown in LB at 37°C. 1 mL of the culture was centrifuged at 12 000 g at room temperature (RT) to collect all cells, washed three times with 1 mL of deionised water (ddH_2O) before being resuspended in 100 µL of ddH_2O. Electrocompetent cells from other bacteria were prepared by diluting overnight culture 100-fold in the fresh LB-media (300 mL) and grown to OD_{600} of 0.4-0.6 at 37 °C with shaking. Media with cells were then removed from a shaker and chilled for 15 min at 4 °C. Bacteria were pelleted by centrifuging at 1000 g for 7 min at 4 °C, washed 3 times with 10 % glycerol solution in ddH_2O before being resuspended in the same solution in a total volume of 500 µL. Prepared electrocompetent cells were portioned by 50 µL and were either used for transformation immediately or stored at -80°C. Electroporation was performed using Eppendorf Electroporator 2510 and Sigma-Aldrich® electroporation cuvettes with a gap of 0.1 cm.

2.2.6. Biofilm formation assay

Biofilm formation assay was performed as described by O'Toole *et al.*, (1999) with some modifications. The required strains were grown overnight in either TSB or LB media at 37°C with shaking. The cultures were diluted to a final cell density of 10^6 colony-forming units (CFU)/mL with either LB or 0.25x diluted TSB media and inoculated into the wells of a flat-bottom 96 well polystyrene microplate (NERBE). The microplate was placed in an airtight box with a wet paper towel to preserve humid conditions and was incubated stationary for 24 h at 37°C. The wells with grown bacteria were

washed three times with ddH_2O to remove planktonic cells and stained for 15 min with 0.1 % (w/v) crystal violet solution. After staining, the wells were washed three times with ddH_2O to remove an excess of the dye. The stained biofilms were evaluated either visually or quantified by solubilizing the dye with 33 % glacial acetic acid for 15 min and measuring the optical density at 580 nm (OD_{580}). The obtained values were normalized by a total bacterial biomass measuring the optical density at 600 nm (OD_{600}). Experiments were performed three times each with 2 technical replicates. Measurements were performed using a Tecan Infinite M200 Pro plate reader.

2.2.7. Generation of *A. baumannii* mutant strains

A. baumannii marker-less gene deletions were obtained according to Oh *et al.* (2015) with some modifications. The upstream and downstream regions of genes to be deleted were amplified, joined into a single fragments with the *aacI3* gene, and cloned into the suicide vector as described in the section 2.2.4. Products were electroporated into *E. coli* JM107 strain and transformants were plated on a selective LB agar media containing 10 mg/L gentamicin. Suicide plasmid was isolated from a propagated colony and electroporated into *A. baumannii* isolate of interest. Resulting transformants were plated on a LB agar plate containing 10 mg/L gentamicin to select colonies, which experienced a first recombination event resulting in the integration of the plasmid into the chromosome as it is unable to replicate in *A. baumannii*. A single transformant was inoculated into LB liquid media without antibiotics, grown for 4-6 hours at 37°C with shaking, streaked onto a LB agar plate containing 10 % sucrose, and grown overnight at 37°C. This step allowed for the selection of strains with a second homologous recombination event, resulting in the loss of the integrated plasmid from the chromosome due to the fact that levansucrase synthesized high molecular-weight fructose polymers are toxic to *A. baumannii*. The resulting strains were either WT strains or mutants with deletions. The graphical schematic of mutant strain generation and genetic mutants that were created using this workflow is displayed in Figure 2.2. All generated mutants were identified and confirmed by PCR with specific primers and by sequencing.

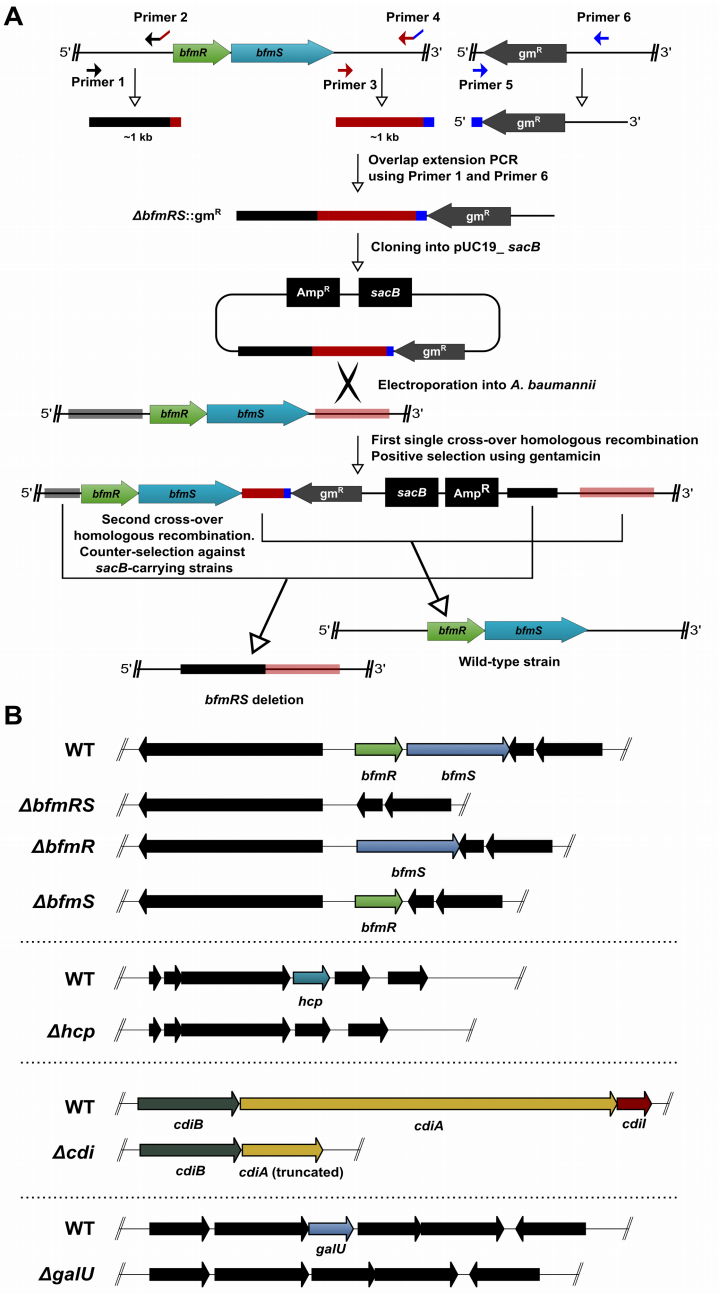

Fig. 2.2. Graphical schematic of marker-less mutant strain generation method used in this work (**A**) and genetic mutants that were created using this workflow (**B**). (**A**) The mutant generation workflow is based on the proposition by Oh *et al.* (2015) and is described in section 2.2.7. The deletion of the whole *bfmRS* operon is provided as an example. Amp^R, ampicillin resistance cassette; gm^R, gentamicin resistance cassette; *sacB*, levansucrase gene; kb, kilobase. Primers 1 – 4 were unique for each target sequence to be deleted and are provided in Table 2.4. Primers 5 and 6 were GentR_R and GentR_F, respectively. (**B**) Genomic organization of genetic mutants used in the work that were created via marker-less deletion method. The list of the mutants can also be found in Table 2.2. WT, wild-type.

2.2.8. Pellicle formation assay

Overnight cultures of *A. baumannii* strains grown in TSB media were diluted with fresh media to a cell density of 10^6 CFU/mL and inoculated into the wells of a flat-bottom 12 well polystyrene microplate (TPP) in a total volume of 3 mL. The cultures were incubated stationary for 30 hours at 30°C. The formed pellicles were inspected visually by observing a floating biomass on the surface of the media. To collect pellicles for the quantification, 200 µL of 2-propanol was added to each well. This allowed to easily transfer pellicles into new tubes using pipette tips. The transferred pellicles were resuspended in 500 µL of 10 mM NaOH, followed by a quick neutralization with HCl. The biomass was quantified by measuring the OD_{600} of suspensions and normalizing to the total volume of inoculation culture (3 mL) so as to be comparable to the planktonic OD_{600} readings.

2.2.9. Motility assays

All motility experiments were performed using bacteria from freshly grown cultures on solid TSB media. Bacteria were picked with a 10 µL pipette tip and were stab inoculated into the centre of freshly prepared motility media in Petri plates (90 mm diameter) and grown in a humid airtight containers at 37°C for 24 h or 48 h for surface motility and twitching motility, respectively. Motility was quantified by measuring the halo of growth around the inoculation site. The surface and twitching motility plates included 20 mL 0.25x TSB media supplemented with 0.25 % and 0.75 % agar, respectively. The prepared plates were allowed to dry with lids removed for 80 min in a laminar flow hood. To assess twitching motility, plates with removed media were stained with 0.1 % crystal violet (w/v). The unbound stain was washed out with water.

2.2.10. Protein secretion assay

The total protein in growth media was evaluated from bacterial cultures grown in TSB media for 30 hours at 30°C. Cells from the cultures were removed by a centrifugation at 10000 g for 10 min at 4°C and an additional filtration through 0.22 micron. In the resulting supernatants, trichloroacetic acid (TCA) to a final concentration of 10 % was added. The precipitated proteins were pelleted by a centrifugation for 60 min at 15000 g at 4°C. The pellets in tubes were washed twice with an ice-cold acetone and dried by incubating at 95°C. The samples were re-suspended with SDS-PAGE sample buffer and analysed using the Laemmli-12% SDS-PAGE system. After

electrophoresis, gels were stained with Coomassie brilliant blue. Protein molecular weight standard (PageRuler™ unstained broad range protein ladder (Thermo Fisher Scientific)) was used as a marker (5 µL per lane). Protein identification by MALDI-TOF mass spectrometry of cut-out bands from gels were undertaken at Proteomics department of Vilnius University Life Sciences Center.

2.2.11. RNA isolation and gene expression analysis

Overnight cultures of *A. baumannii* were diluted to a cell density of 10^6 CFU/mL, inoculated into the wells of 96-well polystyrene plates (Nerbe), and grown at 37°C with shaking until mid-logarithmic phase (OD_{600} of 0.35-0.4). The growth was performed and monitored using Tecan Infinite M200 Pro plate reader. The total RNA was isolated using GeneJET RNA Purification Kit (Thermo Fisher Scientific). The RNA concentration was evaluated with a NanoDrop (Thermo Fisher Scientific). The RNA integrity was checked by agarose gel electrophoresis. Residual DNA was removed with DNase I and cDNA was synthesized using RevertAid First Strand cDNA Synthesis Kit (both Thermo Fisher Scientific). qPCR was performed using primer pairs listed in Table 2.4. The amplification efficiencies of primer pairs exhibited 95–107% (coefficient of determination >0.99), as determined by using the dilutions of genomic DNA. Melting curve analysis was applied to investigate product specificity. Changes in gene expression were calculated as $\Delta\Delta C_t$, using *rpoB* as a house-keeping gene. At least three biological replicates were performed.

2.2.12. Inter-bacterial competition assay

Bacterial strains were grown overnight in TSB media at 37°C with shaking. Grown cultures were washed twice with fresh TSB by a centrifugation for 2 min at 5000 g. Washed bacteria were diluted to a final concentration of 10^8 CFU/mL. Competitions were performed by mixing the prepared cultures at various ratios (indicated in figure legends), and spotting 5 µL of suspensions on TSB media containing 1.5 % agar. The spots were allowed to dry before the plates were proceeded to be incubated for 6 h at 37°C. After the incubation, the spots were excised, vigorously resuspended in 500 µL TSB media, serially diluted, and plated on LB agar plates, containing a selective antibiotic to enumerate surviving bacteria (target and aggressor (if possible)). Strains that were used had a natural resistance or were transformed with a plasmid containing appropriate marker allowing the selective isolation. All experiments included control reactions with *E. coli*

strain DH5α to obtain the total number of bacteria if there were no competition between strains. The obtained number of colonies were calculated as CFU per mL of culture.

2.2.13. Fractionation of Capsular Polysaccharides

Bacterial cultures, grown overnight on LB agar plates were suspended in 1 mL of phosphate-buffered saline (PBS) buffer to a final OD_{600} of 3, and vortexed for 2 min at the maximum speed. Bacteria cells were pelleted by a centrifugation at 10000 g for 10 min. Ethanol to a final concentration of 75 % was added to the supernatants to precipitate capsular polysaccharides, which were pelleted by a centrifugation at 15000 g for 120 min at 4°C. The pellets were air-dried and resuspended in Laemmli-SDS-PAGE sample buffer. The samples were analysed using the Laemmli-12% SDS-PAGE system. After electrophoresis, gels were stained overnight with 0.1 % (w/v) of Alcian Blue as described in Mercaldi *et al.* (2008).

2.2.14. *A. baumannii* growth assays

Overnight cultures of *A. baumannii* strains grown in LB at 37°C with shaking were diluted to a cell density of 10^6 CFU/mL and inoculated into the wells of a flat-bottom 96 well polystyrene microplate (Nerbe) to a final volume of 150 µL. Cultures were grown at 37°C with shaking until reached early logarithmic phase (OD_{600} of 0.25-0.35), where the required additive in a total volume of 10 µL was added and the monitoring was continued. The following additives were used: 0.22 µm filtered supernatant from growth media, sterile LB media, sterile PBS buffer, sterile LB media, purified CdiA protein at 0.3 µg/mL final concentration. Growth was monitored using Tecan Infinite M200 Pro plate reader. Experiment was repeated three times with two technical replicates each.

2.2.15. Purification of CdiA

Overnight cultures of *A. baumannii* V15 *ΔbfmRS* grown in TSB at 37 °C with shaking were diluted to a cell density of 10^7 CFU/mL in a total volume of 750 mL of the fresh TSB. Cultures were allowed to grow stationary for 30 hours at 30 °C. The supernatants of grown cultures were clarified by a centrifugation at 10000 g for 10 min, followed by a filtration through 0.22 µm filter (regenerated cellulose). The CdiA was purified firstly precipitating proteins via the gradual addition of ammonium sulphate to a final concentration of 40 %, under constant mixing. Then, the precipitated proteins were pelleted by a centrifugation at 15000 g for 25 min and

resuspended in 10 mL 0.05 M sodium phosphate buffer (pH 7.0), containing 10 % ammonium sulphate. The suspension was applied to a hydrophobic interaction chromatography column (1 mL Butyl Sepharose® 4 Fast Flow column (GE Healthcare)), which was equilibrated with buffer A (0.05 M sodium phosphate, 1.0 M ammonium sulphate, pH 7.0). The column with bound CdiA was washed with five column volumes of buffer A, followed by elution with buffer B (0.05 M sodium phosphate, pH 7.0) over linear gradient of 14 column volumes. The fractions with eluted CdiA were pooled and concentrated with buffer exchange into PBS using Pierce™ Protein Concentrator PES, with the 100 kDa cut-off value (Thermo Fisher Scientific). Protein concentration was determined using Roti®Quant Bradford protein assay (Roth) with bovine serum albumin standard (Roth) for calibration. Hydrophobic interaction chromatography was performed using ÄKTA FPLC system (GE Healthcare).

2.2.16. Protein size determination by size-exclusion chromatography

The size of purified CdiA was determined using Superose 12 10/300 GL gel filtration column (GE Healthcare) on ÄKTA FPLC system (GE Healthcare). The column was equilibrated with PBS. The following protein molecular mass standards were used for calibration curve: blue dextran, ferritin (440 kDa), catalase (232 kDa), Aldolase (158 kDa), bovine serum albumin (68 kDa) (All Amersham biosciences). The flow conditions were kept constant at 0.6 mL/min. All eluted fractions were collected and subsequently evaluated by SDS-PAGE analysis and by grow inhibition assay as described in section 2.2.14. The molecular weight of CdiA was determined from the calibration curve, which itself was obtained by calculating partitioning coefficients (K_{av}) of eluted molecular weight standards (calculated as $(V_e - V_o)/(V_t - V_o)$, where V_e – elution of a molecule (mL), V_o – column void volume (mL), and V_t – total column volume (24 mL)) and plotting them against the decadic logarithm of standard molecular weight.

2.2.17. Minimal inhibitory concentration (MIC) determination

MICs were performed by the broth micro-dilution method. Briefly, the serial dilutions of purified CdiA were prepared with sterile LB media and dispensed into the wells of a round-bottom 96 well polystyrene microplate (Nerbe) in a total volume of 50 µL. Next, overnight cultures of bacteria grown in LB were diluted with fresh media to a final concentration of 10^6 CFU/mL and 50 µL of suspensions were added to each well in a microplate

containing CdiA dilutions as well as wells that contained only LB media as a growth control. The plate was then incubated for 16 h at 37 °C before recording MIC values, which were defined as the lowest concentration of CdiA that inhibited the visible growth of culture.

2.2.18. Bacteria viability assay

Overnight cultures of bacteria grown in LB were diluted to a final concentration of 10^8 CFU/mL. 100 µL of suspensions were dispensed into the wells of a microplate. 5 µL of either purified CdiA (0.5 µg) or PBS were added, and the plate was incubated at 37 °C. At various time points, 5 µL from suspensions were drawn out, serially diluted, and plated on a selective LB agar plate to enumerate viable bacteria.

2.2.19. Live/dead assay and microscopy analysis

Overnight bacterial cultures grown in LB, were washed twice by a centrifugation at 5000 g for 2 min with PBS, and diluted to a final concentration of 10^8 CFU/mL and distributed into three vials with a total volume of 250 µL. Bacteria were pelleted by a centrifugation at 5000 g for 2 min and resuspended in either PBS (control for live bacteria), 70% 2-propanol (control for dead bacteria), or purified CdiA solution in PBS (final concentration of 5 µg/mL). The suspensions were incubated for 30 minutes or 3 hours at room temperature before the cells were washed 3 times with PBS by a centrifugation at 5000 g for 2 min. The washed cells were concentrated to a cell density of ~10^9 CFU/mL and subjected to cell staining for 15 min in the dark using SYTO9 (Invitrogen) and propidium iodide (Sigma) solution in water at a final concentration of 9.4 nM and 42.4 nM, respectively.

Microscopy experiments were performed by trapping 5 µL of cells between a slide and an 18 mm square cover slip and observing bacteria with Olympus AX70 microscope using UPlanApo objective lens with a final magnification of 1000x. U-WIBA (excitation band-pass at 460-490 nm and emission band-pass at 515-550 nm) and U-MWG (510-550/510-) block filters were used to observe fluorescence for SYTO9 and propidium iodide, respectively. Fluorescent images were taken under the same acquisition setting. The obtained images were merged into a single pseudo-color image using Fiji software (Schindelin *et al.*, 2012).

2.2.20. Homology search and domain identification

Identification of CDI systems in complete and annotated *A. baumannii* genomes (Supplementary table 1) were performed by iteratively searching CdiB homologs in rp75 database (version 2018_09) using JACKHMMER (HmmerWeb version 2.30.0) and the product of gene F911_RS14340 (Harding *et al.*, 2017) as a query. The resulting profile was used to perform HMMSEARCH v. 3.2.1 (HMMER.org) with the inclusion E-value and inclusion domain E-value set at 0.001 against *A. baumannii* protein database created using protein product sequences annotated on the genome assemblies (Supplementary table 1). The CDI coding regions were considered as positive only if the products of downstream genes were identified as large proteins with haemagglutination activity or haemagglutinin repeat domains (potential CdiA protein), followed by a small protein indicating the presence of a potential CdiI. *A. baumannii* genomes were separated into clonal lineage groups by performing *in silico* PCR (primersearch algorithm from EMBOSS suite) using primers and the typing scheme described previously (Turton *et al.*, 2007).

The domain architecture identification in CdiB, CdiA, and CdiI proteins was achieved by performing three iterative searches of each sequence against rp55 database (version 2020_01) using JACKHMMER (HmmerWeb version 2.41.1) with default parameters. The resulting significant hits were used as queries to perform searches with the web version of HHPRED (Zimmermann *et al.*, 2018) against Pfam 32.0 database. The hits were determined as significant if probability value was above 80 %. In the case of CdiA, the searches were performed using the N- and C-terminal halves of the protein separately. Protein alignments were performed with MUSCLE (Edgar, 2004), and visualised as sequence fingerprints using alignment shading software Texshade (version 1.25) (Beitz, 2000).

2.2.21. *In silico* analysis of expression changes of capsule locus genes

Data of published studies regarding *A. baumannii* gene expression changes under various conditions were extracted. The retrieved information included transcriptomics, proteomics, or transposon insertion sequencing from studies, which are listed in Supplementary table 2. All obtained results were sorted by a study and normalized to a relative value of change, when compared to all significantly expressed gene products in that study (scaled from -1 to 0 and from 0 to 1, by calculating using formula per each set of data $(\log_2 x^{\text{gene product of interest}} - \log_2 x^{\text{least significantly expressed gene product}})/(\log_2 x^{\text{most significantly}}$

$^{\text{expressed gene product}}$ - $\log_2 x^{\text{least significantly expressed gene product}}$). The top limit of the most expressed gene product used in the calculations (either induced or repressed) were set at 1000-fold. Hits that went beyond this threshold were considered as maximally expressed/repressed. The data from transposon insertion sequencing were normalized using counts of insertions. The Genes from the K1 locus were obtained from Kaptive database (https://github.com/katholt/Kaptive) (Wyres *et al.*, 2020). Positive hits were identified and confirmed via BLAST against aggregated database containing translated genes with differential expression from all studies using percent identity above 60 % and query coverage above 80 %. The positive hits were also inspected manually.

2.2.22. Statistical analyses

All statistical comparisons were performed using one-way ANOVA (p = 0.05) with a Tukey HSD *post hoc* test. The inter-bacterial competition and viability assays were calculated by taking a decadic logarithm from calculated values as CFU per mL. The changes in gene expression were evaluated only if the differences were more than 2-fold. The asterisks in figures denote the significance (n.s., not significant; *, $p<0.05$; **, $p<0.01$; ***, $p<0.001$). The analyses were performed using R package (version 3.4.4). The graphs were drawn using QtiPlot.

2.2.23. Data availability

The sequence of *A. baumannii* V15 *cdiBAI* locus has been deposited in GenBank under the accession number MK405474.

3. RESULTS

The first part of the Results section describes the role of *A. baumannii* two-component system BfmRS in virulence-associated phenotypes, namely biofilm and pellicle formation, motility, and inter-species competition. The second part, characterizes a competition mechanism termed contact dependent-growth inhibition in *A. baumannii*.

3.1. BfmS is not required for biofilm formation of *A. baumannii*

The two-component system BfmRS has been long known to be responsible for biofilm formation in *A. baumannii* (Tomaras *et al.*, 2008). It has also been determined that BfmS participates in *A. baumannii* motility (Clemmer *et al.*, 2011). However, the role of BfmR regulator in motility is unknown. It is thought that the reciprocal regulation of biofilm formation and motility for bacteria is essential for the stabilisation and maturation of biofilm communities (Guttenplan and Kearns, 2013). Therefore, we set out to investigate how BfmR affects these phenotypes in *A. baumannii*.

For this purpose, from the collection of clinical *A. baumannii* isolates (Povilonis *et al.*, 2013), we have selected isolate V15 (*Ab*V15) (Table 2.1), which showed clear biofilm formation and motility phenotypes. Via markerless gene deletion technique, we have generated knockout strains *ΔbfmR*, *ΔbfmS*, *ΔbfmRS*, deficient in response regulator *bfmR*, signal kinase *bfmS*, or the whole *bfmRS* operon, respectively. We verified the deletions by sequencing and by biofilm formation assays. As can be seen in Fig. 3.1.1 A, the loss of BfmR (*Ab*V15 *ΔbfmR* and *ΔbfmRS* strains), resulted in the loss of the ability to

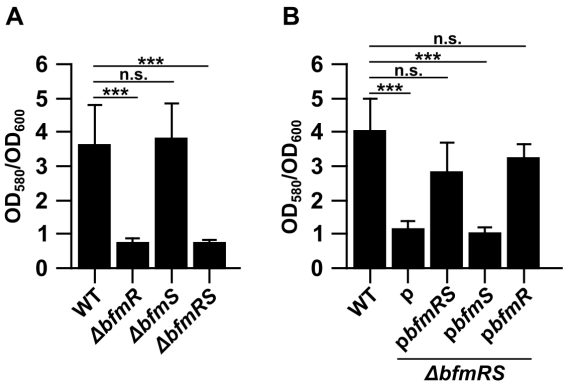

Fig. 3.1.1. Quantitative evaluation of biofilms formed by: (**A**) *Ab*V15 strain (WT) and its mutants *ΔbfmR*, *ΔbfmS*, and *ΔbfmRS*; (**B**) *ΔbfmRS* mutant, complemented with plasmids p*bfmR,* p*bfmS*, p*bfmRS*. Error bars represent standard deviation. ***, p<0.001; n.s., not significant. p denotes empty plasmid used as a control.

form biofilms. The *bfmS* gene deletion did not impact the biofilm formation phenotype (Fig. 3.1.1 A).

We then performed complementation experiments using the *Ab*V15 *ΔbfmRS* mutant complemented with plasmids containing wild-type (WT) genes *bfmR* (p*bfmR*), *bfmS* (p*bfmS*), and *bfmRS* (p*bfmRS*) under an IPTG-inducible promoter. We chose an inducible promoter since constructs with the native promoter sequence were found to be toxic for bacteria (data not shown). The complementation of *ΔbfmRS* with the wild-type operon reinstated the biofilm formation phenotype. The phenotype was also complemented with the sole *bfmR* gene, but not with the *bfmS* gene (Fig. 3.1.1 B), in agreement with previous findings indicating that the deletion of *bfmS* does not impact this phenotype (Tomaras *et al.*, 2008). This is consistent with the observations, that BfmS acts negatively on BfmR, and that the regulator can complement the whole *ΔbfmRS* mutant to the WT (Geisinger *et al.*, 2018; Geisinger and Isberg, 2015).

Since the phenotypes were reinstated under non-inducing conditions, we decided to evaluate the *bfmR* gene transcript levels in both WT strain and *ΔbfmRS* mutant, complemented with p*bfmR*. Results revealed a ~2.9-fold increase of *bfmR* transcript levels (with a standard deviation of ±0.9) in the mutant, when compared to the WT. This indicated that the inducible promoter displays the unregulated transcription of downstream sequences, explaining the reinstated biofilm formation phenotype under non-inducing conditions.

3.2. BfmR negatively regulates surface-associated motility

Next, we investigated the role of BfmR in *A. baumannii* motility. Surface-associated and twitching motility phenotypes were assessed, as these are considered to be regulated by different mechanisms and are independent from each other (Eijkelkamp *et al.*, 2013; Harding *et*

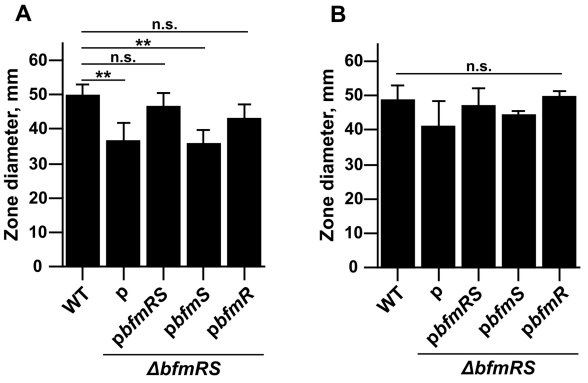

Fig. 3.2.1. Evaluation of (**A**) surface-associated and (**B**) twitching motilities demonstrated by *Ab*V15 strain (WT), *ΔbfmRS* mutant alone or complemented with plasmids p*bfmR* p*bfmS*, p*bfmRS*. Error bars represent standard deviation. **, $p<0.01$, n.s., not significant. p denotes empty plasmid used as a control.

al., 2013). As can be seen in Fig. 3.2.1 A, the *ΔbfmRS* mutant showed an approximately 30 % reduction in the surface-associated motility compared to the WT strain. Complementation with plasmids p*bfmR* or with p*bfmRS* restored the phenotype to the wild-type levels, while complementation with plasmid p*bfmS* did not affect the motility. In contrast to the changes in surface-associated motility, the *ΔbfmRS* mutation did not significantly impact twitching motility (Fig. 3.2.1 B).

Remarkably, induction of the *bfmR* allele in *Ab*V15 *ΔbfmRS* strain with IPTG concentration of 0.01 mM and 0.1 mM, resulted in the inhibition of surface-associated motility phenotype (Fig. 3.2.2 A). Growth assays showed that only 0.1 mM IPTG concentration caused a slight inhibitory effect on the growth phenotype (Fig. 3.2.2 B). We also measured the transcript levels of the *bfmR* gene under inducing conditions. Only at 0.1 mM IPTG concentration the *bfmR* transcript was significantly up-regulated by ~eight-fold compared to non-inducing conditions (Fig. 3.2.2 C).

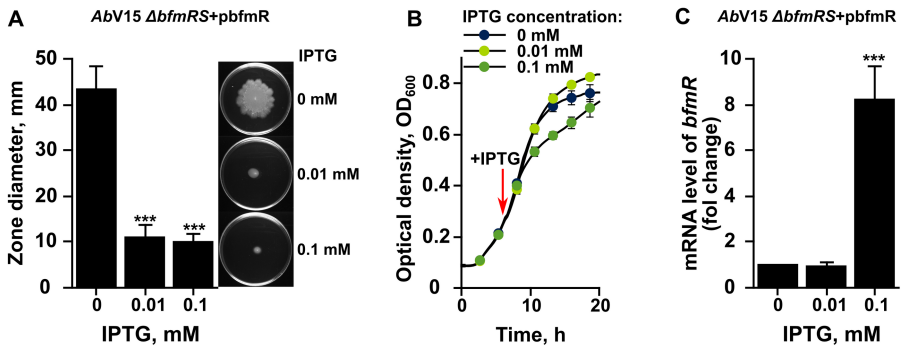

Fig. 3.2.2. (**A**) Inhibition of surface-associated motility under inducing conditions demonstrated by *Ab*V15 *ΔbfmRS* strain complemented with p*bfmR* plasmid. (**B**) Comparison of growth curves obtained from *Ab*V15 *ΔbfmRS* strain complemented with p*bfmR* under inducing conditions. (**C**) mRNA levels of *bfmR* transcript under inducing conditions. Pictures next to the graph **A** show macroscopic images of motility zones. IPTG at various concentrations was used as an inducer, where required. Error bars represent standard deviation. ***, p<0.001, relative to non-induced control.

The same surface-associated motility inhibition phenomenon was observed for the p*bfmRS*-complemented *Ab*V15 *ΔbfmRS* strain at IPTG concentration of 0.1 mM, but not for p*bfmS* plasmid (Fig. 3.2.3 A and B). It must be noted that growth phenotypes in the latter two constructs were not impacted by IPTG concentrations used (data not shown).

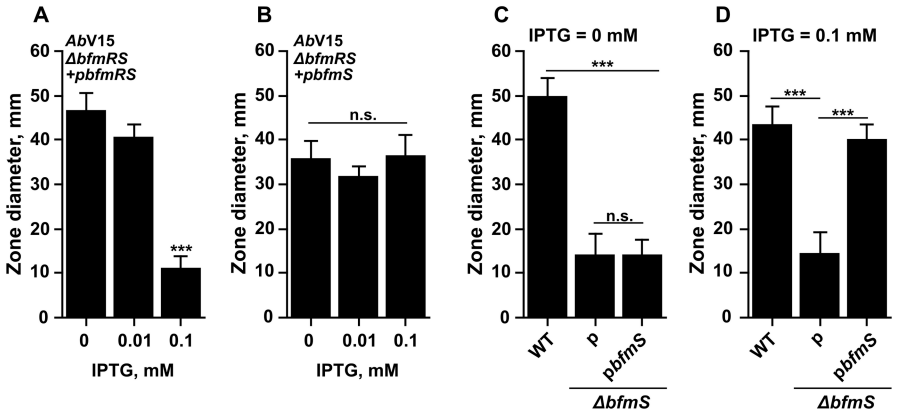

Fig. 3.2.3. (**A-B**) Surface-associated motility under inducing conditions demonstrated by *Ab*V15 *ΔbfmRS* strain complemented with (**A**) p*bfmRS* or (**B**) p*bfmS*. (**C-D**) Surface-associated motility demonstrated by *Ab*V15 strain (WT), *Ab*V15 *ΔbfmS* strain alone or complemented with plasmid p*bfmS* under (**C**) non-inducing or (**D**) inducing conditions. IPTG at various concentrations was used as an inducer, where required. Error bars represent standard deviation. ***, p<0.001, relative to WT; n.s., not significant. p denotes empty plasmid used as a control.

Collectively, these results suggest, that the overexpression of *bfmR* inhibits the surface-associated motility phenotype. Given the previous observations showing that the loss of *bfmS* inhibited *A. baumannii* surface motility (Clemmer *et al.*, 2011), which we also confirmed with our strain (Fig. 3.2.3 C and D), and our observations with the overexpressed constructs (data presented above), the obtained data are fully consistent with the proposed model that BfmS negatively regulates the activity of BfmR (Geisinger *et al.*, 2018; Geisinger and Isberg, 2015). Therefore, for the following experiments, only complementing constructs containing *bfmRS* or *bfmR* genes were used.

3.3. BfmR is required for *A. baumannii* pellicle formation

A recent study by Kentache *et al.* (2017) found that a four-day mature pellicle contains approximately 4.5-fold increased BfmR levels, when compared to a one-day pellicle. Additionally, this study also showed that a mature pellicle displayed increased amounts of CsuA/B pilin, which was shown to be the most abundant component of *A. baumannii* pellicle (Nait Chabane *et al.*, 2014). Therefore, we raised a hypothesis that BfmR might also impact the pellicle phenotype.

For the pellicle formation assay, we selected TSB media and grew strains at 30°C for 30 hours without shaking as these conditions are known to promote pellicle formation (Armitano *et al.*, 2014; Giles *et al.*, 2015). By

growing *Ab*V15, *ΔbfmRS* mutant alone or complemented with plasmids p*bfmRS* or p*bfmR*, we determined that the loss of *bfmRS* abolished pellicle formation. The phenotype was fully restored with either p*bfmRS* or p*bfmR* plasmids (Fig. 3.3.1 A). These results indicate that BfmR is required for pellicle formation of *A. baumannii* V15.

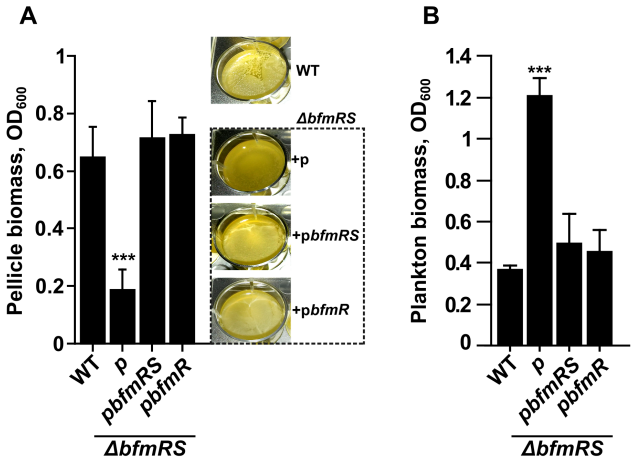

Fig. 3.3.1. Quantitative evaluation of (**A**) pellicle biomass and (**B**) planktonic growth in the pellicle formation assay. The following strains were assessed: *Ab*V15 (WT), *ΔbfmRS* mutant alone or complemented with plasmids p*bfmRS* or p*bfmR*. Biomass in the planktonic growth assay was measured after the removal of pellicle. p denotes empty plasmid used as a control. Pictures next to graph **A** show macroscopic images of formed pellicle on the surface of growth media. Error bars represent standard deviation. ***, denotes statistical significant ($p<0.001$) difference compared to WT strain.

Additionally, WT and *ΔbfmRS* strains, complemented with p*bfmR* or p*bfmRS* plasmids exhibited a significantly reduced amount of planktonic bacteria, when compared to the *ΔbfmRS* mutant (Fig. 3.3.1 B). It is currently proposed that the formation of pellicle prevents oxygen flux into the growth media, which leads to reduced planktonic growth (Eijkelkamp *et al.*, 2013; Liang *et al.*, 2010). Our results suggest that the reduction of planktonic growth might be caused by the fact that most bacterial cells are located in the pellicle itself, as the total biomass (pellicle + planktonic growth) of all strains is at the comparable level.

3.4. Motility and pellicle formation phenotype among *A. baumannii* clinical isolates

We were also interested in how wide-spread is BfmR regulated pellicle phenotype among clinical *A. baumannii* strains as it might facilitate the spread of the pathogen in the clinical environment via the formation of small

droplets (Nait Chabane *et al.*, 2014). For this purpose, we screened clinical *A. baumannii* isolates, representing different genotypically related groups (pulso-types) of strains belonging to the International Clone (IC) I (N=20) and IC II (N=16) clonal lineages (Povilonis *et al.*, 2013). As can be seen in Fig. 3.4.1, the phenotype, although variable in terms of quantity, is nearly exclusively a trait of the IC I strains (17/20), while only a single pellicle former was found among IC II strains analysed. This result indicates that *bfmR*-regulated feature is prevalent only among IC I strains.

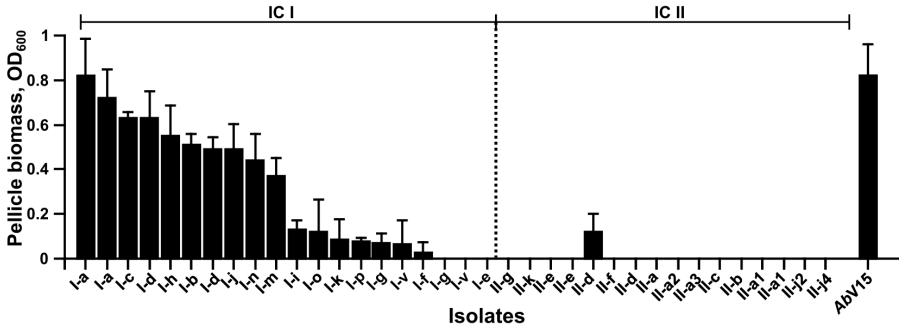

Fig. 3.4.1. Quantitative evaluation of pellicles formed by representative strains belonging to international lineages IC I and IC II. Roman numerals (I or II) indicate clonal lineage, letters indicate pulso-type as determined by Povilonis *et al.* (2013). *Ab*V15 strain was used as a positive pellicle forming control.

Additionally, we asked whether a correlation between two phenotypes – pellicle formation and motility exists among clinical isolates. For this, we performed surface associated and twitching motility assays. As can be seen in Fig. 3.4.2 A, all strains tested displayed a surface-associated motility. Twitching was a more common trait for the majority (16/20) of strains of IC I clonal lineage, while IC II strains essentially did not twitch (Fig. 3.4.2 B).

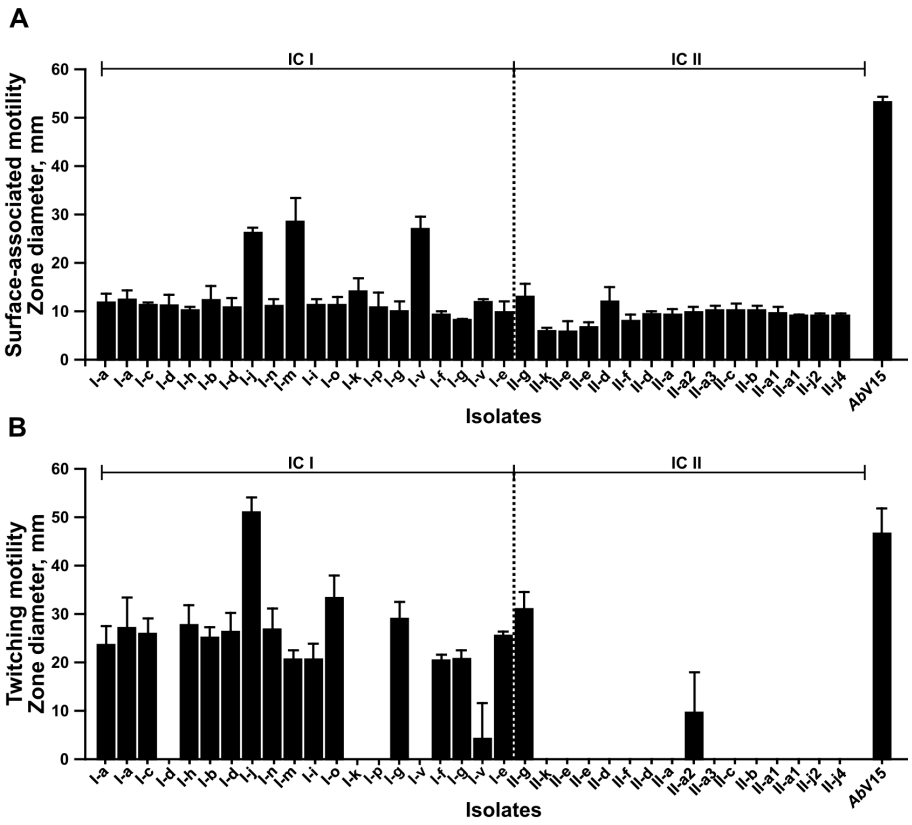

Fig. 3.4.2. Quantitative evaluation of (**A**) surface-associated and (**B**) twitching motility demonstrated by representative strains belonging to international lineages IC I and IC II. Roman numerals (I or II) indicate clonal lineage, letters indicate pulso-type as determined by Povilonis *et al.* (2013). *Ab*V15 strain was used as a positive pellicle forming control.

Our results show that while there was a tendency for a twitching strain to form a pellicle, this motility phenotype was not an indicative sign for pellicle formation.

3.5. Loss of *bfmR* reduces secretion of Hcp into growth media

Pellicle formation is a complex, highly regulated process, which requires various secreted substances such as proteins, polysaccharides, and DNA (Armitano *et al.*, 2014; Kentache *et al.*, 2017). A recent proteomic analysis identified multiple virulence factors expressed in *A. baumannii* pellicle, indicating the clinical significance of this phenotype (Kentache *et al.*, 2017). Therefore, we were interested whether BfmR is responsible for the regulation of pellicle phenotype-associated components.

For this, we have investigated the protein profiles of total protein fractions precipitated from culture media of *Ab*V15 and *Ab*V15 *ΔbfmRS* strains. SDS-PAGE analysis revealed that the *ΔbfmRS* mutant displayed a significant down-regulation of a protein with an approximate molecular mass of 18 kDa. The secretion was reinstated once the mutant strain was complemented with either p*bfmRS* or p*bfmR* plasmids (Fig. 3.5.1 A).

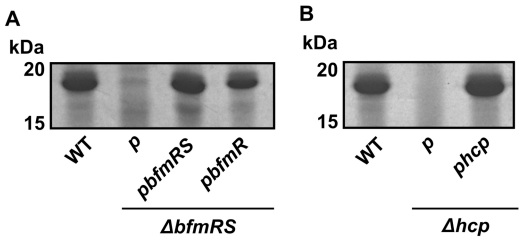

Fig. 3.5.1. 12.5% SDS-PAGE view of trichloroacetic acid precipitated total proteins from filtered growth media supernatants of (**A**) *Ab*V15 (WT), *ΔbfmRS* mutant, and *ΔbfmRS* complemented with plasmids p*bfmRS* or p*bfmR*; (**B**) *Ab*V15 (WT), *Δhcp* mutant alone or complemented with plasmid p*hcp*. Proteins were visualised by staining with Coomassie blue, Numbers on the left denote molecular weight in kDa. Only the region of interest is shown.

We identified the band by mass spectrometry as *A. baumannii* Hcp protein, which is one of the essential components of a bacterial Type VI secretion system (T6SS). Additional confirmation was made by generating the *Δhcp* deletion in *Ab*V15 strain, resulting in the complete loss of secreted Hcp in culture media. The phenotype was reinstated under inducing conditions of 0.1 mM IPTG, by introducing a plasmid p*hcp* with a copy of the native *hcp* gene under inducible promoter (Fig. 3.5.1 B). We hypothesize that induction only conditions for the complementation were required due to the nature of T6SS apparatus, where Hcp before secretion, must assemble into tubular multimeric structure (Coulthurst, 2019).

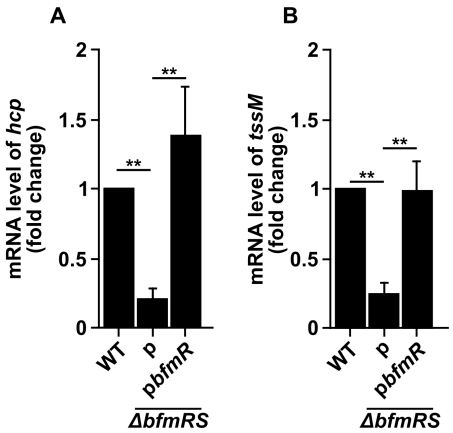

Fig. 3.5.2. Comparison of mRNA levels of (**A**) *hcp* and (**B**) *tssM* transcripts between *Ab*V15 (WT) and *ΔbfmRS* mutant with or without a complementing plasmid p*bfmR*. Data in graphs are displayed as a fold change compared to WT strain which is set at 1. Error bars represent standard deviation. p denotes empty plasmid used as a control. **, $p<0.01$.

The *bfmR*-dependent *hcp* regulation was also observed at the transcriptional level, where we recorded a five-fold reduced *hcp*-specific mRNA quantity in the *ΔbfmRS* mutant, when compared to the WT strain (Fig. 3.5.2 A). This indicated that the whole

T6SS apparatus might be down-regulated, therefore we additionally assessed the mRNA levels of the *tssM* gene in the *ΔbfmRS* mutant. The gene encodes a membrane-anchoring complex, which is essential for T6SS assembly and functional activity (Weber *et al.*, 2013). We found that the *ΔbfmRS* mutant displayed a four-fold down-regulation of *tssM*-specific mRNA quantity, when compared to the WT strain (Fig. 3.5.2 B). The mRNA levels of *tssM* and *hcp* genes in the *ΔbfmRS* mutant were restored to the WT levels, when the mutant was complemented with plasmid p*bfmR* (Fig. 3.5.2 A and B). These results indicate that BfmR is required for the increased secretion of Hcp into the growth media and it is likely that the regulator positively regulates the whole T6SS apparatus.

Finally, we considered the possibility that due to the abundance, bias towards oligomerization, and regulation by BfmR, Hcp might be necessary for pellicle formation by embedding into and stabilising pellicle matrix. Unfortunately, our results showed the loss of *hcp* did not impact the pellicle formation phenotype (Fig. 3.5.3 A), indicating that the secretion of Hcp does not contribute to *A. baumannii* V15 pellicle formation.

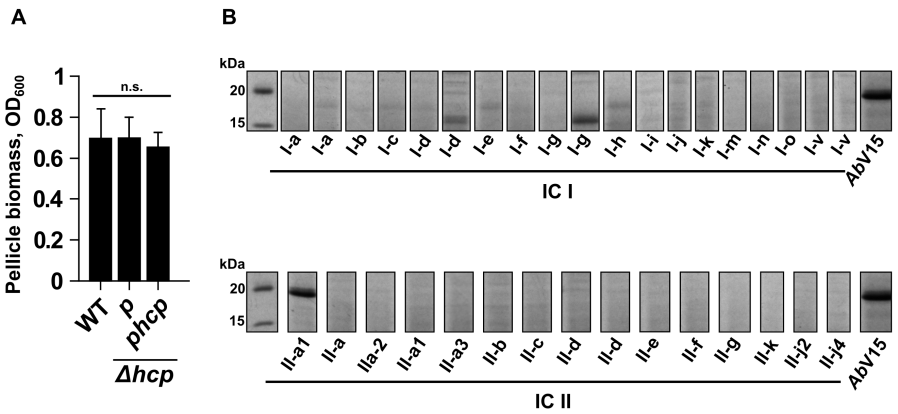

Fig. 3.5.3. (**A**) Quantitative evaluation of pellicle biomass formed by *Ab*V15 (WT), *Δhcp* mutant alone or complemented with the plasmid p*hcp*. p denotes empty plasmid used as a control. Error bars represent standard deviation. n.s., no significant difference. (**B**) 12.5% SDS-PAGE view of trichloroacetic acid precipitated total proteins from centrifuged growth media supernatants of representative strains belonging to international lineages IC I and IC II. Roman numerals (I or II) indicate clonal lineage, letters indicate pulso-type as determined by Povilonis *et al.* (2013). *Ab*V15 strain was used as a positive Hcp secreting control. SDS-PAGE gels were visualised by staining with Coomassie blue. Numbers on the left denote molecular mass of a marker (in kDa).

By performing protein secretion analysis using all representative clinical *A. baumannii* isolates from our collection, we observed that only a single

isolate demonstrated the apparent secretion of Hcp into the growth media (Fig. 3.5.3 B). This suggests that Hcp secretion is not a widespread phenotype among *A. baumannii* isolates, confirming previously published results (Repizo *et al.*, 2015).

3.6. Reduced Hcp secretion does not impact T6SS activity

The presence of Hcp in growth media is considered indicative of an active T6SS (Pukatzki *et al.*, 2009). Thus, we hypothesised that the presence of *bfmR* might impact the activity of T6SS in terms of the increased killing efficiency of target bacteria.

To answer this question, we have undertaken competition experiments, where two strains are mixed together, incubated on solid media before plating serial dilutions to evaluate the remaining cell count. We have selected *E. coli* MC4100 strain as a target. Firstly, we confirmed that the *Ab*V15 strain indeed displays a T6SS-mediated killing phenotype by using wild-type strain and *Δhcp* mutant with or without complementing plasmid containing the native *hcp* allele (p*hcp*). We observed that the *Ab*V15 strain reduced MC4100 numbers by 100-fold, and lost this phenotype once the *Δhcp* deletion was introduced. The phenotype was readily complemented with p*hcp* plasmid under inducing (0.1 mM IPTG) conditions (Fig. 3.6.1 A).

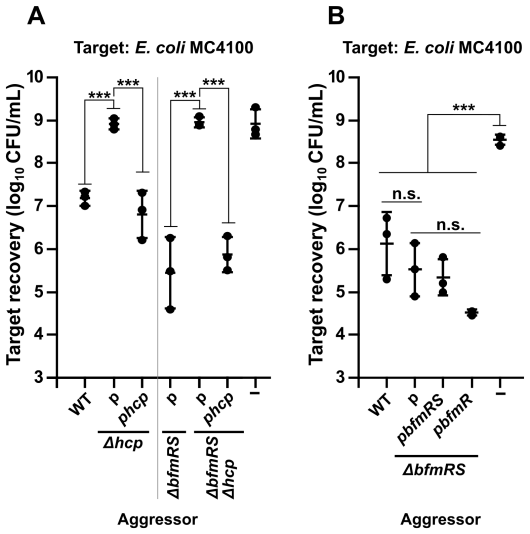

Fig. 3.6.1. Quantitative evaluation of inter-bacterial competition assay displaying the recovered numbers of *E. coli* MC4100 target bacteria. Competitions were performed with the following strains used as aggressors: (**A**) *Ab*V15 (WT), *Δhcp* mutant alone or complemented with plasmid p*hcp, ΔbfmRS* mutant, *ΔbfmRSΔhcp* alone or complemented with plasmid p*hcp.* Competitions were performed under inducing conditions (0.1 mM IPTG). (**B**) *Ab*V15 (WT), *ΔbfmRS* mutant alone or complemented with plasmids p*bfmRS* or p*bfmR*. Aggressor-target ratio of 10:1 was used. p denotes empty plasmid used as a control. Error bars represent standard deviation. The horizontal lines represent mean value. ***, $p<0.001$; n.s., not significant.

We then compared T6SS-mediated killing efficiencies among *Ab*V15 and its *ΔbfmRS* mutant. As can be seen in Fig. 3.6.1 B, the *bfmRS* deletion did not significantly impact killing

phenotype, when compared to the wild-type strain. The complementation of *ΔbfmRS* mutant with plasmids p*bfmRS* or *pbfmR* also did not significantly impact killing phenotype Fig. 3.6.1 B. To confirm that the mutant displayed T6SS-mediated killing phenotype, we generated a double deletion *ΔbfmRSΔhcp* and observed a complete loss of the ability to out-compete *E. coli* MC4100 (Fig. 3.6.1 A). Consistently, the phenotype was rescued by complementation with p*hcp* plasmid under inducing (0.1 mM IPTG) conditions (Fig. 3.6.1 A).

We also performed competition assays with other bacterial species. These included clinical strains of *Pseudomonas aeruginosa* P16 and *Klebsiella pneumoniae* K39. However, we did not observe any differences in killing efficiencies between WT and *ΔbfmRS* strains towards these two species (Fig. 3.6.2 A and B).

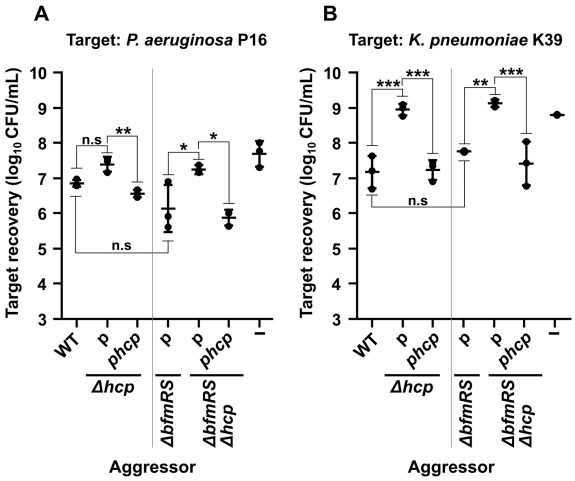

Fig. 3.6.2. Quantitative evaluation of inter-bacterial competition assay displaying recovered numbers of (**A**) *Pseudomonas aeruginosa* P16 and (**B**) *Klebsiella pneumoniae* K36. Competitions were performed with the following strains used as aggressors: *Ab*V15 (WT), *Δhcp* mutant alone or complemented with plasmid p*hcp, ΔbfmRS* mutant, *ΔbfmRSΔhcp* alone or complemented with plasmid p*hcp.* Competitions were performed under inducing conditions (0.1 mM IPTG). Aggressor-target ratio of 20:1 was used. p denotes empty plasmid used as a control. Error bars represent standard deviation. The horizontal lines represent mean value. *, $p<0.05$; **, $p<0.01$; ***, $p<0.001$; n.s., not significant.

Altogether, these results show that *A. baumannii* BfmRS system does not affect T6SS-mediated inter-genus killing. They also indicate that the increased secretion of Hcp into the growth media does not correlate with the increased killing efficiency of target bacteria.

3.7. BfmR down-regulates CDI system

Interesting results were obtained when competitions were performed with a closely related species *Acinetobacter baylyi* ADP1 strain. We observed that *A. baumannii ΔbfmRS* mutant displayed a significantly more aggressive killing phenotype (~10-fold), when compared to the WT, which itself reduced *A. baylyi* ADP1 numbers by 70–200-fold (Fig. 3.7.1 A). The phenotype, displayed by the *ΔbfmRS* mutant, was unaffected despite complementation with either p*bfmRS* or p*bfmR* plasmids (Fig. 3.7.1 A). Moreover, the deletion of *hcp* gene from the *ΔbfmRS* mutant resulted only in a minor reduction of the killing phenotype, while the same deletion in the wild-type strain almost completely abolished T6SS-mediated killing activity (Fig. 3.7.1 B). The phenotype was restored in both strains by complementation with p*hcp* plasmid under inducing (0.1 mM IPTG) conditions (Fig. 3.7.1 B). The obtained results suggest that the loss of BfmRS system causes the activation of T6SS-independent killing mechanism in *A. baumannii*.

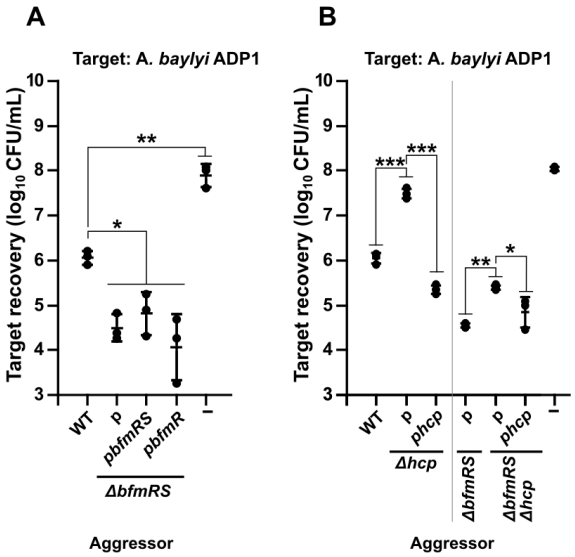

Fig. 3.7.1. Quantitative evaluation of inter-bacterial competition assay displaying recovered numbers of *A. baylyi* ADP1 target bacteria. Competitions were performed with the following strains used as aggressors: (**A**) *Ab*V15 (WT), *ΔbfmRS* mutant alone or complemented with plasmids p*bfmRS* or p*bfmR*. (**B**) *Ab*V15 (WT), *Δhcp* mutant alone or complemented with plasmid p*hcp, ΔbfmRS* mutant, *ΔbfmRSΔhcp* alone or complemented with plasmid p*hcp,* under inducing conditions (0.1 mM IPTG). Aggressor-target ratio of 10:1 was used. p denotes empty plasmid used as a control. Error bars represent standard deviation. *E. coli* DH5α was used as a negative non-competitive control. The horizontal lines represent mean value. *, $p<0.05$; **, $p<0.01$; ***, $p<0.001$.

Since the T6SS-independent killing phenotype was observed only against related species, we hypothesized that it could be mediated via the contact-dependent growth inhibition system, which has been characterised in *Acinetobacter* genus only recently (Harding *et al.*, 2017). We based our hypothesis on the fact that these systems generally target the neighbouring bacteria from the same or related species (Hayes *et al.*, 2014).

Firstly, we identified the CDI system encoded by the *A. baumannii* *Ab*V15 strain. A recent bioinformatic analysis has classified all *Acinetobacter* sp. systems into two types based on the length of clusters. Additionally, it was observed that CdiB transporters are rather conserved among *Acinetobacter* sp. CDI systems (De Gregorio *et al.*, 2019). Therefore, based on the sequence similarity, we created three primer pairs targeting all CDI systems encoded by *A. baumannii*. By identifying the exact sequence of the *cdiB* gene encoded by *Ab*V15, we then easily identified the genomic location and sequence of the two remaining genes, *cdiA* and *cdiI*. The sequenced *cdiBAI* locus has been deposited in GenBank under the accession number MK405474.

Next, we evaluated the *cdiB* gene expression levels in *Ab*V15 and its *ΔbfmRS* mutant. We found that *cdiB* was up-regulated by ~6.4-fold in the mutant, when compared to the wild-type strain (Fig. 3.7.2). We also measured transcript levels in the *ΔbfmRS* mutant complemented with p*bfmR* plasmid and observed a 2.5-fold up-regulation levels of *cdiB*, when compared to the WT *Ab*V15 strain (Fig. 3.7.2).

Altogether, these results suggest that the deletion of *bfmRS* system leads to the up-regulation of contact-dependent growth inhibition locus in *Ab*V15 strain.

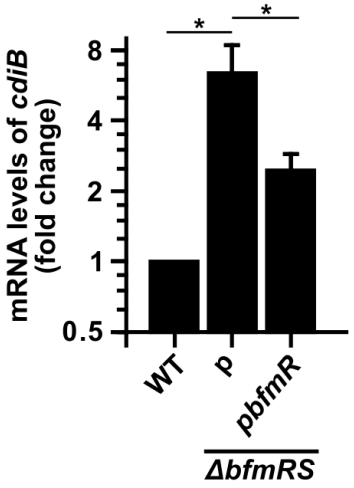

Fig. 3.7.2. Comparison of mRNA levels of *Ab*V15 transcripts *cdiB* between in *Ab*V15 (WT) and *ΔbfmRS* mutant with or without a complementing plasmid p*bfmR*. Data in graphs are displayed as a fold change compared to WT strain which is set at 1. Error bars represent standard deviation. p denotes empty plasmid used as a control. *, $p<0.05$.

3.8. Bioinformatic analysis of a CDI system encoded by *Ab*V15

The analysis of sequenced *cdiBAI* locus of *Ab*V15 allowed us to classify *Ab*V15 CDI system as a type-I system with the highest identity to

bau-A1/pit-A3 CDI systems: CdiB, CdiA, and CdiI proteins displayed identity of 98%, 90%, 66%, respectively (Fig. 3.8.1 A). The length of CdiB, CdiA, and CdiI were determined to be at 579, 2154, 185 amino acids, respectively.

BLASTP searches of CDI locus against all non-redundant protein sequences database (as of 2019-01-15) have identified seven identical CDI loci encoded in other strains: four in *A. baumannii* strains, one system in a *Acinetobacter* sp. strain, and two in *A. pittii* strains.

We also observed that four *A. baumannii* strains, namely AR_0037 (GenBank accession: MPBX01000005.1/bau-D9 CdiA type (De Gregorio *et al.*, 2019)), 1295549 (JFXB01000002.1/bau-B2), 426863 (JFYF01000002.1/ bau-B2), and ATCC19606 (JMRY01000015.1/bau-B2) in addition to their own CDI systems, also encoded genes that were nearly identical to the *cdiI* from *Ab*V15, indicating that these strains are potentially immune to CDI-mediated inhibition by *Ab*V15. Interestingly, the immunity genes were encoded in genomic regions that did not have a CDI system nearby, suggesting a possibility that orphan CDI immunity genes might be widespread among *A. baumannii* strains.

Domain analysis indicated that CdiB consisted of a canonical for Type Vb secretion systems β-barrel pore forming domain (Haemolysin secretion/activation, Pfam database access code: PF03865.13) and two periplasmic polypeptide transport-associated (POTRA) domains (PF08479.11 and PF17287.2), required for interaction with the substrate proteins (Fan *et al.*, 2016) (Fig. 3.8.1 B). Our bioinformatic analysis also identified a domain from opacity family porin proteins (PF02462.15), the function of which in CdiB is currently unclear.

CdiA domain analysis showed that the protein contained a conserved N-terminus signal peptide for the Sec-dependent secretion into the periplasm (PF13018.6). The signal sequence were followed by the two-partner secretion or hemagglutination activity domain, which is required for transport via CdiB across the outer membrane. CdiA also carried two filamentous hemagglutinin (FHA) regions on the N-terminal (FHA1) and C-terminal (FHA2) halves of the protein (Fig. 3.8.1 B). FHA1 has been shown recently to form a β-helix a filament that extends outside the cell, while the FHA2 region domain is sequestered along with CdiA-CT region in the periplasm of inhibitor cell (Ruhe *et al.*, 2018, 2017). The C-terminal half of the CdiA contained CdiA-CT region, which is demarcated by Pre-toxin domain with VENN motif (PF04829.13), and, upon binding the target cell, is cleaved and translocated (Fig. 3.8.1 A and B).

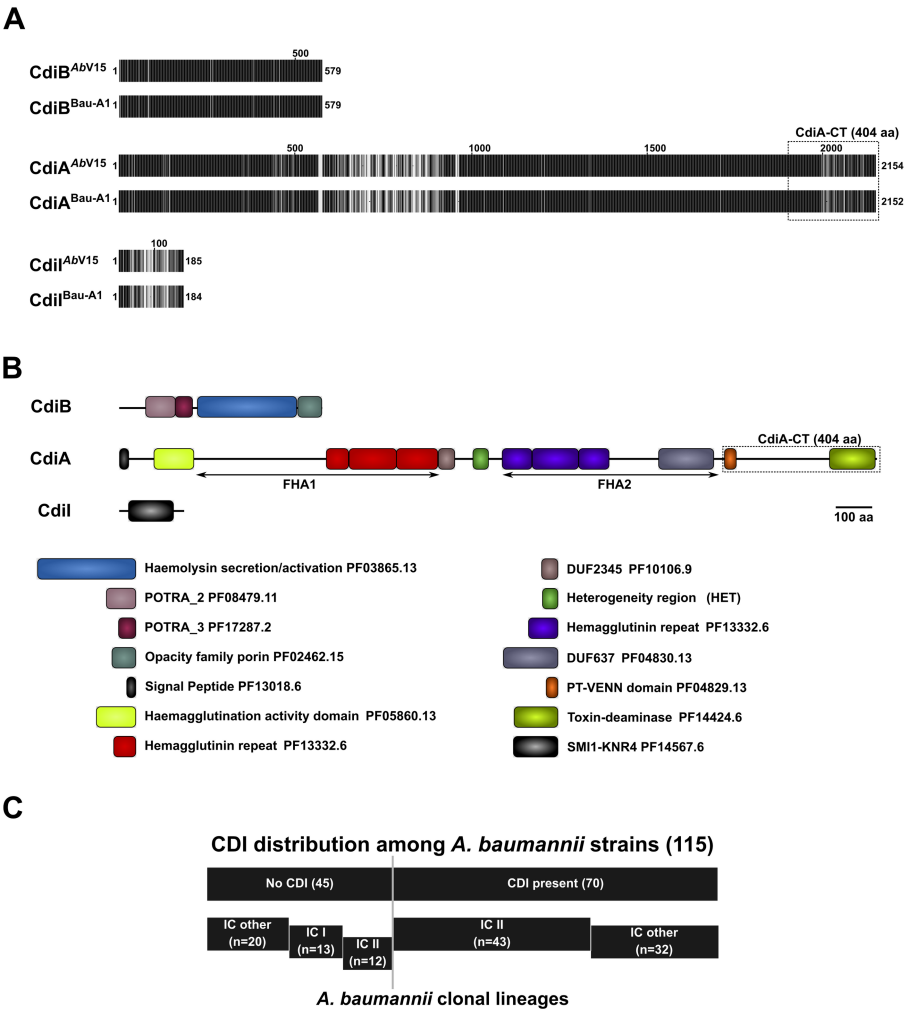

Fig. 3.8.1. (**A**) Multiple amino acid sequence alignment of proteins encoded by *Ab*V15 *cdiBAI* locus with the respective proteins from the most similar type-I CDI system (bau-A1/Genbank accession number: AMFH01000034.1) as determined by De Gregorio *et al.*, (2019). Alignments are displayed as sequence fingerprints that were generated by Texshade software (version 1.25) (Beitz, 2000). Identical and unique amino acids are shaded black and grey, respectively. (**B**) Schematic representation of the domain architectures of *Ab*V15 *cdiBAI* locus proteins. Pfam database accession codes are provided next to domain names. Domains were predicted using HHPRED server (Zimmermann *et al.*, 2018) as described in section 2.2.20. (**C**) The distribution of CDI systems in fully sequenced *A. baumannii* genomes. *A. baumannii* genomes were separated into international clonal lineage groups (IC) by performing *in silico* PCR using primers and the typing scheme described by Turton *et al.* (2007). Roman numerals (I or II) indicate clonal lineage. List of genomes analysed and their Genbank accession numbers are provided in Supplementary table 1. Note that some strains contain more than one CDI system.

Our analysis indicated that the CdiA-CT region contains a conserved toxin-deaminase domain (PF14424.6) from clade BURPS668_1122 (Iyer *et*

al., 2011). These domains were identified recently in a large array of a novel class of bacterial toxin systems, termed polymorphic toxin systems, which are multi-domain secreted proteins that have a toxin module at the C-terminus. The family that this domain has been classified to includes toxins that are secreted via various secretion systems, including T2SS, T5SS, T7SS, T6SS. Unfortunately, substrate preferences have not been determined. However, it was predicted that these enzymes should target cytidine on DNA and/or RNA (Iyer *et al.*, 2011). The CdiI immunity protein contained a Smi1/ Knr4 superfamily domain (PF14567.6), which is common among immunity proteins in bacterial polymorphic toxin systems (Iyer *et al.*, 2011) (Fig. 3.8.1 B).

Unfortunately, due to a weak sequence conservation we were unable to identify regions already known to be involved in the recognition of target cells (receptor binding domain), or cell surface presentation (YP domain) (Ruhe *et al.*, 2018). It was predicted that these domains are situated between two FHA repeat regions. However, we observed previously described heterogeneity (HET) region between the two FHA domains (Fig. 3.8.1 B). HET regions are predicted to form coiled-coils, the structural motif from at least two alpha-helices that are coiled together. It has been suggested that these sequences participate in a protein-protein interaction and possibly can act as receptor binding domains for CDI systems (De Gregorio *et al.*, 2018).

Lastly, we decided to evaluate the distribution of CDI systems among clinical *A. baumannii* isolates from our collection, representing different genotypically related groups (pulso-types) of strains belonging to the International Clone IC I (N=20) and IC II (N=16) lineages (Povilonis *et al.*, 2013). For this purpose, we have screened our isolates using primer pairs targeting *cdiB* genes from all *A. baumannii* encoded CDI systems and observed that the systems were absent in all *A. baumannii* strains assigned to the IC I lineage. In contrast, almost all IC II strains except II-g and II-h strains contained *cdiB* gene. These observations were confirmed by screening the completed *A. baumannii* genomes that are available in NCBI GenBank for the presence of CDI systems (Supplementary Table 1). By using a typing scheme developed by Turton *et al.* (2007), via *in silico* PCR, we assigned strains into international clonal lineages and observed that CDI systems were absent or truncated in all *A. baumannii* strains of international clonal lineage I, while present in the vast majority of strains identified as international clonal lineage II, thereby fully confirming our results obtained with clinical strains (Fig. 3.8.1 C).

Taken together these results indicate that IC I and IC II lineage strains potentially use diverse evolutionary adaptation strategies for intra-species competition via CDI.

3.9. *Ab*V15 CDI is used for intra-genus competition

BfmRS-dependent changes in the expression of *cdiBAI* locus prompted us to further investigate CDI system of *Ab*V15 strain. Firstly, we deleted nearly a whole *cdiA* gene along with *cdiI* in WT, *ΔbfmRS*, and *ΔbfmRSΔhcp* strains. We succeeded in a partial deletion only, due to the large genomic region of *cdiBAI*, which resulted in unsuccessful attempts to acquire clones with a fully deleted operon. We observed that the deletion resulted in the loss of approximately 200 kDa band in SDS-PAGE gel containing the total protein fraction precipitated from the culture media of *Δcdi* and *ΔbfmRSΔcdi* strains, when compared to their parent strains (Fig. 3.9.1). The size of the band corresponded to the predicted molecular weight of the CdiA protein, which is approximately 229 kDa, without a signal peptide. We confirmed the identity of the predicted protein by mass spectrometry analysis.

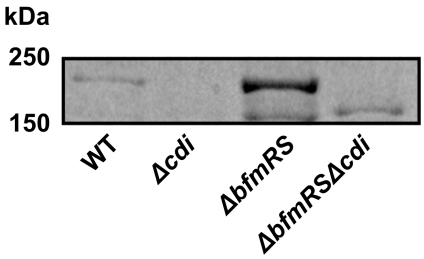

Fig. 3.9.1. 10 % Coomassie blue stained SDS-PAGE of trichloroacetic acid precipitated total protein fracion from growth media supernatants of *Ab*V15 (WT), and *Δcdi*, *ΔbfmRS*, *ΔbfmRSΔcdi* mutants. Numbers on the left denote molecular weight in kDa. Only the relevant part of a gel is shown.

Next, we performed competition assays with the following aggressor strains with presumably inactivated *cdi* loci: *Ab*V15 *ΔbfmRSΔcdi*, and *ΔbfmRSΔhcpΔcdi* mutants. The former mutant was expected to display only the T6SS activity, while the latter – no inhibitory activity towards a target strain. *Ab*V15 wild-type strain, the *ΔbfmRS* mutant, and the *ΔbfmRSΔhcp* mutant were used as positive controls. We have selected *A. baylyi* ADP1 as the target strain.

As can be seen in Fig. 3.9.2 A, the recovered ADP1 cell numbers from competition assays showed a gradual ~10-fold significant decrease with each deletion in the *ΔbfmRS* mutant. Interestingly, even the triple mutant displayed an aggressive phenotype. Although, it was attenuated when compared to either of the *ΔbfmRSΔhcp* or *ΔbfmRSΔcdi* mutans. This suggests the presence of an additional inhibition mechanism. It is reasonable to speculate that *Ab*V15 contains a second CDI locus, which we were unable to

detect with our PCR screen. The presence of two CDI systems have already been observed in some *Acinetobacter* sp. strains (Harding *et al.*, 2017).

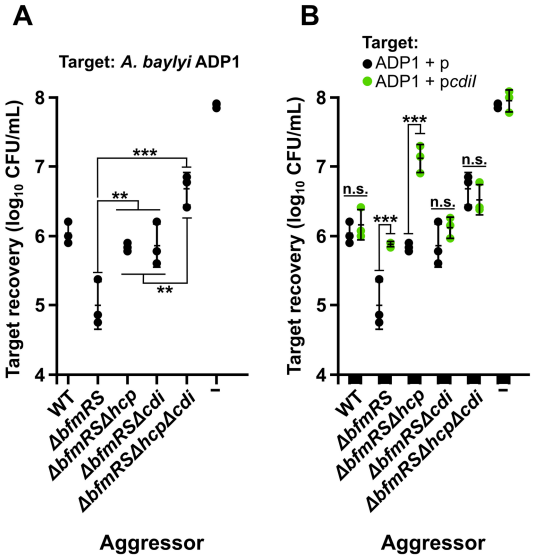

Fig. 3.9.2. Quantitative evaluation of inter-bacterial competition assay displaying recovered numbers of (**A**) *A. baylyi* ADP strain alone or (**B**) complemented with plasmid p*cdiI*, containing immunity gene *cdiI*. Competitions were performed under inducing conditions (5 mM IPTG) with the following strains used as aggressors: AbV15 (WT), *ΔbfmRS, ΔbfmRSΔhcp*, *ΔbfmRSΔcdi*, and *ΔbfmRSΔhcpΔcdi*. Aggressor-target ratio of 10:1 was used. Error bars represent standard deviation. *E. coli* DH5α was used as a negative non-competitive control. The horizontal lines represent mean value. **, $p<0.01$; ***, $p<0.001$; n.s., not significant.

Finally, we also performed competitions using plasmid with the cloned immunity gene *cdiI* under inducible promoter. The plasmid was transformed into *A. baylyi* ADP1. We hypothesized that if the killing was mediated via CDI system, the *cdiI* gene product should protect its host from the CDI activity. Results showed that p*cdiI* plasmid protected *A. baylyi* ADP1 from aggressors, which had a predicted active CDI system (*ΔbfmRS* and *ΔbfmRSΔhcp* mutants), while displayed no effect with the competitions against the predicted CDI-negative mutants (Fig. 3.9.2 B). It must be noted that we did not observe p*cdiI*-mediated increase in resistance towards *Ab*V15 wild-type strain (Fig. 3.9.2 B). We hypothesize, that this might be due to the down-regulated nature of CDI system as we observed that the deletion of *hcp* in *Ab*V15 nearly abolished the killing activity (Fig. 3.7.1 B). Together, these data show that the loss of *bfmRS* activates *Ab*V15 CDI system, which can be used against *A. baylyi* ADP1.

3.10. *Ab*V15 CDI system is used for intra-species competition

Primary targets of the CDI-mediated inhibition are organisms from the same species (Hayes *et al.*, 2014). Therefore, we hypothesized that competitions with *A. baumannii* strains should display increased efficiencies in terms of recovered cell numbers.

To test the hypothesis, we have selected two clinical *A. baumannii* strains II-g and II-h that did not contain a *cdiB* gene (as was described in section 3.8). Additionally, using a primer pair specific for the *cdiI* gene, encoded by *Ab*V15, we confirmed that these strains did not have genetically encoded immunity. All these data predicted that II-g and II-h strains should be susceptible to CDI-mediated attack from the *Ab*V15 strain.

Competition experiments showed that only the II-h strain was highly susceptible to CDI-mediated killing by the *ΔbfmRS* and *ΔbfmRSΔhcp* mutants, and displayed approximately 10^7-fold reduction in the recovered cell numbers (Fig. 3.10.1 A). When competitions were performed with mutants that also had a *cdi* loci deletions, we observed a ~10^2-fold decreased aggressiveness when compared to their parent strains (Fig. 3.10.1 A).

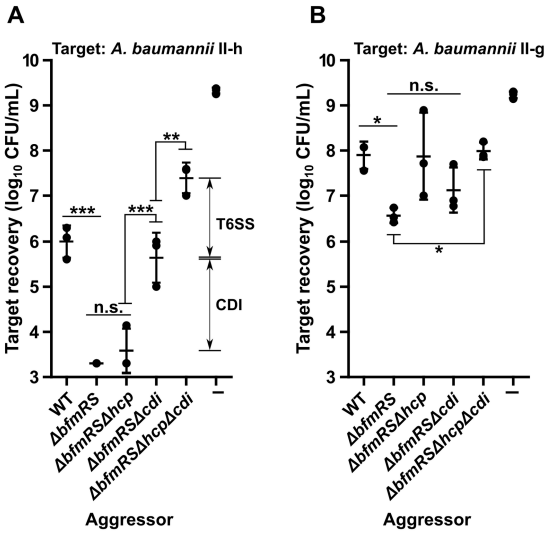

Fig. 3.10.1. Quantitative evaluation of inter-bacterial competition assay displaying the recovered numbers of *A. baumannii* target strains: (**A**) II-h and (**B**) II-g. Competitions were performed with the following strains used as aggressors: *Ab*V15 (WT), *ΔbfmRS*, *ΔbfmRSΔhcp*, *ΔbfmRSΔcdi*, and *ΔbfmRSΔhcpΔcdi*. Aggressor-target ratio of 20:1 was used. Error bars represent standard deviation. *E. coli* DH5α was used as a negative non-competitive control. The horizontal lines represent mean value. *, $p<0.05$; **, $p<0.01$; ***, $p<0.001$; n.s., not significant.

In comparison, the II-g strain showed a weak but significant susceptibility profile to the inhibitory phenotype displayed by the *ΔbfmRS* mutant (Fig. 3.10.1 B). However, because of weak susceptibility, we could not discern between the CDI and T6SS phenotypes using *ΔbfmRSΔhcp* or *ΔbfmRSΔcdi* mutants. We observed that only the *ΔbfmRSΔhcpΔcdi* mutant significantly

rescued the II-g strain, suggesting a cumulative effect of both systems (Fig. 3.10.1 B).

The wild-type *Ab*V15 strain, as expected, displayed mainly T6SS-dependent killing activity, with an overall greatly reduced efficiency, when compared to the *ΔbfmRS* strain (Fig. 3.10.2 A and B also Fig. 3.10.1 A and B).

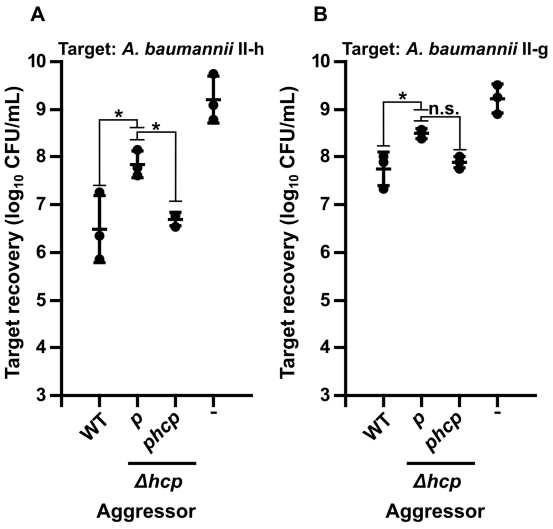

Fig. 3.10.2. Quantitative evaluation of inter-bacterial competition assay displaying the recovered numbers of *A. baumannii* target strains: (**A**) II-h and (**B**) II-g. Competitions were performed with the following strains used as aggressors: *Ab*V15 (WT), and *Δhcp* mutant alone or complemented with the plasmid p*hcp*. Aggressor-target ratio of 20:1 was used. Error bars represent standard deviation. *E. coli* DH5α was used as a negative non-competitive control. The horizontal lines represent mean value. *, $p<0.05$; n.s., not significant.

Based on the findings that *A. baumannii* II-h strain was highly resistant to CDI-mediated inhibition and the previous observation that complementation with plasmid p*bfmR* causes a down-regulation of *cdiBAI* locus, we hypothesised that we should observe a BfmR/BfmRS-mediated partial reduction of aggressive phenotype displayed by CDI-positive strains.

As can be seen in Fig. 3.10.3, the complementation of *ΔbfmRS* mutant with p*bfmR* or p*bfmRS* plasmids resulted in a ~30-fold increase of the recovery numbers of II-h strain, when compared to the non-complemented mutant. Additionally, when T6SS-negative but CDI-positive mutant (*ΔbfmRSΔhcp*) was complemented with the same plasmids, target recovery numbers increased by ~500-fold, compared to the non-complemented strain (Fig. 3.10.3). Lastly, the *ΔbfmRSΔcdi* and *ΔbfmRSΔhcpΔcdi* mutants which were predicted to be CDI-negative displayed no effect on the killing activity regardless complementation by p*bfmR* or p*bfmRS* plasmids (Fig. 3.10.3).

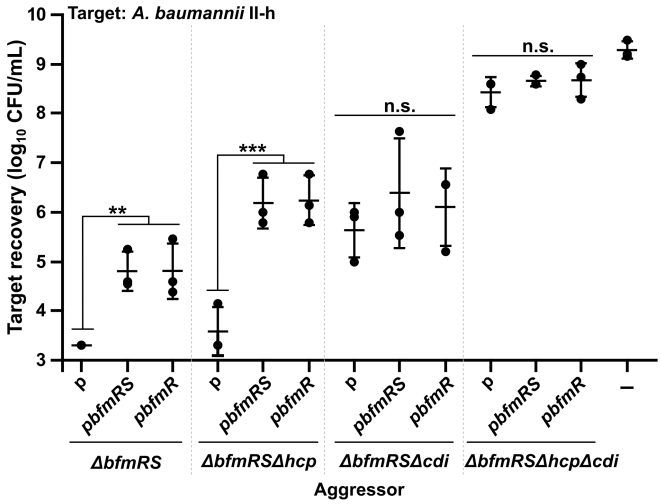

Fig. 3.10.3. Quantitative evaluation of inter-bacterial competition assay displaying the recovered numbers of *A. baumannii* target strain II-h. Competitions were performed with aggressors: *Ab*V15 (WT), and *ΔbfmRS*, *ΔbfmRSΔhcp*, *ΔbfmRSΔcdi*, *ΔbfmRSΔhcpΔcdi* mutants, which were complemented with either p*bfmRS* or p*bfmR*. Aggressor-target ratio of 20:1 was used. *E. coli* DH5α was used as a negative non-competitive control. Error bars represent standard deviation. The horizontal lines represent mean value. **, $p<0.01$; ***, $p<0.001$; n.s., not significant.

Taken together, these results show that *Ab*V15 encodes a CDI system which is active only against some *A. baumannii* strains. Additionally, our phenotypic results are consistent with the *cdiBAI* expression data, indicating that the BfmRS system negatively regulates the *Ab*V15 CDI system.

3.11. Role of capsule in the defence against CDI

We observed, that II-h and II-g *A. baumannii* strains, which were selected for the competition assay, differed in the ability to form capsule (Skerniškytė *et al.*, 2019c). Capsule-deficient strain, II-h, was more susceptible to CDI-mediated inhibition, when compared to capsule forming strain II-g (Fig. 3.10.1 A and B). The presence of capsule might help to hide receptors that a CDI system recognizes leading to a resistant phenotype. Therefore, we asked whether the inhibition of capsule formation would yield *A. baumannii* susceptibility to CDI-mediated inhibition.

We have selected three *A. baumannii* clinical strains, II-c, II-a1 and II-a, belonging to distinct genotypically-related groups – pulsotypes that (1) displayed capsule forming phenotype; (2) were resistant to CDI activity mediated by *Ab*V15 strain (evaluated by performing competition assays using an excess of aggressor to prey ratio of 10:1 (data not shown), and (3) did not have the same *cdi* locus (as determined by the presence of immunity

gene). Additionally, these strains showed differences in terms of resistance to desiccation, hydrophobicity, ability to be phagocytosed by macrophages, and virulence against *Caenorhabditis elegans* (Skerniškytė *et al.*, 2019c).

Firstly, *galU* gene deletions in the selected strains were generated. The gene encodes UTP-glucose-1-phosphate uridylyltransferase, which catalyses the formation of UDP-glucose from glucose-1-phosphate and UTP and is required for the production of capsule in *A. baumannii* (Geisinger and Isberg, 2015).

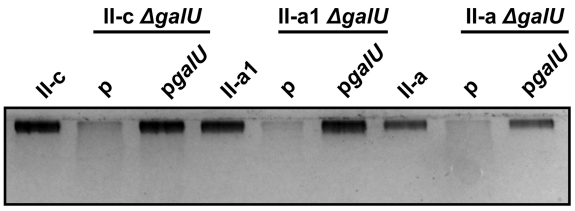

Fig. 3.11.1. 12.5 % SDS-PAGE gel showing capsular polysaccharide profiles of II-c, II-a1, II-a, and their *ΔgalU* mutants with or without the complementing plasmids p*galU* with the wild-type *galU*. Polysaccharides were stained with Alcian Blue.

We observed that the *ΔgalU* mutants lost the ability to produce polysaccharide as judged by 12.5 % SDS-PAGE followed by staining with polysaccharide specific stain Alcian Blue (Fig. 3.11.1). The phenotype was readily reinstated by complementation with p*galU* plasmids that contain the native *galU* genes (Fig. 3.11.1).

Then, we performed the competition assays using *A. baumannii* clinical strains II-c, II-a1, II-a, and their *ΔgalU* mutants with or without complementing p*galU* plasmids. The *Ab*V15 *ΔbfmRSΔhcp* strain was selected as an aggressor. It had an inactive T6SS (to eliminate influence of T6SS-mediated killing effect), but active CDI system, therefore was named as CDI+T6SS- strain. As a CDI-negative control, we selected *ΔbfmRSΔhcpΔcdi* mutant and named it as CDI-T6SS- strain.

The competitions showed that the loss of capsule greatly increased sensitivity to CDI-mediated inhibition of all three tested strains (Fig. 3.11.2 A-F). We observed a ~10^5-10^6-fold decrease in the recovered numbers of the capsule-negative target strains, when competitions were performed with CDI+T6SS-, but not with CDI-T6SS- aggressor strains (Fig. 3.11.2 A-F). The resistance phenotype was fully complemented with p*galU* plasmids (Fig. 3.11.2 A-F). Additionally, the complementation was apparent when the immunity gene was supplied *in trans* with p*cdiI* plasmid (Fig. 3.11.2 A-F).

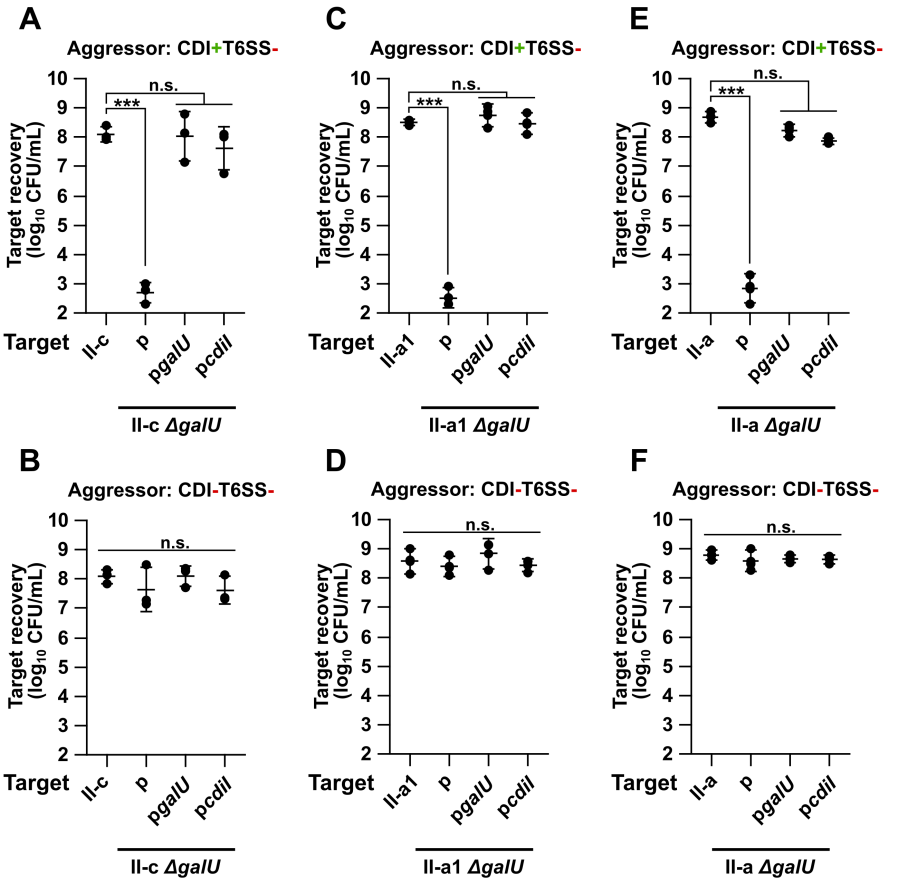

Fig. 3.11.2. Quantitative evaluation of inter-bacterial competition assay displaying the recovered numbers of *A. baumannii* target strains: (**A-B**) II-c; (**C-D**) II-a1; (**E-F**) II-a, and their *ΔgalU* mutants with or without the complementing plasmids p*galU* or p*cdiI*, encoding a wild-type *galU* or immunity to CDI genes, respectively. Competitions were performed with the following aggressors: (**A, C, E**) *ΔbfmRSΔhcp* (CDI+T6SS-), (**B, D, F**) *ΔbfmRSΔhcpΔcdi* (CDI-T6SS-). Aggressor-target ratio of 1:1 was used. Error bars represent standard deviation. The horizontal lines represent mean value. ***, $p<0.001$; n.s., not significant.

We also observed consistent results after the competitions performed with *Ab*V15 strains, which had an active T6SS system: The *ΔbfmRS* mutant with both active systems (CDI+T6SS+) outcompeted capsule-deficient *A. baumannii* strains, while *ΔbfmRSΔcdi* mutant (CDI-T6SS+) did not (Fig. 3.11.3 A-F). The phenotypes were fully complemented with p*galU* or p*cdiI* plasmids (Fig. 3.11.3 A-F).

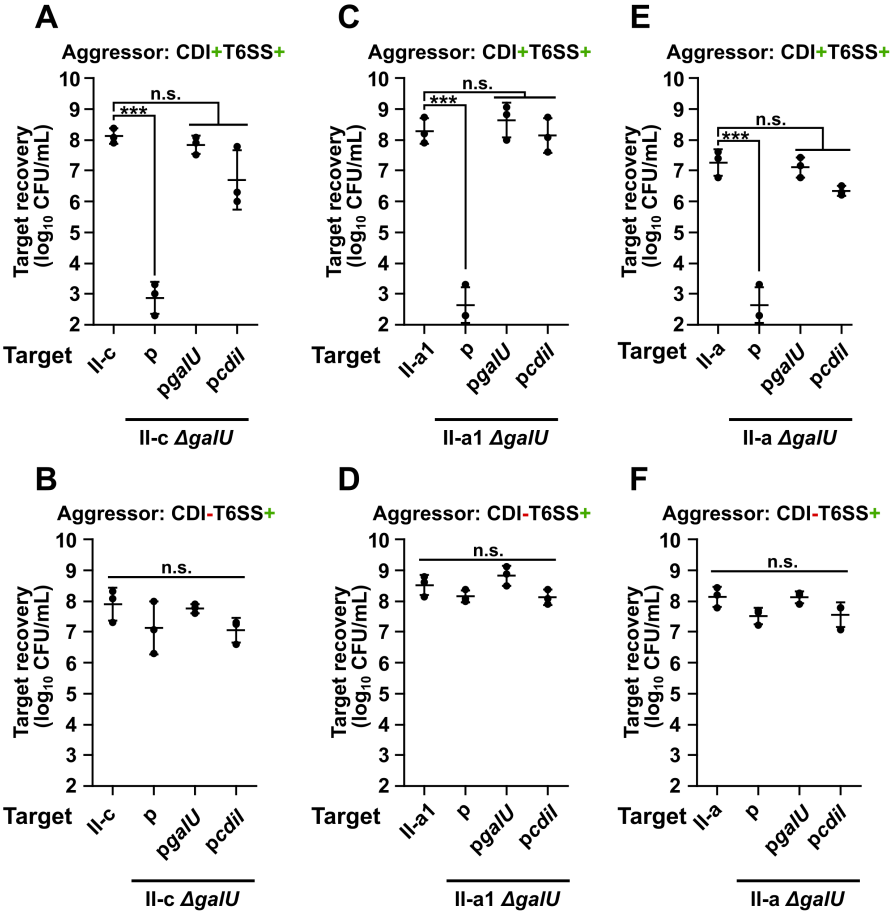

Fig. 3.11.3. Quantitative evaluation of inter-bacterial competition assay displaying the recovered numbers of *A. baumannii* target strains: (**A-B**) II-c; (**C-D**) II-a1; (**E-F**) II-a, and their *ΔgalU* mutants with or without the complementing plasmids p*galU* or p*cdiI*, encoding a wild-type *galU* or immunity to CDI genes, respectively. Competitions were performed with the aggressors: (**A, C, E**) *ΔbfmRS* (CDI+T6SS+), (**B, D, F**) *ΔbfmRSΔcdi* (CDI-T6SS+). Aggressor-target ratio of 1:1 was used. Error bars represent standard deviation. The horizontal lines represent mean value. ***, $p<0.001$; n.s., not significant.

Collectively, these data show that capsule is an essential structure that grants susceptible cells the protection against CDI system.

3.12. Strain-specific role of BfmRS in the protection against CDI

Recent results obtained with *A. baumannii* strain ATCC 17978 showed that the loss of BfmRS results in the reduced capsule polysaccharide synthesis (Geisinger *et al.*, 2018; Geisinger and Isberg, 2015). Based on these observations we hypothesized that the deletion of BfmRS system in our chosen clinical *A. baumannii* strains would lead to decreased capsule

production, which would subsequently increase the susceptibility against CDI.

To test our hypothesis we have generated a *ΔbfmRS* deletion in strains II-c, II-a1, and II-a and evaluated their capsule formation capabilities using 12.5 % SDS-PAGE followed by staining with polysaccharide specific stain Alcian Blue. As can be seen in Fig. 3.12.1, the mutants showed similar quantities of produced capsule, when compared to the respective WT strains. However, we noticed that mutants displayed slightly wider capsular polysaccharide profiles, which were reinstated to wild-type levels upon complementation with p*bfmRS* plasmid Fig. 3.12.1.

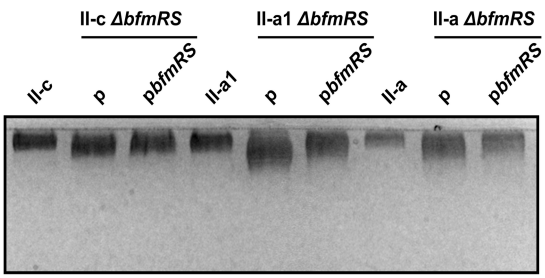

Fig. 3.12.1. 12.5 % SDS-PAGE gel showing capsular polysaccharide profiles of *A. baumannii* clinical strains II-c, II-a1, II-a strains, and their *ΔbfmRS* mutants with or without the complementing plasmid p*bfmRS* with a wild-type *bfmRS*. Polysaccharides were stained with Alcian Blue.

We considered a possibility that wider capsular polysaccharide profiles could indicate modifications in the general capsule structure, which could influence resistance to CDI phenotype. Therefore, we proceeded to perform competitions by selecting *Ab*V15 *ΔbfmRSΔhcp* mutant (CDI+T6SS-) as an aggressor, and II-c, II-a1, and II-a strains and their *ΔbfmRS* mutants with or without complementing p*bfmRS* plasmids, as the target strains. The results showed that only *ΔbfmRS* mutant of II-a strain was susceptible to CDI-mediated inhibition, as we observed a ~400-fold reduction in the recovered cell numbers, which were fully reinstated when the mutant was complemented with plasmids p*bfmRS* or p*cdiI* (Fig. 3.12.2 A)**.** When competitions were performed with CDI-T6SS- aggressor, the recovered cell numbers were similar between all tested strains (Fig. 3.12.2 B). The *bfmRS* deletion in the remaining two strains did not cause susceptibility to CDI-mediated inhibition. We observed that II-c *ΔbfmRS* mutant was susceptible to both CDI+T6SS- and CDI-T6SS- aggressors (Fig. 3.12.2 C and D). Since the phenotype was reinstated by complementation with p*bfmRS*, we speculated that the deletion possibly caused a grow deficiency in co-cultures due to the loss of *bfmRS*. The last strain, II-a1 *ΔbfmRS,* also displayed increased susceptibility to CDI+T6SS- and CDI-T6SS- aggressors (Fig. 3.12.2 E and F). However, the increase was small, when compared to

the observed profiles with strains II-c and II-a. Also, the phenotype could not be significantly complemented with either p*bfmRS* or p*cdiI* plasmids (Fig. 3.12.2 E and F).

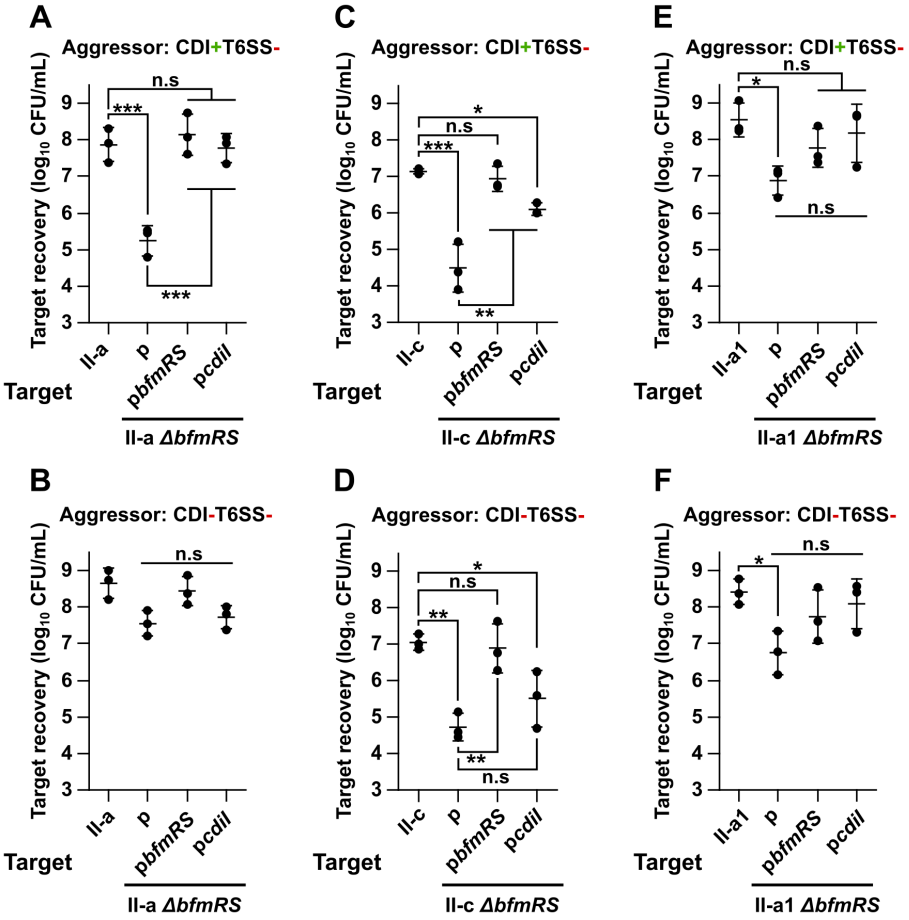

Fig. 3.12.2. Quantitative evaluation of inter-bacterial competition assay displaying the recovered numbers of *A. baumannii* target strains: (**A-B**) II-a; (**C-D**) II-c; (**E-F**) II-a1, and their *ΔbfmRS* mutants with or without the complementing plasmids p*bmfRS* or p*cdiI*, encoding a wild-type *bfmRS* operon or immunity to CDI genes, respectively. Competitions were performed with the following aggressors: (**A, C, E**) *ΔbfmRSΔhcp* (CDI+T6SS-), (**B, D, F**) *ΔbfmRSΔhcpΔcdi* (CDI-T6SS-). Aggressor-target ratio of 1:1 was used. Error bars represent standard deviation. The horizontal lines represent mean value. *, p<0.0; ***, p<0.01; **, p<0.001; n.s., not significant.

Taken together, these results show that *A. baumanni* BfmRS system plays a strain-specific role in the protection against CDI-mediated inhibition. Our observations also indicate that the loss of *bfmRS* does not cause an apparent

reduction in the quantity of capsular polysaccharides, suggesting that the protection is probably mediated via other mechanisms.

3.13. *In silico* analysis of differential expression of *A. baumannii* capsule synthesis loci

In order to identify additional conditions under which *A. baumannii* capsule loci genes and subsequently, capsule formation might be down-regulated, we screened published data on *A. baumannii* total transcriptome, proteome, and genome-wide transposon mutant libraries, and evaluated the expression changes of capsule loci gene products under different conditions. We included data from 81 studies (Supplementary table 2). The data were normalised by scaling values from 0 to 1 so expression ratios would be comparable between different experiments and plotted as a heat map (Fig. 3.13.1).

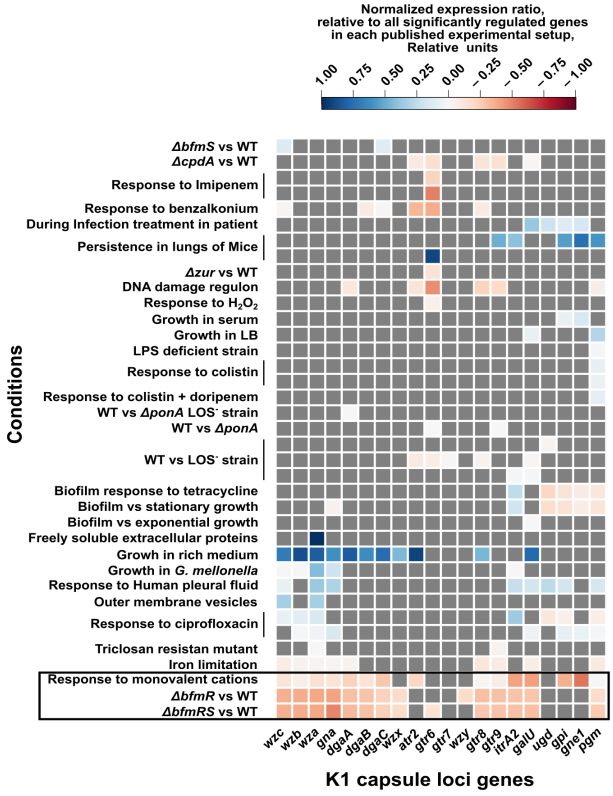

Fig. 3.13.1. Heat map showing aggregated results of differentially expressed K1 polysaccharide synthesis locus gene products that were observed in previously published studies. The map shows normalized relative value of change, when compared to all significantly expressed genes in a particular study. Graph was prepared as described in section 2.2.21. The left of the figure denotes conditions with differential change (for references see Supplementary table 2). The bottom of the figure denotes the names of genes from the locus.

Our analysis revealed only a few conditions that caused significant expression changes in the majority of capsule locus genes (Fig. 3.13.1).The down-regulation was evident in the *ΔbfmR* and *ΔbfmRS* background (Fig. 3.13.1). Moreover, we have observed that an increase in NaCl concentration to 200 mM caused the down-regulation of the majority of genes in the capsule locus (in the range of 2.1-7.4-fold) (Hood *et al.*, 2010) (Fig. 3.13.1). This suggested that under high osmotic conditions due to the down-regulation of capsule synthesis, bacterium might become susceptible to CDI-dependent inhibition. To test this hypothesis, we performed preliminary competition assays under final NaCl concentrations of 240 mM by competing II-a strain against *Ab*V15 *ΔbfmRSΔhcp* (CDI+T6SS-) and *Ab*V15 *ΔbfmRSΔhcpΔcdi* (CDI-T6SS-) strains. Unfortunately, the preliminary results did not reveal a predicted increase of susceptibility towards CDI-dependent inhibition.

3.14. *A. baumannii* secretes a functional CdiA into growth media

It has been well documented that CDI systems require a cell-cell contact to mediate their activity (Hayes *et al.*, 2014). These systems are composed of an outer-membrane β-barrel protein CdiB, which exports a large CdiA protein onto the cell surface, where it, only upon binding a target cell, translocates its C-terminal toxic domain (CdiA-CT) inside the cell (Hayes *et al.*, 2014).

Several studies have identified fragments of a CdiA protein in bacterial growth media. These fragments, in support to previous observations, did not display inhibitory activity (Aoki *et al.*, 2005; Webb *et al.*, 2013). However, it has been reported recently that the whole protein can be found in the secreted fraction of a CDI producing strain (Roussin *et al.*, 2019). In agreement with these results, we also observed the presence of secreted CdiA in growth media but not in cellular fraction of *Ab*V15 *ΔbfmRS* strain (Fig. 3.14.1).

In section 3.7 we also showed that *Ab*V15 *ΔbfmRS* strain displayed the up-regulated expression of CDI locus. Given these data we

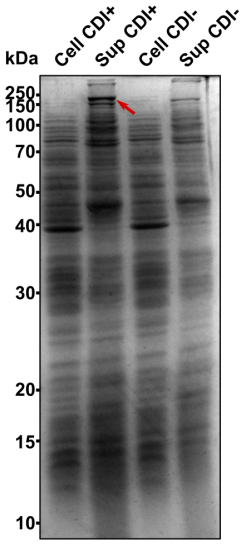

Fig. 3.14.1. Coomassie blue stained 12.5% SDS-PAGE gel containing either total cellular protein fraction (Cell) or trichloroacetic acid precipitated total protein fraction from culture media (Sup) of *A. baumannii* V15 *ΔbfmRS* (CDI+) and *ΔbfmRSΔcdi* (CDI-) strains. Numbers on the left denote molecular weight in kDa. Red arrow denotes CdiA.

asked whether the supernatant of CDI+ strain would be toxic to capsule-negative and susceptible to CDI-mediated inhibition *A. baumannii* strains that we characterised in section 3.11.

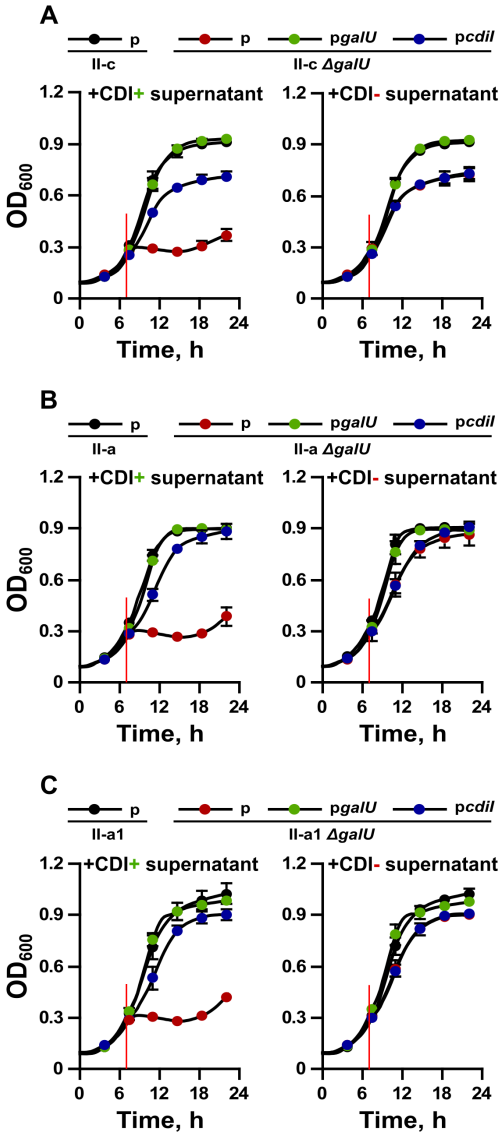

Fig. 3.14.2. Growth inhibition assays of *A. baumannii* clinical strains: (**A**) II-c; (**B**) II-a; (**C**) II-a1; and their *ΔgalU* mutants with or without plasmids p*galU* or p*cdiI*, encoding a wild-type *galU* or immunity to CDI genes, respectively. Red vertical lines denote the time when 10 µL of 0.22 µm filtered culture media from *ΔbfmRS* (CDI+) or *ΔbfmRSΔcdi* (CDI-) were added. Error bars represent standard deviation.

In order to answer this question, we grew capsule-negative (*ΔgalU*) *A. baumannii* strains II-c, II-a, II-a1 until early logarithmic stage and supplied them with 0.22 µm-filtered supernatant fractions of CDI+ and CDI- strains and allowed the growth to continue. Remarkably, we observed that the supernatant from CDI+ strain but not from CDI- strain resulted in a complete growth inhibition of *ΔgalU* strains (Fig. 3.14.2 A-C). The susceptible strains were rescued by complementation with either p*galU* or p*cdiI* plasmids, restoring either capsule formation or resistance to CDI due to the expression of immunity protein (Fig. 3.14.2 A-C). These results indicate that *Ab*V15 supernatants display a CDI activity.

To confirm that the activity is mediated by a full length CdiA protein but not its CdiA-CT domain, we purified the toxic component from growth media and estimated its molecular weight by performing size exclusion chromatography. We hypothesized that if toxicity is

mediated via a full length CdiA we should observe a molecular weight of ~229 kDa, while the predicted weight of only CdiA-CT domain is ~ 44 kDa (the domain prediction was based on the presence of VENN motif at the C-terminus of CdiA (section 3.8).

The CdiA protein was purified using ammonium sulphate precipitation, hydrophobic interaction chromatography and protein concentration with the molecular weight cut-off of 100 kDa. The obtained purity of CdiA was determined to be ~70 % (Fig. 3.14.3 A). The molecular weight of the protein was estimated by size-exclusion chromatography to be approximately 152 kDa (Fig. 3.14.3 B), suggesting that only a part of the full CdiA is secreted into the growth media.

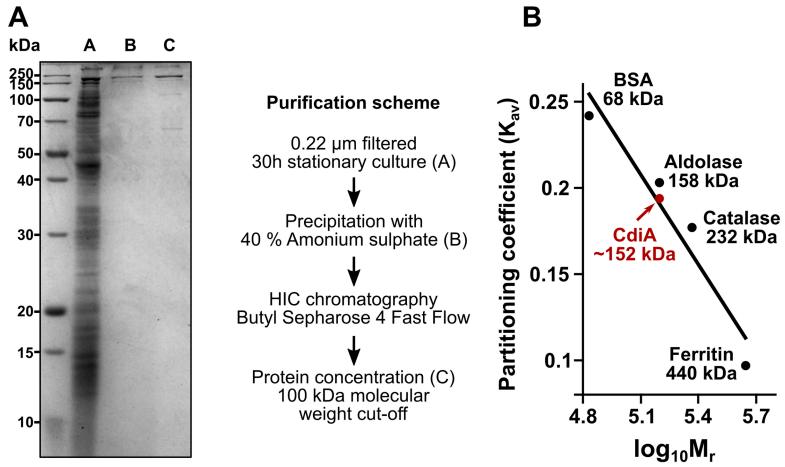

Fig. 3.14.3. (**A**) 12.5% SDS-PAGE view gel CdiA purification results after each purification step, according to the scheme on the right. Numbers on the left of the gel denote molecular mass in kDa. Bands in the gel were stained with Coomassie Brilliant Blue. (**B**) Calibration curve used to determine the molecular weight of CdiA by size-exclusion chromatography. The curve was obtained by calculating partition coefficient K_{av} versus the logarithm of molecular weight standards. Black dots denote proteins used for the calibration curve. Red dot denotes estimated CdiA molecular mass from the curve.

In order to identify, how potent the toxin is, we also have determined the minimum inhibitory concentration (MIC) of CdiA against the *ΔgalU* strains. We calculated that the MIC values of the mutants were 1.25 µg/mL (or 8 nM), while the wild-type strains or mutants complemented with p*galU* or p*cdiI* plasmids displayed at least 10 times higher MIC values. These results indicate that the purified CdiA displays antimicrobial activity, comparable to that of colicins (Sharma *et al.*, 2009), which are toxic proteins, produced by *E. coli* to kill related target cells (Cascales *et al.*, 2007) (please see the Discussion for the brief description of colicin biology).

Altogether, the obtained data show that *Ab*V15 secretes a largely intact CdiA protein into the growth media which retains its activity and enables CDI inhibition without a direct cell-cell contact.

3.15. CdiA inhibits the growth of target cells

Reduced cell recovery numbers after competitions could indicate either that cells were killed, or the growth was inhibited resulting in a persister-like state, where bacteria do not actively divide. Published data, regarding the mechanisms of CDI systems indicate that toxins can perform their activities in both ways (Aoki *et al.*, 2009; Roussin *et al.*, 2019).

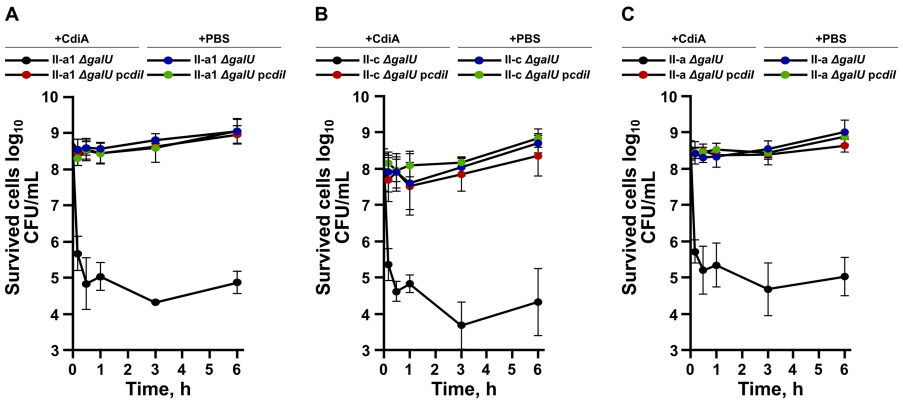

Fig. 3.15.1. Time-dependent viability assay of *ΔgalU* mutants of *A. baumannii* clinical strains II-a1 (**A**), II-c (**B**), II-a (**C**), with or without the complementing plasmid p*cdiI* encoding the immunity to CDI gene. The viability was assessed by mixing strains with either PBS or purified CdiA and evaluating the remaining bacterial colony forming units (CFU) by plating ten-fold dilutions after 0 min, 10 min, 30 min, 1 h, 3 h, 6 h. Values were calculated from at least three independent experiments. Error bars represent standard deviation.

To evaluate the mode of action of CdiA, we first performed viability assays, where over a period of six hours we estimated the recovered cell numbers of the target bacteria that were premixed with the purified CdiA protein. The PBS buffer was used as a negative control. As target bacteria, we selected *ΔgalU* mutants of II-c, II-a1, and II-a strains with or without p*cdiI* plasmid encoding immunity gene. The results revealed that the CdiA concentration 4 times higher the MIC value (section 3.14) on the 10^8 CFU/mL of starting culture of all *ΔgalU* strains, caused a ~500-fold reduction of the cell count after only 10 minutes (Fig. 3.15.1 A-C). Recovered cell numbers remained relatively unchanged for at least another six hours (Fig. 3.15.1 A-C). Control experiments using strains with

immunity gene (complemented with p*cdiI*) or when cultures were premixed with PBS, did not significantly affect the recovery (Fig. 3.15.1 A-C).

Viability experiments were coupled with a live/dead bacteria cell staining using a mix of SYTO9 and Propidium iodide dyes. Green SYTO9 stains all cells in a population, while red propidium iodide enters and stains cells with a damaged cytoplasmic membranes, allowing to discern living and dead cells.

For live/dead staining assay, we selected II-a1 strain and its *ΔgalU* mutant with or without complementing plasmids p*cdiI* or p*galU*. All strains before staining were pre-incubated in either PBS (live control), 2-propanol (dead control) or purified CdiA protein solution for 30 minutes or for 3 hours. The results are presented in Figure 3.15.2.

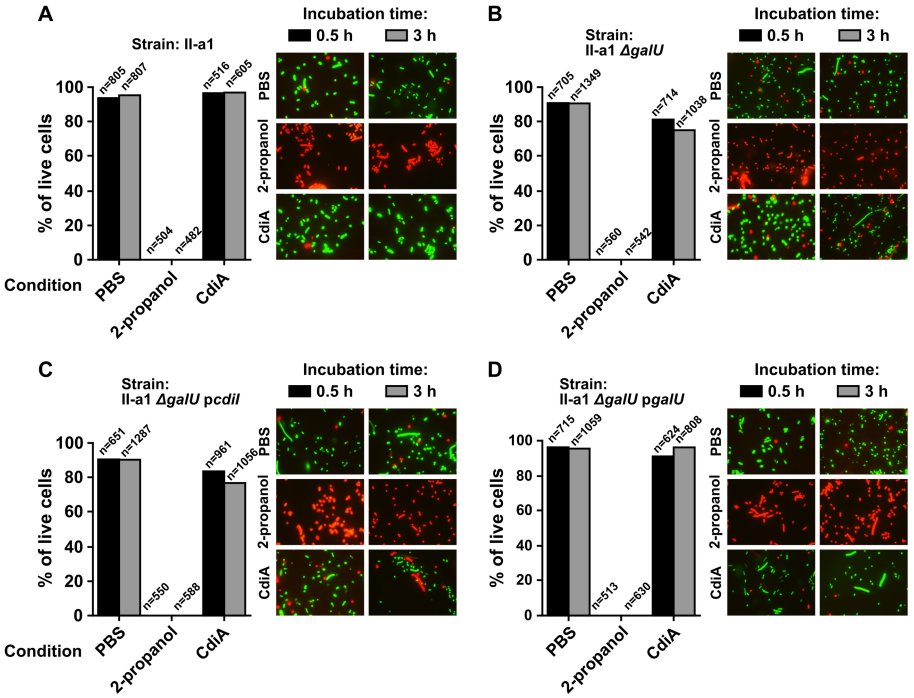

Fig. 3.15.2. Live/dead assays performed with the following *A. baumannii* strains: II-a1 (**A**), its *ΔgalU* mutant (**B**), and the mutant, complemented with plasmids p*cdiI* (**C**) or p*galU* (**D**), encoding immunity to CDI gene or the wild-type *galU* gene, respectively. Bacteria, before each assay, were treated for 30 minutes or 3 hours with either PBS (Live control), 2-propanol (dead control), or purified CdiA. Graphs display the quantitative evaluation of live bacteria from multiple microscopic images. Cells were visualized at 1000x magnification with a fluorescence microscope Olympus AX70 equipped with 100x/1.35 oil immersion lens and WIBA (460–490 nm for excitation and 515–550 nm for emission) and MWG (510-550/590) filter cubes for SYTO9 and propidium iodide, respectively. Numbers above columns indicate total number of bacterial cells counted.

The staining experiments showed that the wild-type II-a1 cells were apparently unaffected by the presence of CdiA and more than 90 % of them were alive independent from the incubation time with the protein (Fig. 3.15.2 A). This data were consistent with the viability calculations for this strain (data not shown). Interestingly, we observed that the majority of II-a1 *ΔgalU* mutant cells that were pre-incubated with the purified CdiA protein for either 30 minutes or 3 hours, still stained green (Fig. 3.15.2 B). The quantitative analysis indicated a slightly reduced live cell numbers – from 90-95%, when incubated with PBS, to ~75-80% after the pre-incubation with CdiA (Fig. 3.15.2 B).The *ΔgalU* mutant, complemented with plasmid p*cdiI*, stained similarly (Fig. 3.15.2 C), while complementation with p*galU* resulted in the indistinguishable from the WT phenotype (Fig. 3.15.2 D).

Together, these data indicate that the observed approximate 1000-fold reduction in survived *ΔgalU* mutant cells in the viability assay after either 30 minutes or 3 hours (Fig. 3.15.1 A-C) might have been caused due to the ability of CdiA to mainly inflict target cell growth arrest.

Conclusion.

Our main findings presented in this thesis are summarized in Fig. 3.15.3.

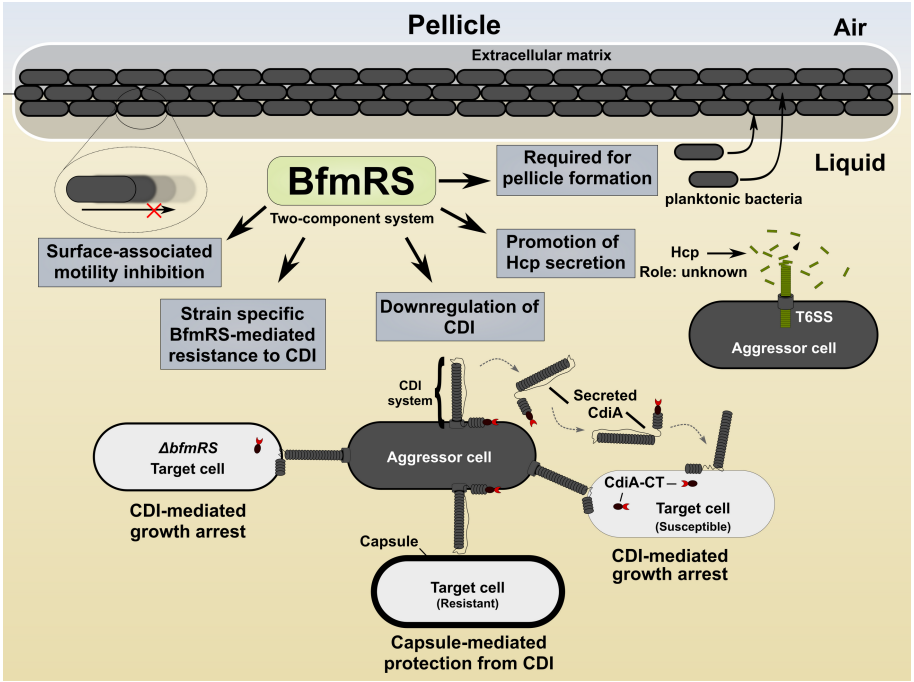

Fig. 3.15.3. Main findings presented in this work regarding the role of *Acinetobacter baumannii* BfmRS system in the environmental fitness and inter-bacterial competition.

We showed here that the two-component BfmRS system from *A. baumannii* reciprocally regulates two physiologically different processes: motility and pellicle formation. We also determined that it regulates intra-species competition via the repression of a CDI system. Peculiarly, we observed that BfmRS might mediate the resistance to CDI competition by strain specific mechanism. However, we noticed that capsule formation might represent a more universal defence mechanism from CDI. Lastly, we are the first to show that due to the secretion of toxic component, which causes target cell growth arrest, CDI inhibition in *A. baumannii* does not require a cell-cell contact.

4. DISCUSSION

In this work we aimed to further our understanding of the role of BfmR regulator from the two-component system BfmRS and its regulatory circuit that might enable *A. baumannii* to better adapt, persist, and spread in clinical settings. Carbapenem-resistant *A. baumannii* is currently classified under the priority 1 pathogens by the World Health Organisation, which indicates that the research and development of new antibacterial strategies against the pathogen is critically important (Tacconelli *et al.*, 2018). Knowledge regarding how organisms interact and respond to their surroundings is key for the design of potential treatment schemes.

One of the mechanisms employed by bacteria to interact with the environment is via two-component signal systems (Groisman, 2016). The ability to manipulate core regulatory circuit of *A. baumannii* might aid in a more efficient control in preventing the persistence of the pathogen in the environment. One of the mechanisms that *A. baumannii* employs to survive under the unfavourable conditions is via biofilm formation, which is regulated by the BfmRS two-component system (Tomaras *et al.*, 2008).

Here, we showed that BfmR regulator does not require the sensor kinase BfmS to reinstate surface biofilm formation. It is well known that bacterial response regulators of two-component systems require phosphorylation of their conserved aspartate to stimulate their activity (Zschiedrich *et al.*, 2016). However, in the case of *A. baumannii* BfmRS system, it has been suggested that BfmS sensor acts negatively on the BfmR regulator by phosphorylating it, resulting in its inactivation (Farrow *et al.*, 2018; Geisinger *et al.*, 2018; Geisinger and Isberg, 2015). Therefore, our data are in agreement with the proposed mechanism of regulation.

This mechanism can also explain a previously observed phenotype, where the mutation of *bfmS* results in the reduction of *A. baumannii* surface-associated motility (Clemmer *et al.*, 2011). The activation of BfmR due to the loss of BfmS might cause the inhibition of the phenotype. Our results confirm this hypothesis as we showed that overproduction of BfmR or BfmRS in the *ΔbfmRS* background completely inhibits *A. baumannii* motility phenotype.

Taken together our findings suggest that BfmR is responsible not only for the promotion of biofilm formation but also for the repression of motility phenotype under inducing conditions, indicating that BfmR can function as a switch from motile to non-motile phases in *A. baumannii* lifestyle. This is

also confirmed by our observations that the loss of *bfmRS* or *bfmR* genes only slightly reduced the surface-associated motility phenotype while the twitching motility was unaffected.

It has been hypothesized, that during the transition to a biofilm lifestyle, the transition from motile to non-motile state might be advantageous for bacteria (Guttenplan and Kearns, 2013). Such phenotype might allow bacteria to conserve energy and do not waste it on two contrasting behaviours. Interestingly, the signalling molecule cyclic-di-GMP (c-di-GMP), composed of two GMP moieties fused into the macrocyclic ring by GGDEF domain containing diguanylate cyclase, regulates motility to biofilm transition in bacterial cells. High levels of c-di-GMP promote biofilm formation, while low levels activate motility (Jenal *et al.*, 2017). A recent analysis of GGDEF domain containing proteins in *A. baumannii* ATCC 17978 showed that the overexpression of some diguanylate cyclases completely abolished surface-associated motility and promoted Csu pili-mediated biofilm formation (Ahmad *et al.*, 2020). Interestingly, one of the diguanylate cyclases tested that completely inhibited motility under the overexpression is encoded nearby the *bfmRS* locus (Fig. 1.11) (Ahmad *et al.*, 2020). This suggests that BfmR-mediated inhibition of surface-associated motility might be enacted via the nearby encoded diguanylate cyclase.

Our investigation into the prevalence of motility phenotypes among clinical *A. baumannii* isolates revealed that the majority of them displayed only minor ability to perform surface-associated motility, suggesting that this phenotype is either not widespread or is repressed under laboratory conditions. Currently, it is unclear how exactly *A. baumannii* mediates surface-associated motility, but it is suggested that multiple factors determine this phenotype (Harding *et al.*, 2018). On the contrary, we observed a clear distinction between isolates in the ability to perform twitching motility as mainly IC I lineage isolates displayed this phenotype. It is known that this phenotype in *Acinetobacter* sp is regulated by Type IV pili (Harding *et al.*, 2013). Our findings could be explained by a recent observation that Type IV pili experienced a specialisation in *A. baumannii* clonal lineages resulting in pilus types that due to the differences in surface electrostatics promote either motility (International clone I) or biofilm formation (International Clone II) (Ronish *et al.*, 2019).

In this study we showed that BfmR is essential for the formation of *A. baumannii* pellicle. It is suggested that this structure is superior to the surface attached biofilms, as it not only allows to persist in hospital environments but also could potentially facilitate the spread via droplets

(Armitano *et al.*, 2014; Nait Chabane *et al.*, 2014). Another advantage against surface biofilms is that pellicle allows bacteria to acquire a favourable ecological niche enabling direct access to oxygen and nutrients from the air and liquid, respectively (Armitano *et al.*, 2014). A recent proteomics study identified multiple virulence factors expressed in the pellicle, suggesting that this phenotype might play an important role in the pathogenesis of *A. baumannii* (Kentache *et al.*, 2017).

The role of BfmRS in pellicle formation supports observations that mature pellicles contain increased BfmR levels (Kentache *et al.*, 2017). Furthermore, it has been recently determined that BfmRS regulated Csu pili are not only required for pellicle formation (Ahmad *et al.*, 2020), but also their component, CsuA/B pilin, has been found to be the most abundant protein in *A. baumannii* pellicle (Nait Chabane *et al.*, 2014). These results explain our observed BfmR-dependent phenotype as the BfmRS system is responsible for the transcriptional regulation of *csuA/BABCDE* locus (Tomaras *et al.*, 2008).

Our screen of clinical *A. baumannii* isolates revealed that pellicle formation was a nearly exclusive phenotype among IC I lineage strains. And although, we observed twitching motility only among the same lineage strains, we could not conclude that these phenotypes are connected as we observed strains, which formed pellicles but did not twitch. A recent study indicated that *A. baumannii* Type IV pili are not required for pellicle formation, as the deletion of *pilA* did not impact the phenotype (Ahmad *et al.*, 2020). Therefore, it is likely that these traits are not related.

A. baumannii pellicle has been shown to also display an increased expression of some T6SS locus genes (Kentache *et al.*, 2017). T6SS systems are widespread among Gram-negative bacteria and are mainly involved in competition among bacteria (Coulthurst, 2019). Interestingly, we found that the supernatants of the *Ab*V15 pellicle contained increased Hcp protein secretion in a BfmR-dependent fashion. This protein is a structural component of T6SS, which with additional proteins assembles into a needle-like apparatus (Coulthurst, 2019). Hcp secretion correlated with the changes in the expression of *hcp* and *tssM* genes that are essential components for the assembly of T6SS apparatus. Given the multiple observations that the secretion of Hcp is a direct indication of an active Type VI secretion system (Pukatzki *et al.*, 2009), we assumed that we should observe an increased killing efficiency against competing bacteria. However, our results revealed that apparent changes in the secretion of Hcp did not correlate with the aggressiveness mediated via T6SS. These results suggest that BfmRS is not

responsible for T6SS-mediated inter-species competition. On the other hand, the increased secretion of Hcp indicated that the protein might participate in other physiological processes of *A. baumannii*.

Type VI secretion systems have been reported to mediate metal ion uptake by the secretion of metal ion scavenging proteins into the extracellular media (Coulthurst, 2019). Additionally, there was an observation of T6SS contribution towards biofilm formation of *Pseudomonas fluorescens* (Gallique *et al.*, 2017). However, our data indicate that a functional *A. baumannii* T6SS does not contribute to biofilm formation nor is required for the uptake of metal ions, when grown under ion-chelating conditions in the presence of EDTA (data not shown).

It is worth noting that the secretion of Hcp into the growth media and hence the T6SS-mediated antibacterial activity is not a universal phenotype among *A. baumannii* as there were observations that some clinical multi-drug resistant strains showed transcriptional activity of *hcp* but did not release the encoded protein into the media and/or killed target cells (Repizo *et al.*, 2015). These observations are consistent with our data indicating that the vast majority of clinical *A. baumannii* isolates did not show an apparent Hcp secretion into the growth media. Recently, it was observed that the activity of *A. baumannii* T6SS is regulated by the two repressors, *tetR1* and *terR2,* which are found on a large conjugative plasmid conferring antimicrobial resistance. Isolates in a colony can lose or gain the plasmid resulting in the increased overall fitness of the colony. Isolates without the plasmid can defend the colony from invaders using T6SS, while individuals with the plasmid ensure the survival of the community under antibiotic pressure (Weber *et al.*, 2015b). However, our PCR screen for these repressors failed to detect them in our collection of isolates, suggesting another T6SS regulatory mechanisms.

In this work we observed that BfmRS is responsible for the down-regulation of contact-dependent growth inhibition system (CDI) of *A. baumannii* V15 strain. These systems belong to a group B of two-partner secretion family, that is a part of Type V secretion systems. CDI systems are composed of a membrane beta-barrel protein (CdiB) that translocates a large exoprotein (CdiA) onto the cell surface. These translocated proteins via their receptor binding domains can recognise, bind, and transfer a CdiA-CT region, encoding a toxic module, into the target cell. This results in growth inhibition or cell death depending on the mechanism of action of a toxin. The auto-inhibition is prevented by a third CDI module, encoding an immunity

gene, whose product binds to and neutralises CdiA-CT activity (Willett *et al.*, 2015b).

Due to the necessity to bind the receptor, CDI is limited only within related bacteria species (Hayes *et al.*, 2014). Our results are consistent with these observations, as we detected the activity against *A. baumannii*, but not against *E. coli* MC4100, *P. aeruginosa*, and *K. pneumoniae*. However, there are a few instances, where CDI systems are used to out-compete strains from related species (Beck *et al.*, 2014; Koskiniemi *et al.*, 2015). Our results show that *A. baumannii* V15 can also out-compete related species – *Acinetobacter baylyi* ADP1 in a CDI-dependent manner. This indicates, that the CDI system targets a rather conserved receptor between these two species.

Interestingly, our bioinformatic analysis showed that CDI systems were absent in clinical *A. baumannii* strains belonging to the IC I international clonal lineage, while the vast majority of the IC II lineage strains carried a CDI module. Such a clear distinction in terms of CDI carriage between worldwide spread *A. baumannii* clonal lineages was not observed before, and the potential of the IC II strains to antagonize related IC I strains might, at least partially, explain the worldwide predominance of this clonal lineage (Karah *et al.*, 2012). However, our analysis showed that some *A. baumannii* strains encoded genes that were nearly identical to the *cdiI* from *Ab*V15. These genes did not have the remaining *cdi* locus components nearby, indicating that not only these isolates are potentially immune to a CDI-mediated inhibition by *Ab*V15, but also it is possible that the accumulation of immunity modules might be widespread among *A. baumannii*.

Our competition assays using clinical *A. baumannii* strains of IC II lineage, that did not contain a known *cdi* locus, revealed that only one of them was susceptible to CDI-mediated inhibition. We observed that the susceptible isolate was capsule-deficient. Since capsule over-production has been previously shown to mediate the resistance against CDI-mediated attack in *E. coli* (Aoki *et al.*, 2008), we asked whether this is also true in *A. baumannii*. Our data allowed to reach a conclusion that *A. baumannii* capsule is indeed an essential phenotypic trait determining the resistance against CDI-mediated inhibition.

A. baumannii capsule formation has been evaluated by a number of studies. Currently, it is considered as one of the main mechanisms that allows the pathogen to survive under desiccation conditions (Harding *et al.*, 2018). It is hypothesised that due to the ability to retain water, capsule polysaccharides can prevent lethal desiccation (Espinal *et al.*, 2012). Also, capsule is essential to defend against complement system, indicating the

important role of this structure in virulence (Russo *et al.*, 2010). Interestingly, there have been reports showing that the loss of capsule results in the increased hydrophobicity, which in turn promotes adherence to surfaces (Kempf *et al.*, 2012; also our unpublished data). This phenotype might aid in the establishment of biofilm communities on surfaces or allow to invade already established ones. In the latter scenario, CDI-mediated inhibition might be an effective defence strategy for the population in the already established biofilm. In agreement, recent data indicate that CDI-positive cells tend to exclude susceptible cells from biofilm formation (Anderson *et al.*, 2014).

In contrast, capsule polysaccharide formation or its absence might be better suited phenotype for different environments. A recent study identified a transcription regulator, which mediates the phenotypic switch of *A. baumannii* isolate AB5075 from virulent opaque phenotype to avirulent translucent phenotype. Interestingly, one of the differences between these two types is that opaque colonies demonstrated a 2-fold increase in capsule thickness (Chin *et al.*, 2018). The study authors hypothesized that the phenotype with reduced capsule production was better suited for life in natural environments due to the increased expression of genes required for the catabolism and uptake of nutrients from various different sources. In addition, the transcription of regulatory factor was more pronounced in lower temperatures, further confirming these suggestions (Chin *et al.*, 2018).

We have shown in this study, that *A. baumannii* V15 is able to secrete a functional CdiA protein into the growth media. This suggests that at least for this strain, a cell-cell contact is not essential to mediate CDI-inhibition. To the best of our knowledge, this is the only observation showing the release of functional CdiA from the cell. Previously, it was shown that only non-functional fragments of CdiA can be released and found in supernatants (Aoki *et al.*, 2005). Our findings suggest that *A. baumannii* CDI-mediated inhibition can influence the growth of susceptible bacteria over the distance, thereby greatly expanding its sphere of influence.

This makes CdiA mechanism more similar to a colicin-like bacteriocins, which are diffusible, receptor-specific, cytotoxic molecules, that translocate their C-terminal domain into the target cell. Their structural organization consisting of N-terminal receptor binding domain, central translocation domain and C-terminal cytotoxic domain resembles that of CdiA (Cascales *et al.*, 2007). Both of these systems are highly species-specific (Cascales *et al.*, 2007; Ruhe *et al.*, 2017). However, colicin production is induced during the SOS response, and the majority of them are released due to cell lysis or

inefficiently via leakage (Cascales *et al.*, 2007). These mechanisms of release are not energy efficient and might lower the overall fitness of a population. On the contrary, CDI export mechanism involves translocation of CdiA protein via its dedicated transporter CdiB (Hayes *et al.*, 2014). This mechanism is much more efficient and sustainable. Additionally, most of the colicin-like bacteriocins are encoded on plasmids, which could result in an easy horizontal spread of immunity among strains. In fact, in natural *E. coli* populations it was found that the frequency of toxin producer strains was up to 50%, while the combined frequencies of resistant strains reached up to 98% (Cascales *et al.*, 2007). It is worth noting that the majority of CDI systems are located on predicted genomic islands, indicating that these systems are/were mobile (Danka *et al.*, 2017). Recent data indicate that these systems might perform a stabilisation of mobile genetic elements as the bearers are constantly under the supervision of sibling cells in a population (Ruhe *et al.*, 2016). This suggests a limited horizontal spread of CDI systems.

In this work, we also estimated the secreted CdiA size to be approximately of 152 kDa, while the full size of the protein is predicted to be ~ 229 kDa. This raises a question of how CdiA is released from the cell surface? It has been suggested that CdiA, after the export to the outer membrane, remains non-covalently bound to CdiB (Willett *et al.*, 2015b). This indicates that the toxin could shed into growth media naturally. However, the determined molecular weight suggests that it is present in growth media as not a full-sized protein. Additionally, it is unclear whether the release from the cell surface is an active mechanism and primary objective of CdiA, or if its release is a non-specific mechanism due to the nature of display.

It has been shown that the loss of the BfmRS two-component system can reduce the ability of some *A. baumannii* strains to produce capsular polysaccharides (Geisinger *et al.*, 2018; Geisinger and Isberg, 2015; Russo *et al.*, 2016). This dependence would potentially make *A. baumannii* strains susceptible to CDI-mediated inhibition, once they turn off BfmRS signalling. In this study, by using *bfmRS* mutants, we have shown that the loss of the system did not result in the reduction of capsule polysaccharides. This result was in agreement with observations made with *A. baumannii* AB307-0294 strain (Russo *et al.*, 2016), and suggests that BfmRS plays a strain-specific role in the ability to cause a reduction in capsule production. Secondly, we observed that *ΔbfmRS* deletion caused a somewhat different capsule polysaccharide profile, with increased quantity of a more variable length

polysaccharides. Currently, the biological meaning of this phenotype is unclear. Lastly, we showed that BfmRS system also plays a strain-specific role in the ability to mediate resistance against CDI-mediated inhibition. Out of the three *ΔbfmRS* mutants tested, only one displayed a clear susceptibility to CDI-inhibition phenotype, while the remaining two strains were either resistant or showed a general growth deficiency in co-cultures that were rescued by complementation with the wild-type *bfmRS* allele. While the mechanism of BfmRS-mediated defence against CDI inhibition is unclear, we hypothesise, that due to the increase in variable length polysaccharides, receptors required for CdiA binding might become more readily accessible, resulting in a higher susceptibility to CDI-mediated inhibition.

Biofilm formation allows the population to protect itself from unfavourable conditions such as predation, presence of antimicrobials, desiccation, chemical perturbations (Yan and Bassler, 2019). It is worth to note that biofilm or pellicle formation requires multiple secreted components such as adhesion factors, nucleic acids, exopolysaccharides, various proteins, lipopolysaccharide and other components to stabilise the structure (Flemming *et al.*, 2016). Once secreted, these factors become available to all individuals in a population, which could lead to the rise of exploiter strains, which do not produce these resources (Xavier, 2011). Additionally, it was shown that the secreted pellicle matrix components (exopolysaccharides and structural protein TasA) are shared between the cells in a population, resulting in the diminished fitness of producing strain, when compared to the non-producing mutant (Dragoš *et al.*, 2018). This suggests that the population might be vulnerable to the invasion of cells that do not contribute to biofilm formation. Also, the same population is vulnerable to the individuals within it, which engage in exploitation behaviour. Interestingly, it was shown recently, that in the majority of bacterial populations, CDI systems are under tight regulation and only a small fraction of bacteria (~0.1%) displays activated systems (Danka *et al.*, 2017).

Our observations, that capsule-deficient strains and only some BfmRS mutant *A. baumannii* strains become susceptible to CDI, suggests several things. First, the repression of CDI indicates that bacteria theoretically might sense when they are growing in a community of siblings, meaning that expression of CDI would by a waste of energy and resources. Second, a small fraction of bacteria, that do express CDI, can protect the population from invaders (Danka *et al.*, 2017). Also, a small number of strains expressing CDI would not significantly impact the fitness of a biofilm colony. Finally, it is clear, that in some *A. baumannii* strains, the biofilm

formation circuitry has a CDI-dependent policing mechanism, meaning that non-related strains can join biofilm colony as long as they contribute to it. Once they switch the BfmRS system off, they might get rapidly eliminated. However, our results also show a rather strain-specific role for the BfmRS system in the regulation of the susceptibility to CDI-mediated inhibition.

While the majority of functions of CDI toxins remain unknown, the experimentally or bioinformatically characterized ones can be separated into several groups: DNase/RNase toxins; nucleic acid deaminases, peptidases, ADP-ribosyl transferases, and pore forming toxins (Iyer *et al.*, 2011; Koskiniemi *et al.*, 2015; Zhang *et al.*, 2012). Interestingly, some toxins were observed to cause a reversible growth inhibition or at least do not cause cell death (Aoki *et al.*, 2009; Roussin *et al.*, 2019), while others caused an immediate cell death (Roussin *et al.*, 2019). A recent study identified *A. baumannii* strain, which encoded both types of systems (Roussin *et al.*, 2019). We determined that the lethal system is categorized in the same type with the similar CdiA modular structure as the CDI described in this work (type I according to De Gregorio *et al.*, (2019)). Peculiarly, our data show that CdiA from *A. baumannii* V15 mainly causes an immediate and effective growth arrest. It is worth noting that the toxin in the aforementioned study was predicted to be a nuclease (Roussin *et al.*, 2019), while the CdiA in our study might belong to a family of toxin-deaminase targeting RNA/DNA cytosines, suggesting a completely different functional activity. Additionally, the authors observed that the CDI system with a lethal mechanism was repressed, while the one with inhibitory activity displayed a constitutive activation. If BfmRS mediated repression is universal among these systems (i.e. Type I systems De Gregorio *et al.*, (2019)), then our observations implicating BfmRS role in CDI regulation, might explain the observed transcriptional repression in the previous study.

Altogether, our results suggest that *A. baumannii* can mediate not only commitment to community behaviour via the BfmRS system, but also mediate competition between sibling cells via contact-dependent growth inhibition system.

CONCLUSIONS

- BfmRS system acts as a positive regulator of *A. baumannii* pellicle formation and a negative regulator of surface-associated motility;
- BfmRS system positively regulates the secretion of Hcp protein, a component of the Type VI secretion system into the growth media without impacting the killing phenotype;
- *A. baumannii* contains a functional contact-dependent growth inhibition system negatively regulated by the two-component system BfmRS;
- *A. baumannii* capsule efficiently protects clinical *A. baumannii* isolates from contact-dependent growth inhibition;
- *A. baumannii* V15 strain secretes a functional CdiA toxin into the growth media causing the growth arrest of susceptible cells.

PUBLICATIONS

- **Krasauskas, R.**, Skerniškytė, J., Martinkus, J., Armalytė, J., and Sužiedėlienė, E. (2020) Capsule Protects *Acinetobacter baumannii* From Inter-Bacterial Competition Mediated by CdiA Toxin. Front. Microbiol. 11:1493.
- **Krasauskas, R.**, Skerniškytė, J., Armalytė, J., and Sužiedėlienė, E. (2019) The role of *Acinetobacter baumannii* response regulator BfmR in pellicle formation and competitiveness via contact-dependent inhibition system. BMC Microbiol. 19: 241.
- Skerniškytė, J., **Krasauskas, R.**, Péchoux, C., Kulakauskas, S., Armalytė, J., and Sužiedėlienė, E. (2019) Surface-Related Features and Virulence Among *Acinetobacter baumannii* Clinical Isolates Belonging to International Clones I and II. Front. Microbiol. 9: 3116.

Scientific presentations

Poster Presentations

- **Krasauskas R.**, Skerniškytė J., Armalytė J., Sužiedėlienė E. „BfmR regulator from *Acinetobacter baumannii* modulates Hcp secretion without effecting killing phenotype mediated by type VI secretion system“. 8th Congress of European Microbiologists (FEMS), Glasgow, UK, July, 2019.
- **Krasauskas R.**, Skerniškytė J., Armalytė J., Sužiedėlienė E. “The role of regulator BfmR in clinically important features of opportunistic pathogen *Acinetobacter baumannii*”. International conference Vita Scientia, Vilnius, Lithuania, 2018.
- **Krasauskas R.**, Skerniškytė J., Armalytė J., Sužiedėlienė E. “Investigation of the role of BfmR regulator in clinically important features of opportunistic pathogen *Acinetobacter baumannii*”. 7th Congress of European Microbiologists (FEMS), Valencia, Spain, July, 2017.
- **Krasauskas R.**, Sužiedėlienė E. “The role of response regulator BfmR on *Acinetobacter baumannii* biofilm formation“ XIVth International Conference of the Lithuanian Biochemical Society, Druskininkai, Lithuania, June 2016.

Oral presentations

- **Krasauskas R.**, Skerniškytė J., Armalytė J., Sužiedėlienė E. „Investigation of the role of BfmR regulator in clinically important features of opportunistic pathogen *Acinetobacter baumannii*“. 10-th Young Scientists conference: „Bioateitis“, Vilnius, Lithuania, 2017.

Funding

Federation of European Microbiological Societies (FEMS) partially financed participation in 7th and 8th Congresses of European Microbiologists.

ACKNOWLEDGEMENTS

First I would like to thank my supervisor Prof. Dr. Edita Sužiedėlienė the head and principal investigator of molecular microbiology lab. I am very grateful for giving me the opportunity to work in your lab since I was undergraduate. Thank you for always finding the time for me when I needed, for your guidance during all these years, insightful comments and discussions, all the help you have given me during the writing of this thesis, and most importantly – for putting all your trust and confidence in me.

I would also like to thank my laboratory and office colleagues Dr. Jūratė Skerniškytė and Dr. Julija Armalytė for insightful discussions, many advices and help performing experiments. I am especially grateful to Dr. Jūratė Skerniškytė for the design and critical commentary on some experiments. Also for conceiving, sharing, and discussing even the craziest ideas about *A. baumannii* physiology, and for being the soul of the lab. I am thanking all the present and previous colleagues and students in the lab during these years for helping with some experiments and for a great atmosphere.

I am indebted to all colleagues from the department of biochemistry and molecular biology for always finding the time and helping with my experiments. I would particularly like to thank Dr. Violeta Jonušienė and Dr. Aušra Sasnauskienė for the reagents and for the access to the fluorescence microscope.

I am thankful to Algirdas Mikšys for comments, ideation, and help in editing the thesis and manuscripts. I would like to thank Audrius Gegeckas for providing a *Bacillus* spp. strain and Centre of Proteomics (Institute of biotechnology) for the mass spectrometry.

Finally, I am grateful for the love and support from my family and friends. Particularly, I am thanking Inga for being understanding when work was prioritized over other things and providing me with love, support, and encouragement during this time.

REFERENCES

1. Adams, F.G., Stroeher, U.H., Hassan, K.A., Marri, S., Brown, M.H., 2018. Resistance to pentamidine is mediated by AdeAB, regulated by AdeRS, and influenced by growth conditions in *Acinetobacter baumannii* ATCC 17978. PloS One 13, e0197412. https://doi.org/10.1371/journal.pone.0197412
2. Adams, M.D., Nickel, G.C., Bajaksouzian, S., Lavender, H., Murthy, A.R., Jacobs, M.R., Bonomo, R.A., 2009. Resistance to colistin in *Acinetobacter baumannii* associated with mutations in the PmrAB two-component system. Antimicrob. Agents Chemother. 53, 3628–3634. https://doi.org/10.1128/AAC.00284-09
3. Ahmad, I., Nygren, E., Khalid, F., Myint, S.L., Uhlin, B.E., 2020. A Cyclic-di-GMP signalling network regulates biofilm formation and surface associated motility of *Acinetobacter baumannii* 17978. Sci. Rep. 10, 1991. https://doi.org/10.1038/s41598-020-58522-5
4. Alekshun, M.N., Levy, S.B., 2007. Molecular mechanisms of antibacterial multidrug resistance. Cell 128, 1037–1050. https://doi.org/10.1016/j.cell.2007.03.004
5. Allen, J.P., Ozer, E.A., Minasov, G., Shuvalova, L., Kiryukhina, O., Satchell, K.J.F., Hauser, A.R., 2020. A comparative genomics approach identifies contact-dependent growth inhibition as a virulence determinant. Proc. Natl. Acad. Sci. U. S. A. https://doi.org/10.1073/pnas.1919198117
6. Álvarez-Fraga, L., Rumbo-Feal, S., Pérez, A., Gómez, M.J., Gayoso, C., Vallejo, J.A., Ohneck, E.J., Valle, J., Actis, L.A., Beceiro, A., Bou, G., Poza, M., 2017. Global assessment of small RNAs reveals a non-coding transcript involved in biofilm formation and attachment in *Acinetobacter baumannii* ATCC 17978. PloS One 12, e0182084. https://doi.org/10.1371/journal.pone.0182084
7. Anderson, M.S., Garcia, E.C., Cotter, P.A., 2014. Kind discrimination and competitive exclusion mediated by contact-dependent growth inhibition systems shape biofilm community structure. PLoS Pathog. 10, e1004076. https://doi.org/10.1371/journal.ppat.1004076
8. Antunes, L.C.S., Visca, P., Towner, K.J., 2014. *Acinetobacter baumannii*: evolution of a global pathogen. Pathog. Dis. 71, 292–301. https://doi.org/10.1111/2049-632X.12125
9. Aoki, S.K., Malinverni, J.C., Jacoby, K., Thomas, B., Pamma, R., Trinh, B.N., Remers, S., Webb, J., Braaten, B.A., Silhavy, T.J., Low, D.A., 2008. Contact-dependent growth inhibition requires the essential outer membrane protein BamA (YaeT) as the receptor and the inner membrane transport protein AcrB. Mol. Microbiol. 70, 323–340. https://doi.org/10.1111/j.1365-2958.2008.06404.x
10. Aoki, S.K., Pamma, R., Hernday, A.D., Bickham, J.E., Braaten, B.A., Low, D.A., 2005. Contact-dependent inhibition of growth in *Escherichia coli*. Science 309, 1245–1248. https://doi.org/10.1126/science.1115109
11. Aoki, S.K., Webb, J.S., Braaten, B.A., Low, D.A., 2009. Contact-dependent growth inhibition causes reversible metabolic downregulation in *Escherichia coli*. J. Bacteriol. 191, 1777–1786. https://doi.org/10.1128/JB.01437-08
12. Aranda, J., Bardina, C., Beceiro, A., Rumbo, S., Cabral, M.P., Barbé, J., Bou, G., 2011. *Acinetobacter baumannii* RecA protein in repair of DNA damage, antimicrobial resistance, general stress response, and virulence. J. Bacteriol. 193, 3740–3747. https://doi.org/10.1128/JB.00389-11

13. Aranda, J., Poza, M., Shingu-Vázquez, M., Cortés, P., Boyce, J.D., Adler, B., Barbé, J., Bou, G., 2013. Identification of a DNA-damage-inducible regulon in *Acinetobacter baumannii*. J. Bacteriol. 195, 5577–5582. https://doi.org/10.1128/JB.00853-13
14. Armalytė, J., Jurėnas, D., Krasauskas, R., Čepauskas, A., Sužiedėlienė, E., 2018. The higBA Toxin-Antitoxin Module From the Opportunistic Pathogen *Acinetobacter baumannii* - Regulation, Activity, and Evolution. Front. Microbiol. 9, 732. https://doi.org/10.3389/fmicb.2018.00732
15. Armitano, J., Méjean, V., Jourlin-Castelli, C., 2014. Gram-negative bacteria can also form pellicles. Environ. Microbiol. Rep. 6, 534–544. https://doi.org/10.1111/1758-2229.12171
16. Ballouz, T., Aridi, J., Afif, C., Irani, J., Lakis, C., Nasreddine, R., Azar, E., 2017. Risk Factors, Clinical Presentation, and Outcome of *Acinetobacter baumannii* Bacteremia. Front. Cell. Infect. Microbiol. 7, 156. https://doi.org/10.3389/fcimb.2017.00156
17. Basler, M., 2015. Type VI secretion system: secretion by a contractile nanomachine. Philos. Trans. R. Soc. B Biol. Sci. 370. https://doi.org/10.1098/rstb.2015.0021
18. Beceiro, A., Llobet, E., Aranda, J., Bengoechea, J.A., Doumith, M., Hornsey, M., Dhanji, H., Chart, H., Bou, G., Livermore, D.M., Woodford, N., 2011. Phosphoethanolamine modification of lipid A in colistin-resistant variants of *Acinetobacter baumannii* mediated by the pmrAB two-component regulatory system. Antimicrob. Agents Chemother. 55, 3370–3379. https://doi.org/10.1128/AAC.00079-11
19. Beck, C.M., Morse, R.P., Cunningham, D.A., Iniguez, A., Low, D.A., Goulding, C.W., Hayes, C.S., 2014. CdiA from *Enterobacter cloacae* delivers a toxic ribosomal RNase into target bacteria. Struct. Lond. Engl. 1993 22, 707–718. https://doi.org/10.1016/j.str.2014.02.012
20. Beck, C.M., Willett, J.L.E., Cunningham, D.A., Kim, J.J., Low, D.A., Hayes, C.S., 2016. CdiA Effectors from Uropathogenic *Escherichia coli* Use Heterotrimeric Osmoporins as Receptors to Recognize Target Bacteria. PLoS Pathog. 12, e1005925. https://doi.org/10.1371/journal.ppat.1005925
21. Beitz, E., 2000. TEXshade: shading and labeling of multiple sequence alignments using LATEX2 epsilon. Bioinforma. Oxf. Engl. 16, 135–139. https://doi.org/10.1093/bioinformatics/16.2.135
22. Bentancor, L.V., Camacho-Peiro, A., Bozkurt-Guzel, C., Pier, G.B., Maira-Litrán, T., 2012. Identification of Ata, a multifunctional trimeric autotransporter of *Acinetobacter baumannii*. J. Bacteriol. 194, 3950–3960. https://doi.org/10.1128/JB.06769-11
23. Bervoets, I., Charlier, D., 2019. Diversity, versatility and complexity of bacterial gene regulation mechanisms: opportunities and drawbacks for applications in synthetic biology. FEMS Microbiol. Rev. 43, 304–339. https://doi.org/10.1093/femsre/fuz001
24. Bhuiyan, M.S., Ellett, F., Murray, G.L., Kostoulias, X., Cerqueira, G.M., Schulze, K.E., Mahamad Maifiah, M.H., Li, J., Creek, D.J., Lieschke, G.J., Peleg, A.Y., 2016. *Acinetobacter baumannii* phenylacetic acid metabolism influences infection outcome through a direct effect on neutrophil chemotaxis. Proc. Natl. Acad. Sci. U. S. A. 113, 9599–9604. https://doi.org/10.1073/pnas.1523116113
25. Boll, J.M., Crofts, A.A., Peters, K., Cattoir, V., Vollmer, W., Davies, B.W., Trent, M.S., 2016. A penicillin-binding protein inhibits selection of colistin-resistant, lipooligosaccharide-deficient *Acinetobacter baumannii*. Proc. Natl. Acad. Sci. U. S. A. 113, E6228–E6237. https://doi.org/10.1073/pnas.1611594113

26. Boll, J.M., Tucker, A.T., Klein, D.R., Beltran, A.M., Brodbelt, J.S., Davies, B.W., Trent, M.S., 2015. Reinforcing Lipid A Acylation on the Cell Surface of *Acinetobacter baumannii* Promotes Cationic Antimicrobial Peptide Resistance and Desiccation Survival. mBio 6, e00478-00415. https://doi.org/10.1128/mBio.00478-15
27. Cabral, M.P., Soares, N.C., Aranda, J., Parreira, J.R., Rumbo, C., Poza, M., Valle, J., Calamia, V., Lasa, I., Bou, G., 2011. Proteomic and functional analyses reveal a unique lifestyle for *Acinetobacter baumannii* biofilms and a key role for histidine metabolism. J. Proteome Res. 10, 3399–3417. https://doi.org/10.1021/pr101299j
28. Cafiso, V., Stracquadanio, S., Lo Verde, F., Dovere, V., Zega, A., Pigola, G., Aranda, J., Stefani, S., 2020. COLR *Acinetobacter baumannii* sRNA Signatures: Computational Comparative Identification and Biological Targets. Front. Microbiol. 10. https://doi.org/10.3389/fmicb.2019.03075
29. Capra, E.J., Laub, M.T., 2012. Evolution of two-component signal transduction systems. Annu. Rev. Microbiol. 66, 325–347. https://doi.org/10.1146/annurev-micro-092611-150039
30. Casadaban, M.J., Cohen, S.N., 1979. Lactose genes fused to exogenous promoters in one step using a Mu-lac bacteriophage: in vivo probe for transcriptional control sequences. Proc. Natl. Acad. Sci. U. S. A. 76, 4530–4533. https://doi.org/10.1073/pnas.76.9.4530
31. Cascales, E., Buchanan, S.K., Duché, D., Kleanthous, C., Lloubès, R., Postle, K., Riley, M., Slatin, S., Cavard, D., 2007. Colicin biology. Microbiol. Mol. Biol. Rev. MMBR 71, 158–229. https://doi.org/10.1128/MMBR.00036-06
32. Catel-Ferreira, M., Marti, S., Guillon, L., Jara, L., Coadou, G., Molle, V., Bouffartigues, E., Bou, G., Shalk, I., Jouenne, T., Vila-Farrés, X., Dé, E., 2016. The outer membrane porin OmpW of *Acinetobacter baumannii* is involved in iron uptake and colistin binding. FEBS Lett. 590, 224–231. https://doi.org/10.1002/1873-3468.12050
33. Cerqueira, G.M., Kostoulias, X., Khoo, C., Aibinu, I., Qu, Y., Traven, A., Peleg, A.Y., 2014. A global virulence regulator in *Acinetobacter baumannii* and its control of the phenylacetic acid catabolic pathway. J. Infect. Dis. 210, 46–55. https://doi.org/10.1093/infdis/jiu024
34. Chang, K.-C., Kuo, H.-Y., Tang, C.Y., Chang, C.-W., Lu, C.-W., Liu, C.-C., Lin, H.-R., Chen, K.-H., Liou, M.-L., 2014. Transcriptome profiling in imipenem-selected *Acinetobacter baumannii*. BMC Genomics 15, 815. https://doi.org/10.1186/1471-2164-15-815
35. Chen, R., Lv, R., Xiao, L., Wang, M., Du, Z., Tan, Y., Cui, Y., Yan, Y., Luo, Y., Yang, R., Song, Y., 2017. A1S_2811, a CheA/Y-like hybrid two-component regulator from *Acinetobacter baumannii* ATCC17978, is involved in surface motility and biofilm formation in this bacterium. MicrobiologyOpen 6. https://doi.org/10.1002/mbo3.510
36. Chen, T.-L., Siu, L.-K., Wu, R.C.-C., Shaio, M.-F., Huang, L.-Y., Fung, C.-P., Lee, C.-M., Cho, W.-L., 2007. Comparison of one-tube multiplex PCR, automated ribotyping and intergenic spacer (ITS) sequencing for rapid identification of *Acinetobacter baumannii*. Clin. Microbiol. Infect. Off. Publ. Eur. Soc. Clin. Microbiol. Infect. Dis. 13, 801–806. https://doi.org/10.1111/j.1469-0691.2007.01744.x
37. Chin, C.Y., Tipton, K.A., Farokhyfar, M., Burd, E.M., Weiss, D.S., Rather, P.N., 2018. A high-frequency phenotypic switch links bacterial virulence and environmental survival in *Acinetobacter baumannii*. Nat. Microbiol. 3, 563–569. https://doi.org/10.1038/s41564-018-0151-5

38. Choi, C.H., Hyun, S.H., Lee, J.Y., Lee, J.S., Lee, Y.S., Kim, S.A., Chae, J.-P., Yoo, S.M., Lee, J.C., 2008a. *Acinetobacter baumannii* outer membrane protein A targets the nucleus and induces cytotoxicity. Cell. Microbiol. 10, 309–319. https://doi.org/10.1111/j.1462-5822.2007.01041.x
39. Choi, C.H., Lee, E.Y., Lee, Y.C., Park, T.I., Kim, H.J., Hyun, S.H., Kim, S.A., Lee, S.-K., Lee, J.C., 2005. Outer membrane protein 38 of *Acinetobacter baumannii* localizes to the mitochondria and induces apoptosis of epithelial cells. Cell. Microbiol. 7, 1127–1138. https://doi.org/10.1111/j.1462-5822.2005.00538.x
40. Choi, C.H., Lee, J.S., Lee, Y.C., Park, T.I., Lee, J.C., 2008b. *Acinetobacter baumannii* invades epithelial cells and outer membrane protein A mediates interactions with epithelial cells. BMC Microbiol. 8, 216. https://doi.org/10.1186/1471-2180-8-216
41. Clemmer, K.M., Bonomo, R.A., Rather, P.N., 2011. Genetic analysis of surface motility in *Acinetobacter baumannii*. Microbiol. Read. Engl. 157, 2534–2544. https://doi.org/10.1099/mic.0.049791-0
42. Coulthurst, S., 2019. The Type VI secretion system: a versatile bacterial weapon. Microbiol. Read. Engl. 165, 503–515. https://doi.org/10.1099/mic.0.000789
43. Coyne, S., Rosenfeld, N., Lambert, T., Courvalin, P., Périchon, B., 2010. Overexpression of resistance-nodulation-cell division pump AdeFGH confers multidrug resistance in *Acinetobacter baumannii*. Antimicrob. Agents Chemother. 54, 4389–4393. https://doi.org/10.1128/AAC.00155-10
44. Craig, L., Forest, K.T., Maier, B., 2019. Type IV pili: dynamics, biophysics and functional consequences. Nat. Rev. Microbiol. 17, 429–440. https://doi.org/10.1038/s41579-019-0195-4
45. Da Silva, G.J., Domingues, S., 2017. Interplay between Colistin Resistance, Virulence and Fitness in *Acinetobacter baumannii*. Antibiot. Basel Switz. 6. https://doi.org/10.3390/antibiotics6040028
46. Dame, R.T., Tark-Dame, M., 2016. Bacterial chromatin: converging views at different scales. Curr. Opin. Cell Biol. 40, 60–65. https://doi.org/10.1016/j.ceb.2016.02.015
47. Danka, E.S., Garcia, E.C., Cotter, P.A., 2017. Are CDI Systems Multicolored, Facultative, Helping Greenbeards? Trends Microbiol. 25, 391–401. https://doi.org/10.1016/j.tim.2017.02.008
48. Darvish Alipour Astaneh, S., Rasooli, I., Mousavi Gargari, S.L., 2014. The role of filamentous hemagglutinin adhesin in adherence and biofilm formation in *Acinetobacter baumannii* ATCC19606(T). Microb. Pathog. 74, 42–49. https://doi.org/10.1016/j.micpath.2014.07.007
49. de Breij, A., Dijkshoorn, L., Lagendijk, E., van der Meer, J., Koster, A., Bloemberg, G., Wolterbeek, R., van den Broek, P., Nibbering, P., 2010. Do biofilm formation and interactions with human cells explain the clinical success of *Acinetobacter baumannii*? PloS One 5, e10732. https://doi.org/10.1371/journal.pone.0010732
50. De Gregorio, E., Del Franco, M., Martinucci, M., Roscetto, E., Zarrilli, R., Di Nocera, P.P., 2015. Biofilm-associated proteins: news from *Acinetobacter*. BMC Genomics 16, 933. https://doi.org/10.1186/s12864-015-2136-6
51. De Gregorio, E., Esposito, E.P., Zarrilli, R., Di Nocera, P.P., 2018. Contact-Dependent Growth Inhibition Proteins in *Acinetobacter baylyi* ADP1. Curr. Microbiol. 75, 1434–1440. https://doi.org/10.1007/s00284-018-1540-y

52. De Gregorio, E., Zarrilli, R., Di Nocera, P.P., 2019. Contact-dependent growth inhibition systems in *Acinetobacter*. Sci. Rep. 9, 154. https://doi.org/10.1038/s41598-018-36427-8
53. De Silva, P.M., Kumar, A., 2019. Signal Transduction Proteins in *Acinetobacter baumannii*: Role in Antibiotic Resistance, Virulence, and Potential as Drug Targets. Front. Microbiol. 10, 49. https://doi.org/10.3389/fmicb.2019.00049
54. De Silva, P.M., Kumar, A., 2018. Effect of Sodium Chloride on Surface-Associated Motility of *Acinetobacter baumannii* and the Role of AdeRS Two-Component System. J. Membr. Biol. 251, 5–13. https://doi.org/10.1007/s00232-017-9985-7
55. Diancourt, L., Passet, V., Nemec, A., Dijkshoorn, L., Brisse, S., 2010. The population structure of *Acinetobacter baumannii*: expanding multiresistant clones from an ancestral susceptible genetic pool. PloS One 5, e10034. https://doi.org/10.1371/journal.pone.0010034
56. Dijkshoorn, L., Nemec, A., Seifert, H., 2007. An increasing threat in hospitals: multidrug-resistant *Acinetobacter baumannii*. Nat. Rev. Microbiol. 5, 939–951. https://doi.org/10.1038/nrmicro1789
57. Dowzicky, M.J., Chmelařová, E., 2019. Antimicrobial susceptibility of Gram-negative and Gram-positive bacteria collected from Eastern Europe: Results from the Tigecycline Evaluation and Surveillance Trial (T.E.S.T.), 2011-2016. J. Glob. Antimicrob. Resist. 17, 44–52. https://doi.org/10.1016/j.jgar.2018.11.007
58. Dragoš, A., Kiesewalter, H., Martin, M., Hsu, C.-Y., Hartmann, R., Wechsler, T., Eriksen, C., Brix, S., Drescher, K., Stanley-Wall, N., Kümmerli, R., Kovács, Á.T., 2018. Division of Labor during Biofilm Matrix Production. Curr. Biol. CB 28, 1903-1913.e5. https://doi.org/10.1016/j.cub.2018.04.046
59. Draughn, G.L., Milton, M.E., Feldmann, E.A., Bobay, B.G., Roth, B.M., Olson, A.L., Thompson, R.J., Actis, L.A., Davies, C., Cavanagh, J., 2018. The Structure of the Biofilm-controlling Response Regulator BfmR from *Acinetobacter baumannii* Reveals Details of Its DNA-binding Mechanism. J. Mol. Biol. 430, 806–821. https://doi.org/10.1016/j.jmb.2018.02.002
60. Duval, M., Simonetti, A., Caldelari, I., Marzi, S., 2015. Multiple ways to regulate translation initiation in bacteria: Mechanisms, regulatory circuits, dynamics. Biochimie 114, 18–29. https://doi.org/10.1016/j.biochi.2015.03.007
61. Edgar, R.C., 2004. MUSCLE: multiple sequence alignment with high accuracy and high throughput. Nucleic Acids Res. 32, 1792–1797. https://doi.org/10.1093/nar/gkh340
62. Eijkelkamp, B.A., Hassan, K.A., Paulsen, I.T., Brown, M.H., 2011a. Investigation of the human pathogen *Acinetobacter baumannii* under iron limiting conditions. BMC Genomics 12, 126. https://doi.org/10.1186/1471-2164-12-126
63. Eijkelkamp, B.A., Stroeher, U.H., Hassan, K.A., Elbourne, L.D.H., Paulsen, I.T., Brown, M.H., 2013. H-NS plays a role in expression of *Acinetobacter baumannii* virulence features. Infect. Immun. 81, 2574–2583. https://doi.org/10.1128/IAI.00065-13
64. Eijkelkamp, B.A., Stroeher, U.H., Hassan, K.A., Papadimitrious, M.S., Paulsen, I.T., Brown, M.H., 2011b. Adherence and motility characteristics of clinical *Acinetobacter baumannii* isolates. FEMS Microbiol. Lett. 323, 44–51. https://doi.org/10.1111/j.1574-6968.2011.02362.x

65. Eijkelkamp, B.A., Stroeher, U.H., Hassan, K.A., Paulsen, I.T., Brown, M.H., 2014. Comparative analysis of surface-exposed virulence factors of *Acinetobacter baumannii*. BMC Genomics 15, 1020. https://doi.org/10.1186/1471-2164-15-1020
66. Espinal, P., Martí, S., Vila, J., 2012. Effect of biofilm formation on the survival of *Acinetobacter baumannii* on dry surfaces. J. Hosp. Infect. 80, 56–60. https://doi.org/10.1016/j.jhin.2011.08.013
67. Fan, E., Chauhan, N., Udatha, D.B.R.K.G., Leo, J.C., Linke, D., 2016. Type V Secretion Systems in Bacteria. Microbiol. Spectr. 4. https://doi.org/10.1128/microbiolspec.VMBF-0009-2015
68. Farrow, J.M., Wells, G., Pesci, E.C., 2018. Desiccation tolerance in *Acinetobacter baumannii* is mediated by the two-component response regulator BfmR. PLoS ONE 13. https://doi.org/10.1371/journal.pone.0205638
69. Fernández-Cuenca, F., Smani, Y., Gómez-Sánchez, M.C., Docobo-Pérez, F., Caballero-Moyano, F.J., Domínguez-Herrera, J., Pascual, A., Pachón, J., 2011. Attenuated virulence of a slow-growing pandrug-resistant *Acinetobacter baumannii* is associated with decreased expression of genes encoding the porins CarO and OprD-like. Int. J. Antimicrob. Agents 38, 548–549. https://doi.org/10.1016/j.ijantimicag.2011.08.002
70. Fernando, D.M., Chong, P., Singh, M., Spicer, V., Unger, M., Loewen, P.C., Westmacott, G., Kumar, A., 2017. Multi-omics approach to study global changes in a triclosan-resistant mutant strain of *Acinetobacter baumannii* ATCC 17978. Int. J. Antimicrob. Agents 49, 74–80. https://doi.org/10.1016/j.ijantimicag.2016.10.014
71. Fiester, S.E., Arivett, B.A., Schmidt, R.E., Beckett, A.C., Ticak, T., Carrier, M.V., Ghosh, R., Ohneck, E.J., Metz, M.L., Sellin Jeffries, M.K., Actis, L.A., 2016. Iron-Regulated Phospholipase C Activity Contributes to the Cytolytic Activity and Virulence of *Acinetobacter baumannii*. PLoS ONE 11. https://doi.org/10.1371/journal.pone.0167068
72. Flemming, H.-C., Wingender, J., Szewzyk, U., Steinberg, P., Rice, S.A., Kjelleberg, S., 2016. Biofilms: an emergent form of bacterial life. Nat. Rev. Microbiol. 14, 563–575. https://doi.org/10.1038/nrmicro.2016.94
73. Flynn, K.M., Dowell, G., Johnson, T.M., Koestler, B.J., Waters, C.M., Cooper, V.S., 2016. Evolution of Ecological Diversity in Biofilms of *Pseudomonas aeruginosa* by Altered Cyclic Diguanylate Signaling. J. Bacteriol. 198, 2608–2618. https://doi.org/10.1128/JB.00048-16
74. Gaddy, J.A., Tomaras, A.P., Actis, L.A., 2009. The *Acinetobacter baumannii* 19606 OmpA protein plays a role in biofilm formation on abiotic surfaces and in the interaction of this pathogen with eukaryotic cells. Infect. Immun. 77, 3150–3160. https://doi.org/10.1128/IAI.00096-09
75. Gallique, M., Decoin, V., Barbey, C., Rosay, T., Feuilloley, M.G.J., Orange, N., Merieau, A., 2017. Contribution of the *Pseudomonas fluorescens* MFE01 Type VI Secretion System to Biofilm Formation. PloS One 12, e0170770. https://doi.org/10.1371/journal.pone.0170770
76. Gao, R., Bouillet, S., Stock, A.M., 2019. Structural Basis of Response Regulator Function. Annu. Rev. Microbiol. 73, 175–197. https://doi.org/10.1146/annurev-micro-020518-115931
77. Garcia, E.C., 2018. Contact-dependent interbacterial toxins deliver a message. Curr. Opin. Microbiol. 42, 40–46. https://doi.org/10.1016/j.mib.2017.09.011

78. Garcia, E.C., Anderson, M.S., Hagar, J.A., Cotter, P.A., 2013. *Burkholderia* BcpA mediates biofilm formation independently of interbacterial contact-dependent growth inhibition. Mol. Microbiol. 89, 1213–1225. https://doi.org/10.1111/mmi.12339
79. Garcia, E.C., Perault, A.I., Marlatt, S.A., Cotter, P.A., 2016. Interbacterial signaling via *Burkholderia* contact-dependent growth inhibition system proteins. Proc. Natl. Acad. Sci. U. S. A. 113, 8296–8301. https://doi.org/10.1073/pnas.1606323113
80. Gebhardt, M.J., Gallagher, L.A., Jacobson, R.K., Usacheva, E.A., Peterson, L.R., Zurawski, D.V., Shuman, H.A., 2015. Joint Transcriptional Control of Virulence and Resistance to Antibiotic and Environmental Stress in *Acinetobacter baumannii*. mBio 6. https://doi.org/10.1128/mBio.01660-15
81. Gebhardt, M.J., Shuman, H.A., 2017. GigA and GigB are Master Regulators of Antibiotic Resistance, Stress Responses, and Virulence in *Acinetobacter baumannii*. J. Bacteriol. 199. https://doi.org/10.1128/JB.00066-17
82. Geisinger, E., Isberg, R.R., 2015. Antibiotic modulation of capsular exopolysaccharide and virulence in *Acinetobacter baumannii*. PLoS Pathog. 11, e1004691. https://doi.org/10.1371/journal.ppat.1004691
83. Geisinger, E., Mortman, N.J., Vargas-Cuebas, G., Tai, A.K., Isberg, R.R., 2018. A global regulatory system links virulence and antibiotic resistance to envelope homeostasis in *Acinetobacter baumannii*. PLoS Pathog. 14, e1007030. https://doi.org/10.1371/journal.ppat.1007030
84. George Garrity, Don J. Brenner, Noel R. Krieg, James R. Staley (Eds.), 2005. Bergey's Manual® of Systematic Bacteriology. Springer US.
85. Ghosh, A., Baltekin, Ö., Wäneskog, M., Elkhalifa, D., Hammarlöf, D.L., Elf, J., Koskiniemi, S., 2018. Contact-dependent growth inhibition induces high levels of antibiotic-tolerant persister cells in clonal bacterial populations. EMBO J. 37. https://doi.org/10.15252/embj.201798026
86. Giammanco, A., Calà, C., Fasciana, T., Dowzicky, M.J., 2017. Global Assessment of the Activity of Tigecycline against Multidrug-Resistant Gram-Negative Pathogens between 2004 and 2014 as Part of the Tigecycline Evaluation and Surveillance Trial. mSphere 2. https://doi.org/10.1128/mSphere.00310-16
87. Giannouli, M., Antunes, L.C.S., Marchetti, V., Triassi, M., Visca, P., Zarrilli, R., 2013. Virulence-related traits of epidemic Acinetobacter baumannii strains belonging to the international clonal lineages I-III and to the emerging genotypes ST25 and ST78. BMC Infect. Dis. 13, 282. https://doi.org/10.1186/1471-2334-13-282
88. Giles, S.K., Stroeher, U.H., Eijkelkamp, B.A., Brown, M.H., 2015. Identification of genes essential for pellicle formation in *Acinetobacter baumannii*. BMC Microbiol. 15, 116. https://doi.org/10.1186/s12866-015-0440-6
89. Gil-Perotin, S., Ramirez, P., Marti, V., Sahuquillo, J.M., Gonzalez, E., Calleja, I., Menendez, R., Bonastre, J., 2012. Implications of endotracheal tube biofilm in ventilator-associated pneumonia response: a state of concept. Crit. Care Lond. Engl. 16, R93. https://doi.org/10.1186/cc11357
90. Golic, A.E., Valle, L., Jaime, P.C., Álvarez, C.E., Parodi, C., Borsarelli, C.D., Abatedaga, I., Mussi, M.A., 2019. BlsA Is a Low to Moderate Temperature Blue Light Photoreceptor in the Human Pathogen *Acinetobacter baumannii*. Front. Microbiol. 10, 1925. https://doi.org/10.3389/fmicb.2019.01925
91. Green, E.R., Mecsas, J., 2016. Bacterial Secretion Systems: An Overview. Microbiol. Spectr. 4. https://doi.org/10.1128/microbiolspec.VMBF-0012-2015

92. Groisman, E.A., 2016. Feedback Control of Two-Component Regulatory Systems. Annu. Rev. Microbiol. 70, 103–124. https://doi.org/10.1146/annurev-micro-102215-095331
93. Guérin, J., Bigot, S., Schneider, R., Buchanan, S.K., Jacob-Dubuisson, F., 2017. Two-Partner Secretion: Combining Efficiency and Simplicity in the Secretion of Large Proteins for Bacteria-Host and Bacteria-Bacteria Interactions. Front. Cell. Infect. Microbiol. 7, 148. https://doi.org/10.3389/fcimb.2017.00148
94. Guttenplan, S.B., Kearns, D.B., 2013. Regulation of flagellar motility during biofilm formation. FEMS Microbiol. Rev. 37, 849–871. https://doi.org/10.1111/1574-6976.12018
95. Hamidian, M., Hawkey, J., Wick, R., Holt, K.E., Hall, R.M., 2019. Evolution of a clade of *Acinetobacter baumannii* global clone 1, lineage 1 via acquisition of carbapenem- and aminoglycoside-resistance genes and dispersion of ISAba1. Microb. Genomics 5. https://doi.org/10.1099/mgen.0.000242
96. Harding, C.M., Hennon, S.W., Feldman, M.F., 2018. Uncovering the mechanisms of *Acinetobacter baumannii* virulence. Nat. Rev. Microbiol. 16, 91–102. https://doi.org/10.1038/nrmicro.2017.148
97. Harding, C.M., Kinsella, R.L., Palmer, L.D., Skaar, E.P., Feldman, M.F., 2016. Medically Relevant *Acinetobacter* Species Require a Type II Secretion System and Specific Membrane-Associated Chaperones for the Export of Multiple Substrates and Full Virulence. PLoS Pathog. 12, e1005391. https://doi.org/10.1371/journal.ppat.1005391
98. Harding, C.M., Pulido, M.R., Di Venanzio, G., Kinsella, R.L., Webb, A.I., Scott, N.E., Pachón, J., Feldman, M.F., 2017. Pathogenic *Acinetobacter* species have a functional type I secretion system and contact-dependent inhibition systems. J. Biol. Chem. 292, 9075–9087. https://doi.org/10.1074/jbc.M117.781575
99. Harding, C.M., Tracy, E.N., Carruthers, M.D., Rather, P.N., Actis, L.A., Munson, R.S., 2013. *Acinetobacter baumannii* strain M2 produces type IV pili which play a role in natural transformation and twitching motility but not surface-associated motility. mBio 4. https://doi.org/10.1128/mBio.00360-13
100. Hare, J.M., Ferrell, J.C., Witkowski, T.A., Grice, A.N., 2014. Prophage induction and differential RecA and UmuDAb transcriptome regulation in the DNA damage responses of *Acinetobacter baumannii* and *Acinetobacter baylyi*. PloS One 9, e93861. https://doi.org/10.1371/journal.pone.0093861
101. Hassan, K.A., Jackson, S.M., Penesyan, A., Patching, S.G., Tetu, S.G., Eijkelkamp, B.A., Brown, M.H., Henderson, P.J.F., Paulsen, I.T., 2013. Transcriptomic and biochemical analyses identify a family of chlorhexidine efflux proteins. Proc. Natl. Acad. Sci. U. S. A. 110, 20254–20259. https://doi.org/10.1073/pnas.1317052110
102. Hayes, C.S., Koskiniemi, S., Ruhe, Z.C., Poole, S.J., Low, D.A., 2014. Mechanisms and biological roles of contact-dependent growth inhibition systems. Cold Spring Harb. Perspect. Med. 4. https://doi.org/10.1101/cshperspect.a010025
103. Heindorf, M., Kadari, M., Heider, C., Skiebe, E., Wilharm, G., 2014. Impact of *Acinetobacter baumannii* superoxide dismutase on motility, virulence, oxidative stress resistance and susceptibility to antibiotics. PloS One 9, e101033. https://doi.org/10.1371/journal.pone.0101033
104. Henry, R., Crane, B., Powell, D., Deveson Lucas, D., Li, Z., Aranda, J., Harrison, P., Nation, R.L., Adler, B., Harper, M., Boyce, J.D., Li, J., 2015. The transcriptomic

response of *Acinetobacter baumannii* to colistin and doripenem alone and in combination in an in vitro pharmacokinetics/pharmacodynamics model. J. Antimicrob. Chemother. 70, 1303–1313. https://doi.org/10.1093/jac/dku536

105. Henry, R., Vithanage, N., Harrison, P., Seemann, T., Coutts, S., Moffatt, J.H., Nation, R.L., Li, J., Harper, M., Adler, B., Boyce, J.D., 2012. Colistin-resistant, lipopolysaccharide-deficient *Acinetobacter baumannii* responds to lipopolysaccharide loss through increased expression of genes involved in the synthesis and transport of lipoproteins, phospholipids, and poly-β-1,6-N-acetylglucosamine. Antimicrob. Agents Chemother. 56, 59–69. https://doi.org/10.1128/AAC.05191-11
106. Higgins, P.G., Dammhayn, C., Hackel, M., Seifert, H., 2010. Global spread of carbapenem-resistant *Acinetobacter baumannii*. J. Antimicrob. Chemother. 65, 233–238. https://doi.org/10.1093/jac/dkp428
107. Ho, B.T., Dong, T.G., Mekalanos, J.J., 2014. A view to a kill: the bacterial type VI secretion system. Cell Host Microbe 15, 9–21. https://doi.org/10.1016/j.chom.2013.11.008
108. Holt, K., Kenyon, J.J., Hamidian, M., Schultz, M.B., Pickard, D.J., Dougan, G., Hall, R., 2016. Five decades of genome evolution in the globally distributed, extensively antibiotic-resistant *Acinetobacter baumannii* global clone 1. Microb. Genomics 2, e000052. https://doi.org/10.1099/mgen.0.000052
109. Hood, M.I., Jacobs, A.C., Sayood, K., Dunman, P.M., Skaar, E.P., 2010. *Acinetobacter baumannii* increases tolerance to antibiotics in response to monovalent cations. Antimicrob. Agents Chemother. 54, 1029–1041. https://doi.org/10.1128/AAC.00963-09
110. Huang, W., Yao, Y., Long, Q., Yang, X., Sun, W., Liu, C., Jin, X., Li, Y., Chu, X., Chen, B., Ma, Y., 2014. Immunization against multidrug-resistant *Acinetobacter baumannii* effectively protects mice in both pneumonia and sepsis models. PloS One 9, e100727. https://doi.org/10.1371/journal.pone.0100727
111. Hunger, M., Schmucker, R., Kishan, V., Hillen, W., 1990. Analysis and nucleotide sequence of an origin of DNA replication in *Acinetobacter calcoaceticus* and its use for *Escherichia coli* shuttle plasmids. Gene 87, 45–51. https://doi.org/10.1016/0378-1119(90)90494-c
112. Iyer, L.M., Zhang, D., Rogozin, I.B., Aravind, L., 2011. Evolution of the deaminase fold and multiple origins of eukaryotic editing and mutagenic nucleic acid deaminases from bacterial toxin systems. Nucleic Acids Res. 39, 9473–9497. https://doi.org/10.1093/nar/gkr691
113. Jacob-Dubuisson, F., Mechaly, A., Betton, J.-M., Antoine, R., 2018. Structural insights into the signalling mechanisms of two-component systems. Nat. Rev. Microbiol. 16, 585–593. https://doi.org/10.1038/s41579-018-0055-7
114. Jacobs, A.C., Blanchard, C.E., Catherman, S.C., Dunman, P.M., Murata, Y., 2014. An ribonuclease T2 family protein modulates *Acinetobacter baumannii* abiotic surface colonization. PloS One 9, e85729. https://doi.org/10.1371/journal.pone.0085729
115. Jacobs, A.C., Hood, I., Boyd, K.L., Olson, P.D., Morrison, J.M., Carson, S., Sayood, K., Iwen, P.C., Skaar, E.P., Dunman, P.M., 2010. Inactivation of phospholipase D diminishes *Acinetobacter baumannii* pathogenesis. Infect. Immun. 78, 1952–1962. https://doi.org/10.1128/IAI.00889-09
116. Jacobs, A.C., Sayood, K., Olmsted, S.B., Blanchard, C.E., Hinrichs, S., Russell, D., Dunman, P.M., 2012. Characterization of the *Acinetobacter baumannii* growth phase-

dependent and serum responsive transcriptomes. FEMS Immunol. Med. Microbiol. 64, 403–412. https://doi.org/10.1111/j.1574-695X.2011.00926.x
117. Jahangiri, A., Rasooli, I., Owlia, P., Imani Fooladi, A.A., Salimian, J., 2018. Highly conserved exposed immunogenic peptides of Omp34 against *Acinetobacter baumannii*: An innovative approach. J. Microbiol. Methods 144, 79–85. https://doi.org/10.1016/j.mimet.2017.11.008
118. Jenal, U., Reinders, A., Lori, C., 2017. Cyclic di-GMP: second messenger extraordinaire. Nat. Rev. Microbiol. 15, 271–284. https://doi.org/10.1038/nrmicro.2016.190
119. Johnson, T.L., Waack, U., Smith, S., Mobley, H., Sandkvist, M., 2015. *Acinetobacter baumannii* Is Dependent on the Type II Secretion System and Its Substrate LipA for Lipid Utilization and In Vivo Fitness. J. Bacteriol. 198, 711–719. https://doi.org/10.1128/JB.00622-15
120. Juttukonda, L.J., Green, E.R., Lonergan, Z.R., Heffern, M.C., Chang, C.J., Skaar, E.P., 2019. *Acinetobacter baumannii* OxyR Regulates the Transcriptional Response to Hydrogen Peroxide. Infect. Immun. 87. https://doi.org/10.1128/IAI.00413-18
121. Kanonenberg, K., Schwarz, C.K.W., Schmitt, L., 2013. Type I secretion systems - a story of appendices. Res. Microbiol. 164, 596–604. https://doi.org/10.1016/j.resmic.2013.03.011
122. Karah, N., Sundsfjord, A., Towner, K., Samuelsen, Ø., 2012. Insights into the global molecular epidemiology of carbapenem non-susceptible clones of *Acinetobacter baumannii*. Drug Resist. Updat. Rev. Comment. Antimicrob. Anticancer Chemother. 15, 237–247. https://doi.org/10.1016/j.drup.2012.06.001
123. Kempf, M., Eveillard, M., Deshayes, C., Ghamrawi, S., Lefrançois, C., Georgeault, S., Bastiat, G., Seifert, H., Joly-Guillou, M.-L., 2012. Cell surface properties of two differently virulent strains of *Acinetobacter baumannii* isolated from a patient. Can. J. Microbiol. 58, 311–317. https://doi.org/10.1139/w11-131
124. Kentache, T., Ben Abdelkrim, A., Jouenne, T., Dé, E., Hardouin, J., 2017. Global Dynamic Proteome Study of a Pellicle-forming *Acinetobacter baumannii* Strain. Mol. Cell. Proteomics MCP 16, 100–112. https://doi.org/10.1074/mcp.M116.061044
125. Kim, S.W., Choi, C.H., Moon, D.C., Jin, J.S., Lee, J.H., Shin, J.-H., Kim, J.M., Lee, Y.C., Seol, S.Y., Cho, D.T., Lee, J.C., 2009. Serum resistance of *Acinetobacter baumannii* through the binding of factor H to outer membrane proteins. FEMS Microbiol. Lett. 301, 224–231. https://doi.org/10.1111/j.1574-6968.2009.01820.x
126. Kim, S.Y., Kim, M.H., Kim, S.I., Son, J.H., Kim, S., Lee, Y.C., Shin, M., Oh, M.H., Lee, J.C., 2019. The sensor kinase BfmS controls production of outer membrane vesicles in *Acinetobacter baumannii*. BMC Microbiol. 19, 301. https://doi.org/10.1186/s12866-019-1679-0
127. Knauf, G.A., Cunningham, A.L., Kazi, M.I., Riddington, I.M., Crofts, A.A., Cattoir, V., Trent, M.S., Davies, B.W., 2018. Exploring the Antimicrobial Action of Quaternary Amines against *Acinetobacter baumannii*. mBio 9. https://doi.org/10.1128/mBio.02394-17
128. Korotkov, K.V., Sandkvist, M., 2019. Architecture, Function, and Substrates of the Type II Secretion System. EcoSal Plus 8. https://doi.org/10.1128/ecosalplus.ESP-0034-2018
129. Korotkov, K.V., Sandkvist, M., Hol, W.G.J., 2012. The type II secretion system: biogenesis, molecular architecture and mechanism. Nat. Rev. Microbiol. 10, 336–351. https://doi.org/10.1038/nrmicro2762

130. Koskiniemi, S., Garza-Sánchez, F., Edman, N., Chaudhuri, S., Poole, S.J., Manoil, C., Hayes, C.S., Low, D.A., 2015. Genetic Analysis of the CDI Pathway from *Burkholderia pseudomallei* 1026b. PLoS ONE 10. https://doi.org/10.1371/journal.pone.0120265
131. Krasauskas, R., Labeikytė, D., Markuckas, A., Povilonis, J., Armalytė, J., Plančiūnienė, R., Kavaliauskas, P., Sužiedėlienė, E., 2015. Purification and characterization of a new β-lactamase OXA-205 from *Pseudomonas aeruginosa*. Ann. Clin. Microbiol. Antimicrob. 14, 52. https://doi.org/10.1186/s12941-015-0113-1
132. Kuo, H.-Y., Chao, H.-H., Liao, P.-C., Hsu, L., Chang, K.-C., Tung, C.-H., Chen, C.-H., Liou, M.-L., 2017. Functional Characterization of *Acinetobacter baumannii* Lacking the RNA Chaperone Hfq. Front. Microbiol. 8, 2068. https://doi.org/10.3389/fmicb.2017.02068
133. Laskowska, E., Kuczyńska-Wiśnik, D., 2019. New insight into the mechanisms protecting bacteria during desiccation. Curr. Genet. https://doi.org/10.1007/s00294-019-01036-z
134. Lee, C.-R., Lee, J.H., Park, M., Park, K.S., Bae, I.K., Kim, Y.B., Cha, C.-J., Jeong, B.C., Lee, S.H., 2017. Biology of *Acinetobacter baumannii*: Pathogenesis, Antibiotic Resistance Mechanisms, and Prospective Treatment Options. Front. Cell. Infect. Microbiol. 7. https://doi.org/10.3389/fcimb.2017.00055
135. Lees-Miller, R.G., Iwashkiw, J.A., Scott, N.E., Seper, A., Vinogradov, E., Schild, S., Feldman, M.F., 2013. A common pathway for O-linked protein-glycosylation and synthesis of capsule in *Acinetobacter baumannii*. Mol. Microbiol. 89, 816–830. https://doi.org/10.1111/mmi.12300
136. Lewis, J.M., Deveson Lucas, D., Harper, M., Boyce, J.D., 2019. Systematic Identification and Analysis of *Acinetobacter baumannii* Type VI Secretion System Effector and Immunity Components. Front. Microbiol. 10, 2440. https://doi.org/10.3389/fmicb.2019.02440
137. Li, Z.-T., Zhang, R.-L., Bi, X.-G., Xu, L., Fan, M., Xie, D., Xian, Y., Wang, Y., Li, X.-J., Wu, Z.-D., Zhang, K.-X., 2015. Outer membrane vesicles isolated from two clinical *Acinetobacter baumannii* strains exhibit different toxicity and proteome characteristics. Microb. Pathog. 81, 46–52. https://doi.org/10.1016/j.micpath.2015.03.009
138. Liang, Y., Gao, H., Chen, J., Dong, Y., Wu, L., He, Z., Liu, X., Qiu, G., Zhou, J., 2010. Pellicle formation in *Shewanella oneidensis*. BMC Microbiol. 10, 291. https://doi.org/10.1186/1471-2180-10-291
139. Lin, M.-F., Lin, Y.-Y., Lan, C.-Y., 2015. The Role of the Two-Component System BaeSR in Disposing Chemicals through Regulating Transporter Systems in *Acinetobacter baumannii*. PloS One 10, e0132843. https://doi.org/10.1371/journal.pone.0132843
140. Lin, M.-F., Lin, Y.-Y., Yeh, H.-W., Lan, C.-Y., 2014. Role of the BaeSR two-component system in the regulation of *Acinetobacter baumannii* adeAB genes and its correlation with tigecycline susceptibility. BMC Microbiol. 14, 119. https://doi.org/10.1186/1471-2180-14-119
141. Liu, D., Liu, Z.-S., Hu, P., Cai, L., Fu, B.-Q., Li, Y.-S., Lu, S.-Y., Liu, N.-N., Ma, X.-L., Chi, D., Chang, J., Shui, Y.-M., Li, Z.-H., Ahmad, W., Zhou, Y., Ren, H.-L., 2016. Characterization of surface antigen protein 1 (SurA1) from *Acinetobacter baumannii* and its role in virulence and fitness. Vet. Microbiol. 186, 126–138. https://doi.org/10.1016/j.vetmic.2016.02.018

142. Lodish, H., Berk, A., Zipursky, S.L., Matsudaira, P., Baltimore, D., Darnell, J., 2000. Bacterial Transcription Initiation. Mol. Cell Biol. 4th Ed. Section 10.2.
143. Loehfelm, T.W., Luke, N.R., Campagnari, A.A., 2008. Identification and characterization of an *Acinetobacter baumannii* biofilm-associated protein. J. Bacteriol. 190, 1036–1044. https://doi.org/10.1128/JB.01416-07
144. López, M., Blasco, L., Gato, E., Perez, A., Fernández-Garcia, L., Martínez-Martinez, L., Fernández-Cuenca, F., Rodríguez-Baño, J., Pascual, A., Bou, G., Tomás, M., 2017. Response to Bile Salts in Clinical Strains of *Acinetobacter baumannii* Lacking the AdeABC Efflux Pump: Virulence Associated with Quorum Sensing. Front. Cell. Infect. Microbiol. 7, 143. https://doi.org/10.3389/fcimb.2017.00143
145. Marchand, I., Damier-Piolle, L., Courvalin, P., Lambert, T., 2004. Expression of the RND-type efflux pump AdeABC in *Acinetobacter baumannii* is regulated by the AdeRS two-component system. Antimicrob. Agents Chemother. 48, 3298–3304. https://doi.org/10.1128/AAC.48.9.3298-3304.2004
146. Marti, S., Nait Chabane, Y., Alexandre, S., Coquet, L., Vila, J., Jouenne, T., Dé, E., 2011. Growth of *Acinetobacter baumannii* in pellicle enhanced the expression of potential virulence factors. PloS One 6, e26030. https://doi.org/10.1371/journal.pone.0026030
147. Martínez-Guitián, M., Vázquez-Ucha, J.C., Álvarez-Fraga, L., Conde-Pérez, K., Lasarte-Monterrubio, C., Vallejo, J.A., Bou, G., Poza, M., Beceiro, A., 2019. Involvement of HisF in the Persistence of *Acinetobacter baumannii* During a Pneumonia Infection. Front. Cell. Infect. Microbiol. 9, 310. https://doi.org/10.3389/fcimb.2019.00310
148. Mascher, T., Helmann, J.D., Unden, G., 2006. Stimulus Perception in Bacterial Signal-Transducing Histidine Kinases. Microbiol. Mol. Biol. Rev. 70, 910–938. https://doi.org/10.1128/MMBR.00020-06
149. Mateo-Estrada, V., Graña-Miraglia, L., López-Leal, G., Castillo-Ramírez, S., 2019. Phylogenomics Reveals Clear Cases of Misclassification and Genus-Wide Phylogenetic Markers for *Acinetobacter*. Genome Biol. Evol. 11, 2531–2541. https://doi.org/10.1093/gbe/evz178
150. Mattick, J.S., 2002. Type IV pili and twitching motility. Annu. Rev. Microbiol. 56, 289–314. https://doi.org/10.1146/annurev.micro.56.012302.160938
151. May, H.C., Yu, J.-J., Zhang, H., Wang, Y., Cap, A.P., Chambers, J.P., Guentzel, M.N., Arulanandam, B.P., 2019. Thioredoxin-A is a virulence factor and mediator of the type IV pilus system in *Acinetobacter baumannii*. PloS One 14, e0218505. https://doi.org/10.1371/journal.pone.0218505
152. McConnell, M.J., Actis, L., Pachón, J., 2013. *Acinetobacter baumannii*: human infections, factors contributing to pathogenesis and animal models. FEMS Microbiol. Rev. 37, 130–155. https://doi.org/10.1111/j.1574-6976.2012.00344.x
153. McConnell, M.J., Rumbo, C., Bou, G., Pachón, J., 2011. Outer membrane vesicles as an acellular vaccine against *Acinetobacter baumannii*. Vaccine 29, 5705–5710. https://doi.org/10.1016/j.vaccine.2011.06.001
154. McQueary, C.N., Kirkup, B.C., Si, Y., Barlow, M., Actis, L.A., Craft, D.W., Zurawski, D.V., 2012. Extracellular stress and lipopolysaccharide modulate *Acinetobacter baumannii* surface-associated motility. J. Microbiol. Seoul Korea 50, 434–443. https://doi.org/10.1007/s12275-012-1555-1

155. Mendez, J.A., Soares, N.C., Mateos, J., Gayoso, C., Rumbo, C., Aranda, J., Tomas, M., Bou, G., 2012. Extracellular proteome of a highly invasive multidrug-resistant clinical strain of *Acinetobacter baumannii*. J. Proteome Res. 11, 5678–5694. https://doi.org/10.1021/pr300496c
156. Mercaldi, M.P., Dams-Kozlowska, H., Panilaitis, B., Joyce, A.P., Kaplan, D.L., 2008. Discovery of the dual polysaccharide composition of emulsan and the isolation of the emulsion stabilizing component. Biomacromolecules 9, 1988–1996. https://doi.org/10.1021/bm800239p
157. Miller, D.P., Wang, Q., Weinberg, A., Lamont, R.J., 2018. Transcriptome analysis of *Porphyromonas gingivalis* and *Acinetobacter baumannii* in polymicrobial communities. Mol. Oral Microbiol. 33, 364–377. https://doi.org/10.1111/omi.12238
158. Moon, D.C., Choi, C.H., Lee, J.H., Choi, C.-W., Kim, H.-Y., Park, J.S., Kim, S.I., Lee, J.C., 2012. *Acinetobacter baumannii* outer membrane protein A modulates the biogenesis of outer membrane vesicles. J. Microbiol. Seoul Korea 50, 155–160. https://doi.org/10.1007/s12275-012-1589-4
159. Morris, F.C., Dexter, C., Kostoulias, X., Uddin, M.I., Peleg, A.Y., 2019. The Mechanisms of Disease Caused by *Acinetobacter baumannii*. Front. Microbiol. 10, 1601. https://doi.org/10.3389/fmicb.2019.01601
160. Mortensen, B.L., Rathi, S., Chazin, W.J., Skaar, E.P., 2014. *Acinetobacter baumannii* response to host-mediated zinc limitation requires the transcriptional regulator Zur. J. Bacteriol. 196, 2616–2626. https://doi.org/10.1128/JB.01650-14
161. Müller, G.L., Tuttobene, M., Altilio, M., Martínez Amezaga, M., Nguyen, M., Cribb, P., Cybulski, L.E., Ramírez, M.S., Altabe, S., Mussi, M.A., 2017. Light Modulates Metabolic Pathways and Other Novel Physiological Traits in the Human Pathogen *Acinetobacter baumannii*. J. Bacteriol. 199. https://doi.org/10.1128/JB.00011-17
162. Mussi, M.A., Gaddy, J.A., Cabruja, M., Arivett, B.A., Viale, A.M., Rasia, R., Actis, L.A., 2010. The opportunistic human pathogen *Acinetobacter baumannii* senses and responds to light. J. Bacteriol. 192, 6336–6345. https://doi.org/10.1128/JB.00917-10
163. Mussi, M.A., Relling, V.M., Limansky, A.S., Viale, A.M., 2007. CarO, an *Acinetobacter baumannii* outer membrane protein involved in carbapenem resistance, is essential for L-ornithine uptake. FEBS Lett. 581, 5573–5578. https://doi.org/10.1016/j.febslet.2007.10.063
164. Nait Chabane, Y., Marti, S., Rihouey, C., Alexandre, S., Hardouin, J., Lesouhaitier, O., Vila, J., Kaplan, J.B., Jouenne, T., Dé, E., 2014. Characterisation of pellicles formed by *Acinetobacter baumannii* at the air-liquid interface. PloS One 9, e111660. https://doi.org/10.1371/journal.pone.0111660
165. Ng, C.-K., How, K.-Y., Tee, K.-K., Chan, K.-G., 2019. Characterization and Transcriptome Studies of Autoinducer Synthase Gene from Multidrug Resistant *Acinetobacter baumannii* Strain 863. Genes 10. https://doi.org/10.3390/genes10040282
166. Norrander, J., Kempe, T., Messing, J., 1983. Construction of improved M13 vectors using oligodeoxynucleotide-directed mutagenesis. Gene 26, 101–106. https://doi.org/10.1016/0378-1119(83)90040-9
167. Nwugo, C.C., Gaddy, J.A., Zimbler, D.L., Actis, L.A., 2011. Deciphering the iron response in *Acinetobacter baumannii*: A proteomics approach. J. Proteomics 74, 44–58. https://doi.org/10.1016/j.jprot.2010.07.010

168. Oh, M.H., Lee, J.C., Kim, J., Choi, C.H., Han, K., 2015. Simple Method for Markerless Gene Deletion in Multidrug-Resistant *Acinetobacter baumannii*. Appl. Environ. Microbiol. 81, 3357–3368. https://doi.org/10.1128/AEM.03975-14
169. Ohneck, E.J., Arivett, B.A., Fiester, S.E., Wood, C.R., Metz, M.L., Simeone, G.M., Actis, L.A., 2018. Mucin acts as a nutrient source and a signal for the differential expression of genes coding for cellular processes and virulence factors in *Acinetobacter baumannii*. PloS One 13, e0190599. https://doi.org/10.1371/journal.pone.0190599
170. O'Toole, G.A., Pratt, L.A., Watnick, P.I., Newman, D.K., Weaver, V.B., Kolter, R., 1999. Genetic approaches to study of biofilms. Methods Enzymol. 310, 91–109. https://doi.org/10.1016/s0076-6879(99)10008-9
171. Pakharukova, N., Tuittila, M., Paavilainen, S., Malmi, H., Parilova, O., Teneberg, S., Knight, S.D., Zavialov, A.V., 2018. Structural basis for *Acinetobacter baumannii* biofilm formation. Proc. Natl. Acad. Sci. U. S. A. 115, 5558–5563. https://doi.org/10.1073/pnas.1800961115
172. Peleg, A.Y., Seifert, H., Paterson, D.L., 2008. *Acinetobacter baumannii*: emergence of a successful pathogen. Clin. Microbiol. Rev. 21, 538–582. https://doi.org/10.1128/CMR.00058-07
173. Penesyan, A., Nagy, S.S., Kjelleberg, S., Gillings, M.R., Paulsen, I.T., 2019. Rapid microevolution of biofilm cells in response to antibiotics. NPJ Biofilms Microbiomes 5, 34. https://doi.org/10.1038/s41522-019-0108-3
174. Pérez, A., Merino, M., Rumbo-Feal, S., Álvarez-Fraga, L., Vallejo, J.A., Beceiro, A., Ohneck, E.J., Mateos, J., Fernández-Puente, P., Actis, L.A., Poza, M., Bou, G., 2017. The FhaB/FhaC two-partner secretion system is involved in adhesion of *Acinetobacter baumannii* AbH12O-A2 strain. Virulence 8, 959–974. https://doi.org/10.1080/21505594.2016.1262313
175. Pinto, D., Liu, Q., Mascher, T., 2019. ECF σ factors with regulatory extensions: the one-component systems of the σ universe. Mol. Microbiol. 112, 399–409. https://doi.org/10.1111/mmi.14323
176. Poltak, S.R., Cooper, V.S., 2011. Ecological succession in long-term experimentally evolved biofilms produces synergistic communities. ISME J. 5, 369–378. https://doi.org/10.1038/ismej.2010.136
177. Poole, K., 2012. Bacterial stress responses as determinants of antimicrobial resistance. J. Antimicrob. Chemother. 67, 2069–2089. https://doi.org/10.1093/jac/dks196
178. Povilonis, J., Seputiene, V., Krasauskas, R., Juskaite, R., Miskinyte, M., Suziedelis, K., Suziedeliene, E., 2013. Spread of carbapenem-resistant *Acinetobacter baumannii* carrying a plasmid with two genes encoding OXA-72 carbapenemase in Lithuanian hospitals. J. Antimicrob. Chemother. 68, 1000–1006. https://doi.org/10.1093/jac/dks499
179. Pukatzki, S., McAuley, S.B., Miyata, S.T., 2009. The type VI secretion system: translocation of effectors and effector-domains. Curr. Opin. Microbiol. 12, 11–17. https://doi.org/10.1016/j.mib.2008.11.010
180. Repizo, G.D., Espariz, M., Seravalle, J.L., Salcedo, S.P., 2019. Bioinformatic Analysis of the Type VI Secretion System and Its Potential Toxins in the *Acinetobacter* Genus. Front. Microbiol. 10. https://doi.org/10.3389/fmicb.2019.02519
181. Repizo, G.D., Gagné, S., Foucault-Grunenwald, M.-L., Borges, V., Charpentier, X., Limansky, A.S., Gomes, J.P., Viale, A.M., Salcedo, S.P., 2015. Differential Role of the T6SS in *Acinetobacter baumannii* Virulence. PloS One 10, e0138265. https://doi.org/10.1371/journal.pone.0138265

182. Richmond, G.E., Evans, L.P., Anderson, M.J., Wand, M.E., Bonney, L.C., Ivens, A., Chua, K.L., Webber, M.A., Sutton, J.M., Peterson, M.L., Piddock, L.J.V., 2016. The *Acinetobacter baumannii* Two-Component System AdeRS Regulates Genes Required for Multidrug Efflux, Biofilm Formation, and Virulence in a Strain-Specific Manner. mBio 7. https://doi.org/10.1128/mBio.00430-16
183. Rodman, N., Martinez, J., Fung, S., Nakanouchi, J., Myers, A.L., Harris, C.M., Dang, E., Fernandez, J.S., Liu, C., Mendoza, A.M., Jimenez, V., Nikolaidis, N., Brennan, C.A., Bonomo, R.A., Sieira, R., Ramirez, M.S., 2019. Human Pleural Fluid Elicits Pyruvate and Phenylalanine Metabolism in *Acinetobacter baumannii* to Enhance Cytotoxicity and Immune Evasion. Front. Microbiol. 10, 1581. https://doi.org/10.3389/fmicb.2019.01581
184. Ronish, L.A., Lillehoj, E., Fields, J.K., Sundberg, E.J., Piepenbrink, K.H., 2019. The structure of PilA from *Acinetobacter baumannii* AB5075 suggests a mechanism for functional specialization in *Acinetobacter* type IV pili. J. Biol. Chem. 294, 218–230. https://doi.org/10.1074/jbc.RA118.005814
185. Rosenfeld, N., Bouchier, C., Courvalin, P., Périchon, B., 2012. Expression of the resistance-nodulation-cell division pump AdeIJK in *Acinetobacter baumannii* is regulated by AdeN, a TetR-type regulator. Antimicrob. Agents Chemother. 56, 2504–2510. https://doi.org/10.1128/AAC.06422-11
186. Roussin, M., Rabarioelina, S., Cluzeau, L., Cayron, J., Lesterlin, C., Salcedo, S.P., Bigot, S., 2019. Identification of a Contact-Dependent Growth Inhibition (CDI) System That Reduces Biofilm Formation and Host Cell Adhesion of *Acinetobacter baumannii* DSM30011 Strain. Front. Microbiol. 10, 2450. https://doi.org/10.3389/fmicb.2019.02450
187. Ruhe, Z.C., Low, D.A., Hayes, C.S., 2013a. Bacterial contact-dependent growth inhibition. Trends Microbiol. 21, 230–237. https://doi.org/10.1016/j.tim.2013.02.003
188. Ruhe, Z.C., Nguyen, J.Y., Chen, A.J., Leung, N.Y., Hayes, C.S., Low, D.A., 2016. CDI Systems Are Stably Maintained by a Cell-Contact Mediated Surveillance Mechanism. PLoS Genet. 12. https://doi.org/10.1371/journal.pgen.1006145
189. Ruhe, Z.C., Nguyen, J.Y., Xiong, J., Koskiniemi, S., Beck, C.M., Perkins, B.R., Low, D.A., Hayes, C.S., 2017. CdiA Effectors Use Modular Receptor-Binding Domains To Recognize Target Bacteria. mBio 8. https://doi.org/10.1128/mBio.00290-17
190. Ruhe, Z.C., Subramanian, P., Song, K., Nguyen, J.Y., Stevens, T.A., Low, D.A., Jensen, G.J., Hayes, C.S., 2018. Programmed Secretion Arrest and Receptor-Triggered Toxin Export during Antibacterial Contact-Dependent Growth Inhibition. Cell 175, 921-933.e14. https://doi.org/10.1016/j.cell.2018.10.033
191. Ruhe, Z.C., Townsley, L., Wallace, A.B., King, A., Van der Woude, M.W., Low, D.A., Yildiz, F.H., Hayes, C.S., 2015. CdiA promotes receptor-independent intercellular adhesion. Mol. Microbiol. 98, 175–192. https://doi.org/10.1111/mmi.13114
192. Ruhe, Z.C., Wallace, A.B., Low, D.A., Hayes, C.S., 2013b. Receptor polymorphism restricts contact-dependent growth inhibition to members of the same species. mBio 4. https://doi.org/10.1128/mBio.00480-13
193. Rumbo, C., Tomás, M., Fernández Moreira, E., Soares, N.C., Carvajal, M., Santillana, E., Beceiro, A., Romero, A., Bou, G., 2014. The *Acinetobacter baumannii* Omp33-36 Porin Is a Virulence Factor That Induces Apoptosis and Modulates Autophagy in Human Cells. Infect. Immun. 82, 4666–4680. https://doi.org/10.1128/IAI.02034-14

194. Rumbo-Feal, S., Gómez, M.J., Gayoso, C., Álvarez-Fraga, L., Cabral, M.P., Aransay, A.M., Rodríguez-Ezpeleta, N., Fullaondo, A., Valle, J., Tomás, M., Bou, G., Poza, M., 2013. Whole transcriptome analysis of *Acinetobacter baumannii* assessed by RNA-sequencing reveals different mRNA expression profiles in biofilm compared to planktonic cells. PloS One 8, e72968. https://doi.org/10.1371/journal.pone.0072968
195. Rumbo-Feal, S., Pérez, A., Ramelot, T.A., Álvarez-Fraga, L., Vallejo, J.A., Beceiro, A., Ohneck, E.J., Arivett, B.A., Merino, M., Fiester, S.E., Kennedy, M.A., Actis, L.A., Bou, G., Poza, M., 2017. Contribution of the *A. baumannii* A1S_0114 Gene to the Interaction with Eukaryotic Cells and Virulence. Front. Cell. Infect. Microbiol. 7, 108. https://doi.org/10.3389/fcimb.2017.00108
196. Russo, T.A., Luke, N.R., Beanan, J.M., Olson, R., Sauberan, S.L., MacDonald, U., Schultz, L.W., Umland, T.C., Campagnari, A.A., 2010. The K1 capsular polysaccharide of *Acinetobacter baumannii* strain 307-0294 is a major virulence factor. Infect. Immun. 78, 3993–4000. https://doi.org/10.1128/IAI.00366-10
197. Russo, T.A., Manohar, A., Beanan, J.M., Olson, R., MacDonald, U., Graham, J., Umland, T.C., 2016. The Response Regulator BfmR Is a Potential Drug Target for *Acinetobacter baumannii*. mSphere 1. https://doi.org/10.1128/mSphere.00082-16
198. Saberi, F., Kamali, M., Najafi, A., Yazdanparast, A., Moghaddam, M.M., 2016. Natural antisense RNAs as mRNA regulatory elements in bacteria: a review on function and applications. Cell. Mol. Biol. Lett. 21, 6. https://doi.org/10.1186/s11658-016-0007-z
199. Saranathan, R., Pagal, S., Sawant, A.R., Tomar, A., Madhangi, M., Sah, S., Satti, A., Arunkumar, K.P., Prashanth, K., 2017. Disruption of tetR type regulator adeN by mobile genetic element confers elevated virulence in *Acinetobacter baumannii*. Virulence 8, 1316–1334. https://doi.org/10.1080/21505594.2017.1322240
200. Schindelin, J., Arganda-Carreras, I., Frise, E., Kaynig, V., Longair, M., Pietzsch, T., Preibisch, S., Rueden, C., Saalfeld, S., Schmid, B., Tinevez, J.-Y., White, D.J., Hartenstein, V., Eliceiri, K., Tomancak, P., Cardona, A., 2012. Fiji: an open-source platform for biological-image analysis. Nat. Methods 9, 676–682. https://doi.org/10.1038/nmeth.2019
201. Schultz, M.B., Pham Thanh, D., Tran Do Hoan, N., Wick, R.R., Ingle, D.J., Hawkey, J., Edwards, D.J., Kenyon, J.J., Phu Huong Lan, N., Campbell, J.I., Thwaites, G., Thi Khanh Nhu, N., Hall, R.M., Fournier-Level, A., Baker, S., Holt, K.E., 2016. Repeated local emergence of carbapenem-resistant *Acinetobacter baumannii* in a single hospital ward. Microb. Genomics 2, e000050. https://doi.org/10.1099/mgen.0.000050
202. Seputiene, V., Linkevicius, M., Bogdaite, A., Povilonis, J., Planciūniene, R., Giedraitiene, A., Pavilonis, A., Suziedeliene, E., 2010. Molecular characterization of extended-spectrum β-lactamase-producing *Escherichia coli* and *Klebsiella pneumoniae* isolates from hospitals in Lithuania. J. Med. Microbiol. 59, 1263–1265. https://doi.org/10.1099/jmm.0.021972-0
203. Sevilla, E., Bes, M.T., González, A., Peleato, M.L., Fillat, M.F., 2019. Redox-Based Transcriptional Regulation in Prokaryotes: Revisiting Model Mechanisms. Antioxid. Redox Signal. 30, 1651–1696. https://doi.org/10.1089/ars.2017.7442
204. Sharma, O., Datsenko, K.A., Ess, S.C., Zhalnina, M.V., Wanner, B.L., Cramer, W.A., 2009. Genome-wide screens: novel mechanisms in colicin import and cytotoxicity. Mol. Microbiol. 73, 571–585. https://doi.org/10.1111/j.1365-2958.2009.06788.x

205. Sharma, R., Arya, S., Patil, S.D., Sharma, A., Jain, P.K., Navani, N.K., Pathania, R., 2014. Identification of Novel Regulatory Small RNAs in *Acinetobacter baumannii*. PLoS ONE 9. https://doi.org/10.1371/journal.pone.0093833
206. Singh, J.K., Adams, F.G., Brown, M.H., 2018. Diversity and Function of Capsular Polysaccharide in *Acinetobacter baumannii*. Front. Microbiol. 9, 3301. https://doi.org/10.3389/fmicb.2018.03301
207. Skerniškytė, J., Karazijaitė, E., Deschamps, J., Krasauskas, R., Armalytė, J., Briandet, R., Sužiedėlienė, E., 2019a. Blp1 protein shows virulence-associated features and elicits protective immunity to *Acinetobacter baumannii* infection. BMC Microbiol. 19, 259. https://doi.org/10.1186/s12866-019-1615-3
208. Skerniškytė, J., Karazijaitė, E., Deschamps, J., Krasauskas, R., Briandet, R., Sužiedėlienė, E., 2019b. The Mutation of Conservative Asp268 Residue in the Peptidoglycan-Associated Domain of the OmpA Protein Affects Multiple *Acinetobacter baumannii* Virulence Characteristics. Mol. Basel Switz. 24. https://doi.org/10.3390/molecules24101972
209. Skerniškytė, J., Krasauskas, R., Péchoux, C., Kulakauskas, S., Armalytė, J., Sužiedėlienė, E., 2019c. Surface-Related Features and Virulence Among *Acinetobacter baumannii* Clinical Isolates Belonging to International Clones I and II. Front. Microbiol. 9, 3116. https://doi.org/10.3389/fmicb.2018.03116
210. Skiebe, E., de Berardinis, V., Morczinek, P., Kerrinnes, T., Faber, F., Lepka, D., Hammer, B., Zimmermann, O., Ziesing, S., Wichelhaus, T.A., Hunfeld, K.-P., Borgmann, S., Gröbner, S., Higgins, P.G., Seifert, H., Busse, H.-J., Witte, W., Pfeifer, Y., Wilharm, G., 2012. Surface-associated motility, a common trait of clinical isolates of *Acinetobacter baumannii*, depends on 1,3-diaminopropane. Int. J. Med. Microbiol. IJMM 302, 117–128. https://doi.org/10.1016/j.ijmm.2012.03.003
211. Smani, Y., McConnell, M.J., Pachón, J., 2012. Role of fibronectin in the adhesion of *Acinetobacter baumannii* to host cells. PloS One 7, e33073. https://doi.org/10.1371/journal.pone.0033073
212. Snitkin, E.S., Zelazny, A.M., Gupta, J., NISC Comparative Sequencing Program, Palmore, T.N., Murray, P.R., Segre, J.A., 2013. Genomic insights into the fate of colistin resistance and *Acinetobacter baumannii* during patient treatment. Genome Res. 23, 1155–1162. https://doi.org/10.1101/gr.154328.112
213. Soojhawon, I., Pattabiraman, N., Tsang, A., Roth, A.L., Kang, E., Noble, S.M., 2017. Discovery of novel inhibitors of multidrug-resistant *Acinetobacter baumannii*. Bioorg. Med. Chem. 25, 5477–5482. https://doi.org/10.1016/j.bmc.2017.08.014
214. Srinivasan, V.B., Vaidyanathan, V., Rajamohan, G., 2015. AbuO, a TolC-like outer membrane protein of *Acinetobacter baumannii*, is involved in antimicrobial and oxidative stress resistance. Antimicrob. Agents Chemother. 59, 1236–1245. https://doi.org/10.1128/AAC.03626-14
215. Stahl, J., Bergmann, H., Göttig, S., Ebersberger, I., Averhoff, B., 2015. *Acinetobacter baumannii* Virulence Is Mediated by the Concerted Action of Three Phospholipases D. PloS One 10, e0138360. https://doi.org/10.1371/journal.pone.0138360
216. Sugawara, E., Nikaido, H., 2012. OmpA is the principal nonspecific slow porin of *Acinetobacter baumannii*. J. Bacteriol. 194, 4089–4096. https://doi.org/10.1128/JB.00435-12
217. Sun, D., Crowell, S.A., Harding, C.M., De Silva, P.M., Harrison, A., Fernando, D.M., Mason, K.M., Santana, E., Loewen, P.C., Kumar, A., Liu, Y., 2016. KatG and KatE

confer *Acinetobacter* resistance to hydrogen peroxide but sensitize bacteria to killing by phagocytic respiratory burst. Life Sci. 148, 31–40. https://doi.org/10.1016/j.lfs.2016.02.015

218. Szwedziak, P., Pilhofer, M., 2019. Bidirectional contraction of a type six secretion system. Nat. Commun. 10, 1565. https://doi.org/10.1038/s41467-019-09603-1
219. Tacconelli, E., Carrara, E., Savoldi, A., Harbarth, S., Mendelson, M., Monnet, D.L., Pulcini, C., Kahlmeter, G., Kluytmans, J., Carmeli, Y., Ouellette, M., Outterson, K., Patel, J., Cavaleri, M., Cox, E.M., Houchens, C.R., Grayson, M.L., Hansen, P., Singh, N., Theuretzbacher, U., Magrini, N., WHO Pathogens Priority List Working Group, 2018. Discovery, research, and development of new antibiotics: the WHO priority list of antibiotic-resistant bacteria and tuberculosis. Lancet Infect. Dis. 18, 318–327. https://doi.org/10.1016/S1473-3099(17)30753-3
220. Talà, A., Progida, C., De Stefano, M., Cogli, L., Spinosa, M.R., Bucci, C., Alifano, P., 2008. The HrpB-HrpA two-partner secretion system is essential for intracellular survival of *Neisseria meningitidis*. Cell. Microbiol. 10, 2461–2482. https://doi.org/10.1111/j.1462-5822.2008.01222.x
221. Tilley, D., Law, R., Warren, S., Samis, J.A., Kumar, A., 2014. CpaA a novel protease from *Acinetobacter baumannii* clinical isolates deregulates blood coagulation. FEMS Microbiol. Lett. 356, 53–61. https://doi.org/10.1111/1574-6968.12496
222. Tipton, K.A., Chin, C.-Y., Farokhyfar, M., Weiss, D.S., Rather, P.N., 2018. Role of Capsule in Resistance to Disinfectants, Host Antimicrobials, and Desiccation in *Acinetobacter baumannii*. Antimicrob. Agents Chemother. 62. https://doi.org/10.1128/AAC.01188-18
223. Tipton, K.A., Dimitrova, D., Rather, P.N., 2015. Phase-Variable Control of Multiple Phenotypes in *Acinetobacter baumannii* Strain AB5075. J. Bacteriol. 197, 2593–2599. https://doi.org/10.1128/JB.00188-15
224. Tiwari, S., Jamal, S.B., Hassan, S.S., Carvalho, P.V.S.D., Almeida, S., Barh, D., Ghosh, P., Silva, A., Castro, T.L.P., Azevedo, V., 2017. Two-Component Signal Transduction Systems of Pathogenic Bacteria As Targets for Antimicrobial Therapy: An Overview. Front. Microbiol. 8, 1878. https://doi.org/10.3389/fmicb.2017.01878
225. Tomaras, A.P., Dorsey, C.W., Edelmann, R.E., Actis, L.A., 2003. Attachment to and biofilm formation on abiotic surfaces by *Acinetobacter baumannii*: involvement of a novel chaperone-usher pili assembly system. Microbiol. Read. Engl. 149, 3473–3484. https://doi.org/10.1099/mic.0.26541-0
226. Tomaras, A.P., Flagler, M.J., Dorsey, C.W., Gaddy, J.A., Actis, L.A., 2008. Characterization of a two-component regulatory system from *Acinetobacter baumannii* that controls biofilm formation and cellular morphology. Microbiol. Read. Engl. 154, 3398–3409. https://doi.org/10.1099/mic.0.2008/019471-0
227. Touchon, M., Cury, J., Yoon, E.-J., Krizova, L., Cerqueira, G.C., Murphy, C., Feldgarden, M., Wortman, J., Clermont, D., Lambert, T., Grillot-Courvalin, C., Nemec, A., Courvalin, P., Rocha, E.P.C., 2014. The genomic diversification of the whole *Acinetobacter* genus: origins, mechanisms, and consequences. Genome Biol. Evol. 6, 2866–2882. https://doi.org/10.1093/gbe/evu225
228. Turton, J.F., Gabriel, S.N., Valderrey, C., Kaufmann, M.E., Pitt, T.L., 2007. Use of sequence-based typing and multiplex PCR to identify clonal lineages of outbreak strains of *Acinetobacter baumannii*. Clin. Microbiol. Infect. Off. Publ. Eur. Soc. Clin. Microbiol. Infect. Dis. 13, 807–815. https://doi.org/10.1111/j.1469-0691.2007.01759.x

229. Tuttobene, M.R., Cribb, P., Mussi, M.A., 2018. BlsA integrates light and temperature signals into iron metabolism through Fur in the human pathogen *Acinetobacter baumannii*. Sci. Rep. 8, 7728. https://doi.org/10.1038/s41598-018-26127-8
230. Vandecraen, J., Chandler, M., Aertsen, A., Van Houdt, R., 2017. The impact of insertion sequences on bacterial genome plasticity and adaptability. Crit. Rev. Microbiol. 43, 709–730. https://doi.org/10.1080/1040841X.2017.1303661
231. Vila, J., Martí, S., Sánchez-Céspedes, J., 2007. Porins, efflux pumps and multidrug resistance in *Acinetobacter baumannii*. J. Antimicrob. Chemother. 59, 1210–1215. https://doi.org/10.1093/jac/dkl509
232. Vincent, J.-L., Rello, J., Marshall, J., Silva, E., Anzueto, A., Martin, C.D., Moreno, R., Lipman, J., Gomersall, C., Sakr, Y., Reinhart, K., EPIC II Group of Investigators, 2009. International study of the prevalence and outcomes of infection in intensive care units. JAMA 302, 2323–2329. https://doi.org/10.1001/jama.2009.1754
233. Wandersman, C., Delepelaire, P., 2004. Bacterial iron sources: from siderophores to hemophores. Annu. Rev. Microbiol. 58, 611–647. https://doi.org/10.1146/annurev.micro.58.030603.123811
234. Wang, N., Ozer, E.A., Mandel, M.J., Hauser, A.R., 2014. Genome-wide identification of *Acinetobacter baumannii* genes necessary for persistence in the lung. mBio 5, e01163-01114. https://doi.org/10.1128/mBio.01163-14
235. Webb, J.S., Nikolakakis, K.C., Willett, J.L.E., Aoki, S.K., Hayes, C.S., Low, D.A., 2013. Delivery of CdiA nuclease toxins into target cells during contact-dependent growth inhibition. PloS One 8, e57609. https://doi.org/10.1371/journal.pone.0057609
236. Weber, B.S., Harding, C.M., Feldman, M.F., 2015a. Pathogenic *Acinetobacter*: from the Cell Surface to Infinity and Beyond. J. Bacteriol. 198, 880–887. https://doi.org/10.1128/JB.00906-15
237. Weber, B.S., Kinsella, R.L., Harding, C.M., Feldman, M.F., 2017. The Secrets of *Acinetobacter* Secretion. Trends Microbiol. 25, 532–545. https://doi.org/10.1016/j.tim.2017.01.005
238. Weber, B.S., Ly, P.M., Irwin, J.N., Pukatzki, S., Feldman, M.F., 2015b. A multidrug resistance plasmid contains the molecular switch for type VI secretion in *Acinetobacter baumannii*. Proc. Natl. Acad. Sci. U. S. A. 112, 9442–9447. https://doi.org/10.1073/pnas.1502966112
239. Weber, B.S., Miyata, S.T., Iwashkiw, J.A., Mortensen, B.L., Skaar, E.P., Pukatzki, S., Feldman, M.F., 2013. Genomic and functional analysis of the type VI secretion system in *Acinetobacter*. PloS One 8, e55142. https://doi.org/10.1371/journal.pone.0055142
240. Weidensdorfer, M., Ishikawa, M., Hori, K., Linke, D., Djahanschiri, B., Iruegas, R., Ebersberger, I., Riedel-Christ, S., Enders, G., Leukert, L., Kraiczy, P., Rothweiler, F., Cinatl, J., Berger, J., Hipp, K., Kempf, V.A.J., Göttig, S., 2019. The *Acinetobacter* trimeric autotransporter adhesin Ata controls key virulence traits of *Acinetobacter baumannii*. Virulence 10, 68–81. https://doi.org/10.1080/21505594.2018.1558693
241. Weiss, A., Broach, W.H., Lee, M.C., Shaw, L.N., 2016. Towards the complete small RNome of *Acinetobacter baumannii*. Microb. Genomics 2. https://doi.org/10.1099/mgen.0.000045
242. Willett, J.L.E., Gucinski, G.C., Fatherree, J.P., Low, D.A., Hayes, C.S., 2015a. Contact-dependent growth inhibition toxins exploit multiple independent cell-entry pathways. Proc. Natl. Acad. Sci. U. S. A. 112, 11341–11346. https://doi.org/10.1073/pnas.1512124112

243. Willett, J.L.E., Ruhe, Z.C., Goulding, C.W., Low, D.A., Hayes, C.S., 2015b. Contact-Dependent Growth Inhibition (CDI) and CdiB/CdiA Two-Partner Secretion Proteins. J. Mol. Biol. 427, 3754–3765. https://doi.org/10.1016/j.jmb.2015.09.010
244. Wong, D., Nielsen, T.B., Bonomo, R.A., Pantapalangkoor, P., Luna, B., Spellberg, B., 2017. Clinical and Pathophysiological Overview of *Acinetobacter* Infections: a Century of Challenges. Clin. Microbiol. Rev. 30, 409–447. https://doi.org/10.1128/CMR.00058-16
245. Wood, C.R., Ohneck, E.J., Edelmann, R.E., Actis, L.A., 2018. A Light-Regulated Type I Pilus Contributes to *Acinetobacter baumannii* Biofilm, Motility, and Virulence Functions. Infect. Immun. 86. https://doi.org/10.1128/IAI.00442-18
246. Wood, W.B., 1966. Host specificity of DNA produced by *Escherichia coli*: bacterial mutations affecting the restriction and modification of DNA. J. Mol. Biol. 16, 118–133. https://doi.org/10.1016/s0022-2836(66)80267-x
247. Woodcock, D.M., Crowther, P.J., Doherty, J., Jefferson, S., DeCruz, E., Noyer-Weidner, M., Smith, S.S., Michael, M.Z., Graham, M.W., 1989. Quantitative evaluation of *Escherichia coli* host strains for tolerance to cytosine methylation in plasmid and phage recombinants. Nucleic Acids Res. 17, 3469–3478. https://doi.org/10.1093/nar/17.9.3469
248. Wright, M.S., Haft, D.H., Harkins, D.M., Perez, F., Hujer, K.M., Bajaksouzian, S., Benard, M.F., Jacobs, M.R., Bonomo, R.A., Adams, M.D., 2014. New insights into dissemination and variation of the health care-associated pathogen *Acinetobacter baumannii* from genomic analysis. mBio 5, e00963-00913. https://doi.org/10.1128/mBio.00963-13
249. Wright, M.S., Jacobs, M.R., Bonomo, R.A., Adams, M.D., 2017. Transcriptome Remodeling of *Acinetobacter baumannii* during Infection and Treatment. mBio 8. https://doi.org/10.1128/mBio.02193-16
250. Wyres, K.L., Cahill, S.M., Holt, K.E., Hall, R.M., Kenyon, J.J., 2020. Identification of *Acinetobacter baumannii* loci for capsular polysaccharide (KL) and lipooligosaccharide outer core (OCL) synthesis in genome assemblies using curated reference databases compatible with Kaptive. Microb. Genomics. https://doi.org/10.1099/mgen.0.000339
251. Xavier, J.B., 2011. Social interaction in synthetic and natural microbial communities. Mol. Syst. Biol. 7, 483. https://doi.org/10.1038/msb.2011.16
252. Xu, Q., Chen, T., Yan, B., Zhang, Linyue, Pi, B., Yang, Y., Zhang, Linghong, Zhou, Z., Ji, S., Leptihn, S., Akova, M., Yu, Y., Hua, X., 2019. Dual Role of gnaA in Antibiotic Resistance and Virulence in *Acinetobacter baumannii*. Antimicrob. Agents Chemother. 63. https://doi.org/10.1128/AAC.00694-19
253. Yan, J., Bassler, B.L., 2019. Surviving as a Community: Antibiotic Tolerance and Persistence in Bacterial Biofilms. Cell Host Microbe 26, 15–21. https://doi.org/10.1016/j.chom.2019.06.002
254. Yanisch-Perron, C., Vieira, J., Messing, J., 1985. Improved M13 phage cloning vectors and host strains: nucleotide sequences of the M13mp18 and pUC19 vectors. Gene 33, 103–119. https://doi.org/10.1016/0378-1119(85)90120-9
255. Yoon, E.-J., Balloy, V., Fiette, L., Chignard, M., Courvalin, P., Grillot-Courvalin, C., 2016. Contribution of the Ade Resistance-Nodulation-Cell Division-Type Efflux Pumps to Fitness and Pathogenesis of *Acinetobacter baumannii*. mBio 7. https://doi.org/10.1128/mBio.00697-16
256. Zahn, M., D'Agostino, T., Eren, E., Baslé, A., Ceccarelli, M., van den Berg, B., 2015. Small-Molecule Transport by CarO, an Abundant Eight-Stranded β-Barrel Outer

Membrane Protein from *Acinetobacter baumannii*. J. Mol. Biol. 427, 2329–2339. https://doi.org/10.1016/j.jmb.2015.03.016

257. Zarrilli, R., Bagattini, M., Esposito, E.P., Triassi, M., 2018. *Acinetobacter* Infections in Neonates. Curr. Infect. Dis. Rep. 20, 48. https://doi.org/10.1007/s11908-018-0654-5
258. Zarrilli, R., Pournaras, S., Giannouli, M., Tsakris, A., 2013. Global evolution of multidrug-resistant *Acinetobacter baumannii* clonal lineages. Int. J. Antimicrob. Agents 41, 11–19. https://doi.org/10.1016/j.ijantimicag.2012.09.008
259. Zhang, D., de Souza, R.F., Anantharaman, V., Iyer, L.M., Aravind, L., 2012. Polymorphic toxin systems: Comprehensive characterization of trafficking modes, processing, mechanisms of action, immunity and ecology using comparative genomics. Biol. Direct 7, 18. https://doi.org/10.1186/1745-6150-7-18
260. Zimmermann, L., Stephens, A., Nam, S.-Z., Rau, D., Kübler, J., Lozajic, M., Gabler, F., Söding, J., Lupas, A.N., Alva, V., 2018. A Completely Reimplemented MPI Bioinformatics Toolkit with a New HHpred Server at its Core. J. Mol. Biol. 430, 2237–2243. https://doi.org/10.1016/j.jmb.2017.12.007
261. Zschiedrich, C.P., Keidel, V., Szurmant, H., 2016. Molecular Mechanisms of Two-Component Signal Transduction. J. Mol. Biol. 428, 3752–3775. https://doi.org/10.1016/j.jmb.2016.08.003

SUPPLEMENTARY MATERIAL

Supplementary table 1. A list of complete *A. baumannii* genomes used in the analyses and their NCBI GenBank accession numbers. IC groups were determined by the *in silico* PCR using primer pairs described by Turton *et al.* (2007).

Assembly accession	Genome accession	Strain name	IC group
GCA_000018445.1	CP000863.1	ACICU	IC II
GCA_000021145.1	CP001172.1	AB307-0294	IC I
GCA_000021245.2	CP001182.2	AB0057	IC I
GCA_000069245.1	CU459141.1	AYE	IC I
GCA_000186665.4	CP003967.2	D1279779	IC_other
GCA_000187205.4	CP003500.1	MDR-TJ	IC II
GCA_000188215.1	CP001921.1	1656-2	IC II
GCA_000226275.2	CP001937.2	MDR-ZJ06	IC_other
GCA_000302575.1	CP003856.1	TYTH-1	IC II
GCA_000419385.1	CP003846.1	BJAB07104	IC II
GCA_000419405.1	CP003847.1	BJAB0715	IC_other
GCA_000419425.1	CP003849.1	BJAB0868	IC_other
GCA_000498375.2	CP017152.1	DU202	IC II
GCA_000505685.2	CP006768.1	ZW85-1	IC_other
GCA_000576535.1	CP006963.1	AB07	IC II
GCA_000695855.3	CP007535.2	AC29	IC II
GCA_000746605.1	CP009256.1	AB031	IC_other
GCA_000746645.1	CP009257.1	AB030	IC_other
GCA_000761175.1	CP009534.1	AbH12O-A2	IC_other
GCA_000786735.1	CP007712.1	LAC-4	IC_other
GCA_000814345.1	CP010397.1	6200	IC_other
GCA_000828795.1	AP013357.1	NCGM 237	IC_other
GCA_000828935.1	AP014649.1	IOMTU 433	IC_other
GCA_000830055.1	CP010781.1	A1	IC I
GCA_000939415.2	CP015483.1	ORAB01	IC II
GCA_000963815.1	CP008706.1	AB5075-UW	IC I
GCA_001026965.1	CP010779.1	XH386	IC II
GCA_001077555.2	CP021342.1	B8342	IC_other
GCA_001077565.2	CP021345.1	B11911	IC_other
GCA_001077655.1	CP012006.1	Ab04-mff	IC_other
GCA_001077675.1	CP012004.1	ATCC 17978-mff	IC_other
GCA_001077965.2	CP021347.1	B8300	IC_other
GCA_001261895.2	LN868200.1	R2090	IC_other
GCA_001399655.1	CP012952.1	D36	IC I
GCA_001457535.1	LN865143.1	CIP70.10	IC_other
GCA_001514375.1	CP013924.1	KBN10P02143	IC II
GCA_001517645.1	LN997846.1	R2091	IC_other
GCA_001543995.1	CP014215.1	YU-R612	IC II
GCA_001573065.1	CP014538.1	XH860	IC II
GCA_001573085.1	CP014539.1	XH859	IC II
GCA_001573105.1	CP014540.1	XH857	IC_other
GCA_001573125.1	CP014541.1	XH856	IC II
GCA_001578145.1	CP014528.1	XH858	IC_other
GCA_001636235.1	CP015364.1	3207	IC_other
GCA_001721705.1	CP012587.1	CA-17	IC_other
GCA_001806345.1	CP017642.1	KAB01	IC II
GCA_001806365.1	CP017644.1	KAB02	IC II
GCA_001806385.1	CP017646.1	KAB03	IC II
GCA_001806405.1	CP017648.1	KAB04	IC II
GCA_001806425.1	CP017650.1	KAB05	IC II
GCA_001806445.1	CP017652.1	KAB06	IC II
GCA_001806465.1	CP017654.1	KAB07	IC II

GCA_001806485.1	CP017656.1	KAB08	IC II
GCA_001887305.1	CP018143.1	HRAB-85	IC II
GCA_001895985.1	CP018256.1	AF-673	IC II
GCA_001896005.1	CP018254.1	AF-401	IC_other
GCA_001902375.1	CP018421.1	XDR-BJ83	IC II
GCA_001922205.1	CP016295.1	CMC-CR-MDR-Ab4	IC II
GCA_001922225.1	CP016298.1	CMC-MDR-Ab59	IC II
GCA_001922245.1	CP016300.1	CMC-CR-MDR-Ab66	IC II
GCA_001922425.2	CP018861.2	11510	IC_other
GCA_001941765.1	CP019034.1	AB042	IC_other
GCA_002082625.2	CP020584.1	JBA13	IC II
GCA_002082645.1	CP020586.1	CBA7	IC_other
GCA_002082685.1	CP020590.1	15A34	IC_other
GCA_002082705.1	CP020574.1	15A5	IC II
GCA_002082725.1	CP020592.1	USA2	IC II
GCA_002082745.1	CP020591.1	SSA6	IC_other
GCA_002082785.1	CP020597.1	HWBA8	IC_other
GCA_002082805.1	CP020598.1	WKA02	IC_other
GCA_002082825.1	CP020595.1	USA15	IC I
GCA_002082845.1	CP020579.1	SAA14	IC II
GCA_002082865.1	CP020578.1	SSA12	IC II
GCA_002082885.1	CP020581.1	SSMA17	IC II
GCA_002116925.1	CP015121.1	ab736	IC_other
GCA_002210065.1	CP021782.1	A85	IC I
GCA_002504145.1	CP018332.1	A1296	IC_other
GCA_002741415.1	CP024418.1	A388	IC_other
GCA_002753915.1	CP024576.1	AbPK1	IC II
GCA_002761575.1	CP024124.1	AYP-A2	IC II
GCA_002762095.1	CP024611.1	Ab4977	IC II
GCA_002762115.1	CP024613.1	Ab4568	IC II
GCA_002762155.1	CP024612.1	Ab4653	IC II
GCA_002843665.1	CP025266.1	SMC_Paed_Ab_BL01	IC II
GCA_002902885.1	CP026125.1	ABNIH28	IC_other
GCA_002947845.1	CP026711.1	AR_0063	IC_other
GCA_002948475.1	CP026943.1	S1 AB1A2	IC II
GCA_002948925.1	CP026761.1	AR_0078	IC_other
GCA_002950495.1	CP026750.1	WCHAB005133	IC II
GCA_002996805.1	CP027528.1	AR_0083	IC I
GCA_002999195.1	CP027246.1	WCHAB005078	IC I
GCA_003006035.1	CP027530.1	AR_0088	IC_other
GCA_003010655.1	CP027607.1	AR_0102	IC II
GCA_003010675.1	CP027611.1	AR_0101	IC_other
GCA_003029495.1	CP027123.1	AR_0056	IC II
GCA_003181015.1	CP029569.1	DA33098	IC II
GCA_003202135.1	CP021496.1	ZS3	IC II
GCA_003264295.1	CP019217.1	XH731	IC II
GCA_003296225.1	CP030106.1	DA33382	IC I
GCA_003345235.1	CP026338.1	810CP	IC_other
GCA_003431385.1	CP022283.1	7804	IC_other
GCA_003431865.1	CP027178.1	AR_0070	IC_other
GCA_003516005.1	CP023031.1	7847	IC II
GCA_003522665.1	CP023020.1	9201	IC_other
GCA_003522705.1	CP023022.1	10324	IC_other
GCA_003522785.1	CP023026.1	10042	IC II
GCA_003522845.1	CP023029.1	9102	IC I
GCA_003522885.1	CP023034.1	5845	IC II
GCA_003547115.1	CP027183.1	AR_0052	IC_other
GCA_003591615.1	CP023140.1	XH906	IC II
GCA_900088705.1	LT594095.1	BAL062	IC II
GCA_900478145.1	LS483472.1	NCTC13421	IC I

Supplementary table 2. References to studies, which data were used to screen the expression changes of genes from capsule synthesis loci under various conditions.

Conditions	Note	Reference
Triclosan resistan mutant		Fernando *et al.* (2017)
Outer membrane vesicles	A38 strain compared to 5806 strain	Li *et al.* (2015)
Biofilm vs exponential growth Biofilm vs late growth Exponential vs late growth Salicylic acid treated vs exponential growth Salicylic acid treated vs late growth Late growth vs biofilm Late growth vs exponential growht		Cabral *et al.* (2011)
Freely soluble extracellular proteins Found in OMVs and FSEP Found in OMV only	 Found in outer membrane vesicles and freely soluble extracellular proteins Found in outer membrane vesicles only	Mendez *et al.* (2012)
Biofilm vs stationary growth Response to ciprofloxacin Response to ciprofloxacin Biofilm response to tetracycline Biofilm response to tetracycline	 Ciprofloxacin exposed biofilm compared to control biofilm Ciprofloxacin exposed biofilm compared to stationary growth Versus biofilm Versus stationary growth	Penesyan *et al.* (2019)
Response to chlorhexidine		Hassan *et al.* (2013)
WT vs LOS$^-$ strain WT vs LOS$^-$ strain WT vs LOS$^-$ strain WT vs *ΔponA* WT vs *ΔponA* LOS$^-$ strain	AYE compared to lipooligosaccharide negative strain Strain 19606 compared to lipooligosaccharide negative strain Strain 5075 compared to lipooligosaccharide negative strain	Boll *et al.* (2016)
ΔgacA vs WT *ΔgacS* vs WT		Cerqueira *et al.* (2014)
Response to colistin + doripenem Response to colistin Response to colistin Response to doripenem LPS deficient strain vs WT	2mg/L Colistin doripenem treatment for 60 min 2mg/L Colistin treatment for 15 min 2mg/L Colistin treatment for 60 min 2mg/L Doripenem treatment for 60 min	Henry *et al.* (2015)
Growth in LB Growth in LB Growth in serum Growth in serum	Exponential growth phase Stationary growth phase Exponential growth phase Stationary growth phase	Jacobs *et al.* (2012)
Transcriptome changes in *Porphyromonas gingivalis A. baumannii* polymicrobial community		Miller *et al.* (2018)
Response to monovalent cations		Hood *et al.* (2010)
LPS deficient strain vs WT		Henry *et al.* (2012)
Δhns vs WT		Eijkelkamp *et al.* (2013)
Response to H_2O_2 treatment		Juttukonda *et al.* (2019)
Light vs dark conditions		Müller *et al.* (2017)
DNA damage regulon		Aranda *et al.* (2013)
Δzur vs WT		Mortensen *et al.* (2014)
ΔadeAB vs WT S1 strain *ΔadeB* vs WT AYE strain *ΔadeRS* vs WT AYE strain		Richmond *et al.* (2016)

Genes that decrease persistence in lungs of mice		Wang *et al.* (2014)
Genes required for growth in rich media		
Genes required for persistence in lungs of mice		
Growth in *Galleria mellonella*		Gebhardt *et al.* (2015)
During Infection treatment	Patient 280	Wright *et al.* (2017)
During Infection treatment	Patient 315	
During Infection treatment	Patient 348	
During Infection treatment	Patient 410	
During Infection treatment	Patient 475	
During Infection treatment	Patient 588	
During Infection treatment	Patient 66	
During Infection treatment	Patient 81	
Response to benzalkonium		Knauf *et al.* (2018)
Iron limitation		Eijkelkamp *et al.* (2011a)
Response to Imipenem	0.5mg/l imipenem	Chang *et al.* (2014)
Response to Imipenem	2mg/l imipenem	
ΔcpdA vs WT		Giles *et al.* (2015)
Biofilm vs exponential growth		Rumbo-Feal *et al.* (2013)
Biofilm vs stationary phase		
Exponential vs stationary growth		
Rnase T2 mutant vs WT		Jacobs *et al.* (2014)
Mitomycin C induced DNA damage		Hare *et al.* (2014)
Cells treated with 0.5% mucin		Ohneck *et al.* (2018)
ΔadeRS vs WT		Adams *et al.* (2018)
ΔtrxA vs WT		May *et al.* (2019)
ΔbfmRS vs WT		Geisinger *et al.* (2018)
ΔbfmR vs WT		
ΔbfmS vs WT		
ΔadeB vs ΔadeB in 0.5% bile salt		López *et al.* (2017)
ΔadeB vs ΔadeL in 0.5% bile salt		
ΔadeB vs WT in 0.5% bile salt		
ΔadeL vs ΔadeL in 0.5% bile salt		
ΔadeL vs WT in 0.5% bile salt		
ΔadeL vs WT in 0.5% bile salt		
Response to Human pleural fluid		Rodman *et al.* (2019)
ΔabaI vs WT		Ng *et al.* (2019)

Vilnius University Press
9 Saulėtekio Ave., Building III, LT-10222 Vilnius
Email: info@leidykla.vu.lt, www.leidykla.vu.lt
Print run 12 copies